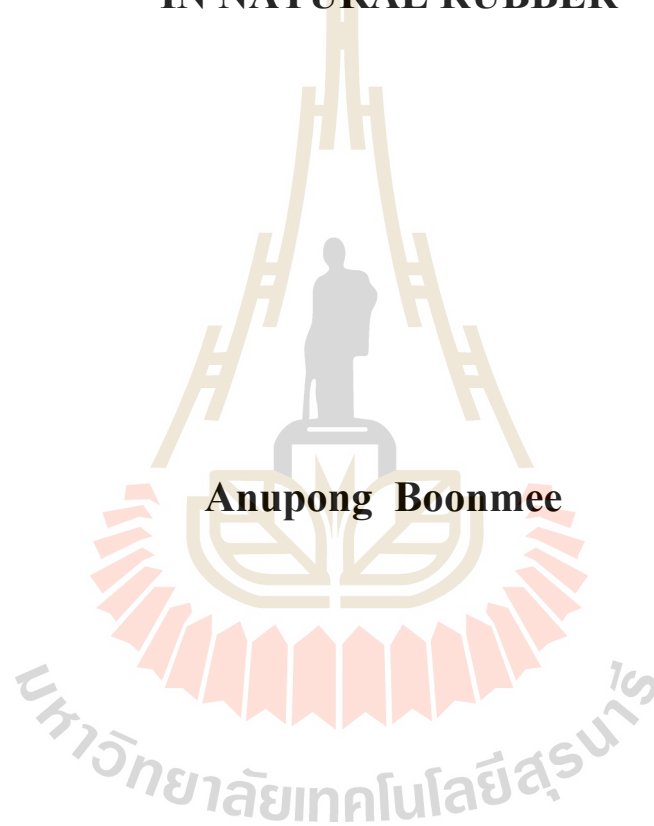


**PREPARATION AND CHARACTERIZATION OF  
SILICA NANOPARTICLES FROM SUGARCANE  
BAGASSE ASH FOR USE AS A FILLER  
IN NATURAL RUBBER**



**A Thesis Submitted in Partial Fulfillment of the Requirements for the  
Degree of Master of Engineering Program in Materials Engineering**

**Suranaree University of Technology**

**Academic Year 2019**

การเตรียมและตรวจสอบนาโนซิลิกาจากถ้ำซานอ้อยเพื่อใช้เป็น  
สารตัวเติมในยางธรรมชาติ




วิทยานิพนธ์นี้เป็นส่วนหนึ่งของการศึกษาตามหลักสูตรปริญญาวิศวกรรมศาสตรมหาบัณฑิต  
สาขาวิชาวิศวกรรมวัสดุ  
มหาวิทยาลัยเทคโนโลยีสุรนารี  
ปีการศึกษา 2562

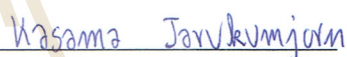
**PREPARATION AND CHARACTERIZATION OF SILICA  
NANOPARTICLES FROM SUGARCANE BAGASSE ASH  
FOR USE AS A FILLER IN NATURAL RUBBER**

Suranaree University of Technology has approved this thesis submitted in partial fulfillment of the requirements for a Master's Degree.


Thesis Examining Committee

  
\_\_\_\_\_  
(Assoc. Prof. Dr. Chaiwat Ruksakulpiwat)

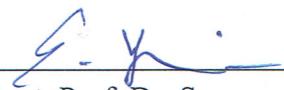
Chairperson

  
\_\_\_\_\_  
(Assoc. Prof. Dr. Kasama Jarukumjorn)

Member (Thesis Advisor)

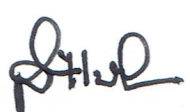
  
\_\_\_\_\_  
(Prof. Dr. Jatuporn Wittayakun)

Member

  
\_\_\_\_\_  
(Asst. Prof. Dr. Supagorn Rugmai)

Member

  
\_\_\_\_\_  
(Assoc. Prof. Ft. Lt. Dr. Kontom Chamniprasart)

  
\_\_\_\_\_  
(Prof. Dr. Santi Maensiri)

Vice Rector for Academic Affairs  
and Internationalization

Dean of Institute of Engineering

อนุพงศ์ บุญมี : การเตรียมและตรวจสอบนาโนซิลิกาจากเถ้าชานอ้อยเพื่อใช้เป็นสารตัวเติม  
ในยางธรรมชาติ (PREPARATION AND CHARACTERIZATION OF SILICA  
NANOPARTICLES FROM SUGARCANE BAGASSE ASH FOR USE AS A FILLER  
IN NATURAL RUBBER) อาจารย์ที่ปรึกษา : รองศาสตราจารย์ ดร. กษมา จารุกัจฉา,  
117 หน้า.

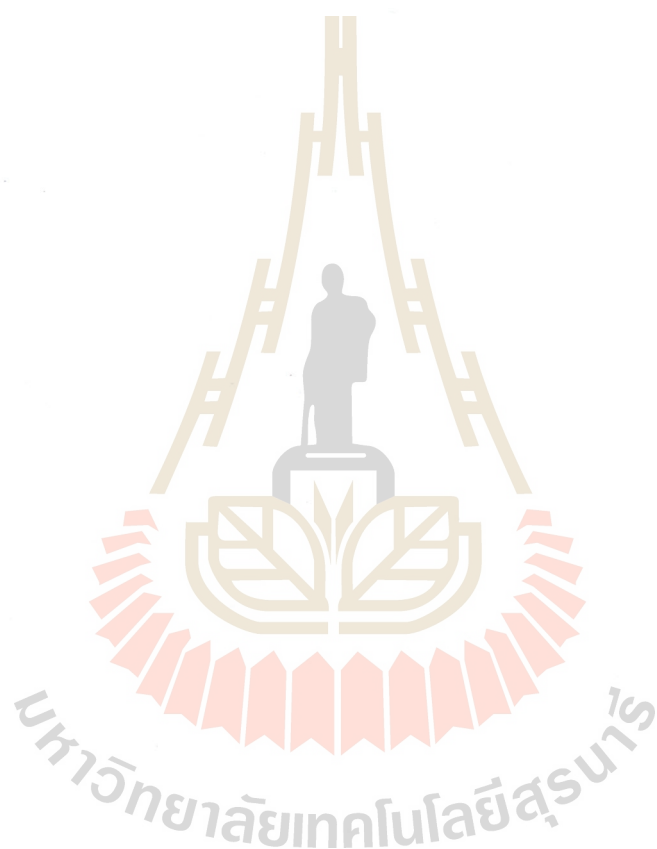
ในวิทยานิพนธ์นี้เตรียมนาโนซิลิกาจากเถ้าชานอ้อยโดยกระบวนการโซล-เจล ได้นาโนซิลิกาความบริสุทธิ์สูงมีขนาดอนุภาคระหว่าง  $90 \pm 10$  นาโนเมตร ฟูเรียร์ทรานส์ฟอร์มอินฟราเรด สเปกตรัมของนาโนซิลิกายืนยันคุณลักษณะของซิลิกา การวิเคราะห์การเลี้ยวเบนของรังสีเอกซ์บ่งชี้ว่านาโนซิลิกาเป็นอสัณฐาน ในขณะที่เถ้าชานอ้อยแสดงโครงสร้างผลึกของโลหะออกไซด์ที่เหลืออยู่ การอบแห้งแบบแช่เยือกแข็งให้อนุภาคนาโนซิลิกาที่มีพื้นที่ผิวจำเพาะและรูพรุนสูงกว่า เมื่อเทียบกับการอบแห้งด้วยความร้อนทั่วไป

ค่าทอร์กสูงสุดและค่าทอร์กต่ำสุดของยางธรรมชาติคอมโพสิตเพิ่มขึ้นอย่างต่อเนื่องเมื่อเพิ่มปริมาณนาโนซิลิกา เนื่องจากการเพิ่มขึ้นของความแข็งแรงของคอมโพสิต และการลดลงของการเปลี่ยนแปลงรูปร่างโมเลกุลของยางธรรมชาติ เวลาสกรอว์ และเวลาคงรูปของยางธรรมชาติคอมโพสิตเพิ่มขึ้น เมื่อเพิ่มปริมาณนาโนซิลิกา เนื่องจากการดูดซับสารตัวเร่งในกระบวนการเกิดพันธะแบบเชื่อมโยงโดยพื้นผิวของซิลิกา ยางธรรมชาติคอมโพสิตที่เติมนาโนซิลิกาที่อบแห้งแบบแช่เยือกแข็งให้เวลาการสกรอว์ และเวลาคงรูปนานกว่ายางธรรมชาติคอมโพสิตที่เติมนาโนซิลิกาที่อบแห้งด้วยความร้อน เนื่องจากการมีพื้นที่ผิวที่สูงกว่าของนาโนซิลิกาที่อบแห้งแบบแช่เยือกแข็งนำไปสู่การรบกวนกระบวนการเกิดพันธะแบบเชื่อมโยง ความหนืดมูนิของยางธรรมชาติคอมโพสิตเพิ่มขึ้นตามปริมาณนาโนซิลิกา โมดูลัสและความแข็งแรงของยางธรรมชาติคอมโพสิตเพิ่มขึ้น ในขณะที่การยืดตัว ณ จุดแตกหักลดลง เมื่อเพิ่มปริมาณนาโนซิลิกา เนื่องจากการเพิ่มขึ้นของความแข็งแรง ความทนทานต่อแรงดึงของยางธรรมชาติคอมโพสิตเพิ่มขึ้นตามปริมาณนาโนซิลิกา ถึง 5 ส่วนในหนึ่งร้อยส่วนของยางธรรมชาติ และลดลงที่ปริมาณนาโนซิลิกาสูงขึ้นเนื่องจากการเกาะกลุ่มกันของนาโนซิลิกา ความทนทานต่อการขัดถูของคอมโพสิตเพิ่มขึ้น เมื่อเติมนาโนซิลิกาจนถึง 3 ส่วนในหนึ่งร้อยส่วนของยางธรรมชาติ และลดลงที่ปริมาณนาโนซิลิกาสูงขึ้น ความหนาแน่นของพันธะเชื่อมโยงของคอมโพสิตเพิ่มขึ้นตามปริมาณนาโนซิลิกา และลดลงที่ปริมาณนาโนซิลิกา 10 ส่วนในหนึ่งร้อยส่วนของยางธรรมชาติ

การเติมบิส [3-(ไตรเอทอกซีไซลิล) โพรพิล] เตตระซัลไฟด์เป็นสารก่อกวนลงในกับยางธรรมชาติคอมโพสิตเพิ่มค่าทอร์กสูงสุด และค่าทอร์กต่ำสุดของคอมโพสิต เนื่องจากปรับปรุงความเข้ากันได้ดีขึ้นระหว่างนาโนซิลิกาและยางธรรมชาติ เวลาสกรอว์และเวลาคงรูปของยาง



ธรรมชาติคอมพิวเตอร์ที่มีสารคู่ควบไซเลนสั้นกว่าของยางธรรมชาติคอมพิวเตอร์ที่ไม่ใส่สารคู่ควบไซเลน เนื่องจากการดูดซับสารตัวเร่งที่น้อยลง การปรับปรุงมอดูลัส ความทนทานต่อแรงดึง ความแข็ง ความทนทานต่อการฉีกขาด และความทนทานต่อการขัดถูของคอมพิวเตอร์ เมื่อมีสารคู่ควบไซเลน เนื่องจากการเพิ่มขึ้นของการยึดติระหว่างนาโนซิลิกาและยางธรรมชาติ การใส่สารคู่ควบไซเลนเพิ่มความหนาแน่นของพันธะเชื่อมขวางของคอมพิวเตอร์ เพราะสารคู่ควบไซเลนให้บางส่วนของกำมะถันแก่คอมพิวเตอร์ทำให้เพิ่มปริมาณกำมะถันอิสระ



สาขาวิชา วิศวกรรมพอลิเมอร์

ปีการศึกษา 2562

ลายมือชื่อนักศึกษา เอกพงศ์ อรุณฉวี

ลายมือชื่ออาจารย์ที่ปรึกษา กษมา สารภักดิ์

ANUPONG BOONMEE : PREPARATION AND CHARACTERIZATION  
OF SILICA NANOPARTICLES FROM SUGARCANE BAGASSE ASH  
FOR USE AS A FILLER IN NATURAL RUBBER. THESIS ADVISOR :  
ASSOC. PROF. KASAMA JARUKUMJORN, Ph.D., 117 PP.

SILICA NANOPARTICLES/SUGARCANE BAGASSE ASH/NATURAL RUBBER/  
COMPOSITES/SILANE COUPLING AGENT

In this thesis, silica nanoparticles from sugarcane bagasse ash (SBA) were prepared using a sol-gel process. High purity of silica nanoparticles in the size range of  $90\pm 10$  nm were obtained. Fourier transform infrared spectrum of prepared silica nanoparticles confirmed silica characteristics. X-ray diffraction analysis indicated that silica nanoparticles were amorphous while SBA showed a crystalline structure from metal oxide residues. Freeze drying (FD) process provided silica nanoparticles with higher specific surface area and porosity compared to conventional heat drying (HD) process.

Maximum torque (MH) and minimum torque (ML) of natural rubber (NR) composites continuously increased with increasing silica nanoparticle content due to an increment of stiffness of the composites and a reduction of the deformation of NR molecules. Scorch time and cure time of NR composites increased with increasing silica nanoparticle content due to the adsorption of accelerator in vulcanization process by silica surface. FD-silica/NR composites provided longer scorch time and cure time compared to HD-silica/NR composites due to higher active surface area of FD-silica leading to disturbance of the vulcanization process. Mooney viscosity of NR composites increased with silica nanoparticle content. Modulus and hardness of NR composites

were increased while elongation at break was decreased with increasing silica nanoparticle content because of an increase in stiffness. Tensile strength of NR composites increased with silica nanoparticle content up to 5 phr then dropped at higher silica nanoparticle content due to aggregate formation of silica nanoparticles. Abrasion resistance of the composites was enhanced with the incorporation of silica nanoparticle up to 3 phr and declined at higher content of silica nanoparticle. Crosslink density of the composites increased with increasing silica nanoparticle content and decreased at 10 phr of silica nanoparticles.

The incorporation of Bis [3-(triethoxysilyl) propyl] tetrasulfide (Si-69) as a coupling agent into NR composites increased MH and ML of the composites due to the improved compatibility between silica nanoparticles and NR matrix. Scorch time and cure time of the composites with silane coupling agent were shorter than those of the composites without silane coupling agent because of less absorption of accelerator. Modulus, tensile strength, hardness, tear strength and abrasion resistance of the composites were improved with the presence of silane coupling agent because of enhanced adhesion between silica and NR. Incorporating silane coupling agent increased crosslink density of the composites because silane coupling agent donated some of its sulfur to the compound to implicitly raised the amount of free sulfur.

School of Polymer Engineering

Academic Year 2019

Student's Signature Anupong Boonmee

Advisor's Signature Kasama Janyekumjorn

## ACKNOWLEDGEMENT

I gratefully acknowledge the financial supports from Suranaree University of Technology and Khonburi Power Plant Co., Ltd. subordinated to Khonburi Sugar Public Co., Ltd. for supplying sugarcane bagasse ash and PI industry Co., Ltd for supplying chemicals used in rubber compounding.

I would like to express my sincere gratitude to my thesis advisor, Assoc. Prof. Dr. Kasama Jarukumjorn, for her excellent supervision, inspiring guidance and encouragement throughout the period of the study. Sincere appreciation is also extended to Prof. Dr. Jatuporn Wittayakun for his valuable excellent suggestion in the details of silica nanoparticles preparation. My appreciation also goes to Assoc. Prof. Dr. Chaiwat Ruksakulpiwat for his excellent suggestion in the details of rubber compound preparation and testing. In addition, I wish to express my gratitude to Assoc. Prof. Dr. Wimonlak Sutapun and Asst. Prof. Dr. Supagorn Rugmai for their valuable suggestions and guidance given as committee members. Furthermore, I am deeply indebted to lecturers, staff members, and all friends of School of Polymer Engineering for their helps, supports and encouragement.

Finally, my graduation would not be achieved without best wish from my beloved friend and parents who give me a valuable life with their endless love, warmth, support, and encourage me throughout the course of this study at Suranaree University of Technology.

Anupong Boonmee

# TABLE OF CONTENTS

	<b>Page</b>
ABSTRACT (THAI) .....	I
ABSTRACT (ENGLISH) .....	III
ACKNOWLEDGEMENTS .....	V
TABLE OF CONTENTS .....	VI
LIST OF TABLES .....	XI
LIST OF FIGURES .....	XII
SYMBOLS AND ABBRIVIATIONS .....	XVI
<b>CHAPTER</b>	
<b>I INTRODUCTION</b> .....	<b>1</b>
1.1 General background.....	1
1.2 Research objectives.....	6
1.3 Scope and limitation of the study.....	6
<b>II LITERATURE REVIEW</b> .....	<b>9</b>
2.1 Silica nanoparticles.....	10
2.2 Preparation and characterization of silica nanoparticles from sugarcane bagasse ash.....	11
2.3 The effect of drying techniques on surface properties and particles size of silica nanoparticles.....	18

## TABLE OF CONTENTS (Continued)

	<b>Page</b>
2.4 Properties of silica reinforcing natural rubber composites.....	21
2.5 Compatibility improvement of silica/NR composites.....	25
2.5.1 NR matrix modification.....	26
2.5.2 Silica surface modification.....	27
2.5.3 Addition of compatibilizer.....	28
<b>III METHODOLOGY</b> .....	<b>32</b>
3.1 Materials.....	32
3.2 Experimental.....	32
3.2.1 Preparation of silica nanoparticles from sugarcane bagasse ash.....	32
3.2.1.1 Leaching sugarcane bagasse ash with acid.....	32
3.2.1.2 Extraction of sodium silicate from acid treated sugarcane bagasse ash.....	33
3.2.1.3 Preparation of silica nanoparticles from extracted sodium silicate.....	34
3.2.2 Characterization of sugarcane bagasse ash, sodium silicate and silica nanoparticles from sugarcane bagasse ash.....	36

## TABLE OF CONTENTS (Continued)

	<b>Page</b>
3.2.3 Preparation of silica nanoparticles/NR composites.....	37
3.2.4 Characterization of NR and NR composites.....	38
3.2.4.1 Cure characteristics.....	38
3.2.4.2 Mooney viscosity.....	38
3.2.4.3 Mechanical properties.....	38
3.2.4.4 Abrasion resistance.....	39
3.2.4.5 Morphology.....	39
3.2.4.6 Crosslink density.....	39
<b>IV RESULTS AND DISCUSSION .....</b>	<b>41</b>
4.1 Characterization of sodium silicate from sugarcane bagasse ash.....	41
4.1.1 Chemical structure.....	41
4.2 Effect of drying techniques on properties of silica nanoparticles.....	42
4.2.1 Chemical structure.....	42
4.2.2 Chemical composition.....	44
4.2.3 Surface properties.....	44
4.2.4 Particle size and particles size distribution.....	45
4.2.5 Morphology.....	46



## TABLE OF CONTENTS (Continued)

	<b>Page</b>
4.3 Effect of silica nanoparticle content on properties of silica nanoparticles/NR composites.....	48
4.3.1 Cure characteristics and Mooney viscosity.....	48
4.3.2 Mechanical properties.....	52
4.3.2.1 Tensile properties.....	52
4.3.2.2 Tear properties.....	55
4.3.2.3 Hardness.....	58
4.3.3 Abrasion resistance.....	58
4.3.4 Crosslink density.....	60
4.3.5 Morphology.....	61
4.4 Effect of Si-69 on properties of silica nanoparticles/NR composites.....	64
4.4.1 Cure characteristics and Mooney viscosity.....	64
4.4.2 Mechanical properties.....	67
4.4.2.1 Tensile properties.....	67
4.4.2.2 Tear properties.....	70
4.4.2.3 Hardness.....	71
4.4.3 Abrasion resistance.....	73
4.4.4 Crosslink density.....	74
4.4.5 Morphology.....	75





## LIST OF TABLES

Table	Page
2.1 Silica content in sugarcane bagasse ash from different sources.....	12
3.1 Formulation of NR composites.....	37
4.1 Chemical composition of SBA and prepared silica nanoparticles.....	44
4.2 Surface properties and particle size of prepared silica nanoparticles.....	45
4.3 Cure characteristics and Mooney viscosity of NR and NR composites filled with FD-silica and HD-silica.....	50
4.4 Mechanical properties of NR and NR composites filled with FD-silica and HD-silica.....	57
4.5 Volume loss and crosslink density of NR and NR composites filled with FD-silica and HD-silica.....	59
4.6 Cure characteristics and Mooney viscosity of NR and NR composites filled with FD-silica and HD-silica with and without Si-69.....	65
4.7 Mechanical properties of NR and NR composites filled with FD-silica and HD-silica with and without Si-69.....	72
4.8 Volume loss and crosslink density of NR and NR composites filled with FD-silica and HD-silica with and without Si-69.....	74

## LIST OF FIGURES

Figure	Page
2.1	The schematic of surface structure of silica nanoparticles.....10
3.1	Leaching process of sugarcane bagasse ash.....33
3.2	Extraction process of sodium silicate from sugarcane bagasse ash..... 34
3.3	Preparation process of silica nanoparticles from sodium silicate.....35
3.4	(a) Sugarcane bagasse ash and (b) Silica nanoparticles.....36
3.5	Tensile test specimen.....38
3.6	Tear test specimen.....39
4.1	FTIR spectra of commercial sodium silicate and prepared sodium silicate....41
4.2	FTIR spectra of HD-silica nanoparticles and FD-silica nanoparticles.....43
4.3	XRD diffraction patterns of FD-silica nanoparticles HD-silica nanoparticles and SBA.....43
4.4	Particle size distribution of FD-silica nanoparticles and HD-silica nanoparticles.....46
4.5	SEM images at 50000X magnification of FD-silica nanoparticles and HD-silica nanoparticles.....47
4.6	TEM images of FD-silica nanoparticles and HD-silica nanoparticles.....47
4.7	Effect of silica nanoparticle content on maximum torque and minimum torque of NR composites.....50

## LIST OF FIGURES (Continued)

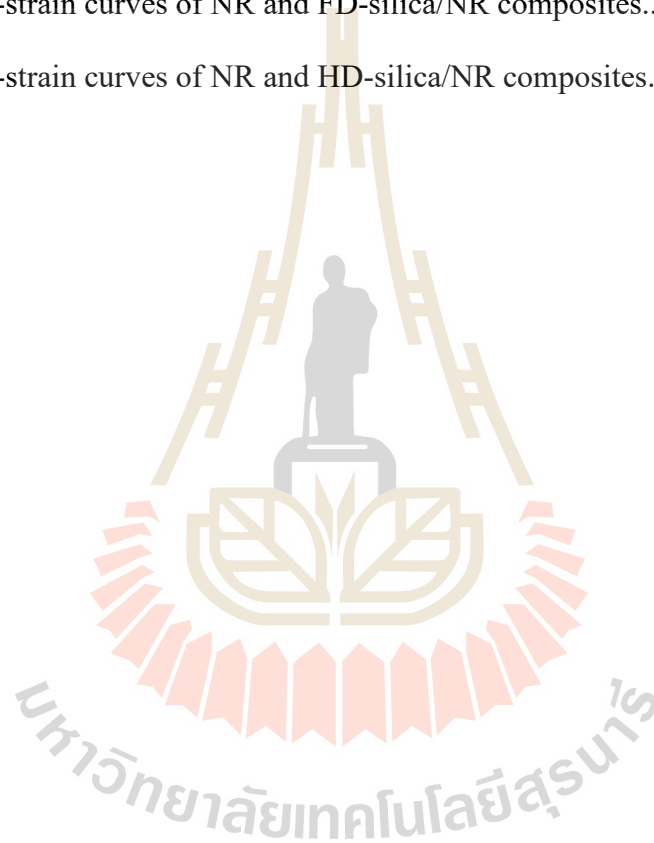
Figure	Page
4.8	Effect of silica nanoparticle content on scorch time and cure time of NR composites.....51
4.9	Effect of silica nanoparticle content on Mooney viscosity of NR composites.....51
4.10	Effect of silica nanoparticle content on modulus at 100% elongation of NR composites.....53
4.11	Effect of silica nanoparticle content on modulus at 300% elongation of NR composites.....54
4.12	Effect of silica nanoparticle content on elongation at break of NR composites.....54
4.13	Effect of silica nanoparticle content on tensile strength of NR composites....55
4.14	Effect of silica nanoparticle content on tear strength of NR composites.....56
4.15	Effect of silica nanoparticle content on hardness of NR composites.....58
4.16	Effect of silica nanoparticle content on volume loss of NR composites.....60
4.17	Effect of silica nanoparticle content on crosslink density of NR composites..61
4.18	SEM images of tensile fractured surface at 100X and 10000X of NR and NR composites..... 63
4.19	Effect of Si-69 on maximum torque and minimum torque of NR composites filled with FD-silica and HD silica.....66

## LIST OF FIGURES (Continued)

<b>Figure</b>	<b>Page</b>
4.20 Effect of Si-69 on scorch time and cure time of NR composites filled with FD-silica and HD-silica.....	66
4.21 Effect of Si-69 on Mooney viscosity of NR composites filled with FD-silica and HD-silica.....	67
4.22 Effect of Si-69 on modulus at 100% elongation of NR composites filled with FD-silica and HD-silica.....	68
4.23 Effect of Si-69 on modulus at 300% elongation of NR composites filled with FD-silica and HD-silica.....	39
4.24 Effect of Si-69 on elongation at break of NR composites filled with FD-silica and HD-silica.....	69
4.25 Effect of Si-69 on tensile strength of NR composites filled with FD-silica and HD-silica.....	70
4.26 Effect of Si-69 on tear strength of NR composites filled with FD-silica and HD-silica.....	71
4.27 Effect of Si-69 on hardness of NR composites filled with FD-silica and HD-silica.....	73
4.28 Effect of Si-69 on volume loss of NR composites filled with FD-silica and HD-silica.....	74
4.29 Effect of Si-69 on crosslink density of NR composites filled with FD-silica and HD-silica.....	75

## LIST OF FIGURES (Continued)

<b>Figure</b>		<b>Page</b>
4.30	SEM images at 100X of NR and NR composites filled with FD-silica and HD-silica with and without Si-69.....	76
A.1	Stress-strain curves of NR and FD-silica/NR composites.....	93
A.2	Stress-strain curves of NR and HD-silica/NR composites.....	93



## SYMBOLS AND ABBREVIATIONS

NR	=	Natural rubber
FAO	=	Agriculture Organization of United Nation
SBA	=	Sugarcane bagasse ash
H <sub>2</sub> SO <sub>4</sub>	=	Sulfuric acid
HCl	=	Hydrochloric acid
HNO <sub>3</sub>	=	Nitric acid
ENR	=	Epoxidized natural rubber
M	=	Molarity concentration
NaOH	=	Sodium hydroxide
ATR	=	Attenuated total reflection
Si-69	=	Bis [3-(triethoxysilyl) propyl]tetrasulfide
MH	=	Maximum torque
ML	=	Minimum torque
t <sub>s1</sub>	=	Scorch time
t <sub>90</sub>	=	Cure time
SiO <sub>2</sub>	=	Silica
XRF	=	X-ray fluorescent spectrometer
FTIR	=	Fourier-transform infrared spectrometer
AD	=	Alcohol dehydration
FD	=	Freeze drying

**SYMBOLS AND ABBREVIATIONS (Continued)**

HD	=	Heat drying
phr	=	Part per hundred of rubber
FSi	=	Fumed silica
PSi	=	Precipitated silica
wt%	=	Percent by weight
SEM	=	Scanning electron microscope
nm	=	Nanometer
$\mu\text{m}$	=	Micrometer
STR	=	Standard Thailand rubber
CBS	=	N-cyclohexyl-2-benzothiazole-2-sulphenamide
ml	=	Milliliter
mol	=	Mole
MDR	=	Moving die rheometer
UTM	=	Universal testing machine
dN-m	=	Deci Newton meter
MPa	=	Mega Pascal
$V_e$	=	Crosslink density
keV	=	Kilo electron volt
rpm	=	Revolution per minute



# CHAPTER I

## INTRODUCTION

### 1.1 General background

Thailand is the largest stocks and producer of natural rubber (NR) in the world. Food and Agriculture Organization of United Nation (FAO) reported the worldwide consumption of rubber totally around 27.5 million tons in 2016 which consists of 48% natural rubber, 20% styrene butadiene rubber, 12% polybutadiene rubber, 5% ethylene propylene-diene rubber, 2% chloroprene rubber, 2% nitrile rubber and 11% of other synthetic rubbers. Thus, in terms of quantity by type, NR is still the largest consumption of rubber. However, natural rubber price has dropped markedly in the past years because of the oversupply of NR from all around the world. Research and development such as improving properties of natural rubber composite plays an important role as a remedy for this worsening situation.

Natural rubber is one of the main rubbers and widely used to prepare many rubber products such as automotive tire, gasket and seal, rubber goods product etc. NR is a renewable material. It combines excellent and wide range of mechanical and dynamical properties for various applications. Properties and performances of rubber compounds depend mainly on the right compounding ingredient combination, including rubber additives and reinforcing fillers. Different types of reinforcing fillers affect significantly the properties of NR compounds (Rattanasom et al., 2007; Ahmed et al., 2014). In the rubber industry, carbon black and other non-black filler are used as

reinforcing fillers. Carbon black is used for the black products such as automotive tire, conveying belt or product that do not need much gorgeous appearance.

The introduction of silica particles into NR matrix as a non-black filler has been recently attracted interested. It possesses certain advantages over that of carbon black such as better abrasion resistance and lower rolling resistance. Silica particles is often used in producing white as well as colored articles. For the same reason, replacement of carbon black by silica has been growing steadily, especially in the tire industry. Moreover, silica particles has been used as a reinforcing filler in natural rubber industry for improving mechanical and thermal properties of natural rubber composites such as tensile strength, tear strength, hardness, abrasion resistance and thermal stability (Rattanasom et al., 2007). However, the production of silica particles for commercial applications is still high cost, high energy consumption and hazardous to the worker (Faizul et al., 2013).

Nowadays, nanotechnology is rapidly sweeping through all vital fields of science and technology. This involves in synthesis, characterization, and application of material and devices on the nanometer scale. At the nanoscale, physical, chemical, and biological properties are different from the properties of individual atoms and molecules of bulk matter. Therefore, the synthesis of silica nanoparticles with various methods have been studied with much success in several areas. Using silica nanoparticles as a filler in engineering composite application provides an opportunity to develop new classes of advanced materials.

Sol-gel process is a proper route to synthesis silica nanoparticles due to its ability to form high purity and homogenous products at proper conditions. Tetraethyl orthosilicate (TEOS) is commonly used as a precursor in alkaline medium to produce

silica nanoparticles. Particle size, particle size distribution and surface properties of silica nanoparticles prepared from TEOS are highly depended on experimental conditions that affect rate of hydrolysis and condensation reactions such as the type and concentration of alkoxides, catalyst's nature and concentration, time of aging and drying method etc. (Jafarzadeh et al., 2009). Drying is a simple process which involves the transition of fluid to solid leading to the formation of solid materials. It is the important step in the production of silica nanoparticles process. Collision and coalescence of the primary particles are the main factors of agglomeration in a silica nanoparticles system. Moreover, the intense aging process that occurs during the drying of sol can lead to complex agglomeration behavior arising from polycondensation reactions (Hench and West, 1990). So, a careful controlled drying process may lead to the formation of good dispersed and non-agglomeration of silica nanoparticles.

In addition, sodium silicate is another alternative precursor for synthesis of silica nanoparticles. Sodium silicate offers typical advantages over TEOS including refined and uniform particle size along with the high concentration of silica nanoparticles (Weichold et al., 2008). Extensive researches have been carried out to extract sodium silicate from sugarcane bagasse ash (Norsuraya et al., 2016; Huabcharoen et al., 2017) because of its safe in handling, high content of silicon and low-cost resources which are abundant availability in agriculture country. Sugarcane bagasse ash is waste in sugar industry and by-products from Bio-power station. It needs to be disposed properly, otherwise it may cause a major environmentally sustainable issue. Office of the Cane and Sugar Board in Thailand reported the production of sugarcane in 2014/2015 were 105.96 million tons/year. After extracted juice, the sugarcane bagasse amount 27.55 million tons/year was allowed for Bio-Power production process. Followed Cordeiro

method, about 0.62% by mass of the sugar cane remains as ash after combustion processes (Cordeiro et al., 2010). So, the amount of bagasse ash was around 660,000 tons/year in Thailand. Using sugarcane bagasse ash as a source of sodium silicate for produce silica nanoparticles for natural rubber composite applications not only provides a solution for waste disposal but also recovers a valuable material from agricultural wastes. The deposition of silica in the sugarcane is influenced by the quantity and availability of silicon in soil (Norsuraya et al., 2016).

Alkaline extraction is a proper route to extract sodium silicate from sugarcane bagasse ash. Sodium hydroxide (NaOH) solutions are conventionally used in alkaline extraction to extract silica from sugarcane bagasse ash. However, acid leaching is the important step to remove some residual metal oxide impurity. Huabcharoen et al. (2017) reported silica content of sugarcane bagasse ash before and after acid leaching were 77.2 % and 90.6 %, respectively. Leaching sugarcane bagasse ash by acids removes dirt and soil and metal oxides, especially alkali metal oxides (Huabcharoen et al., 2017; Ghorbani et al., 2015).

The properties of silica nanoparticles filled NR composite are generally depended on silica nanoparticles characteristics such as specific surface area, particle size as well as the ability of dispersion in NR matrix (Chuayjuljit et al., 2001). The main drawback of silica reinforced natural rubber composites is poor adhesion between silica surface and NR matrix. Silica surface is densely populated with siloxane and silanol groups which make the silica filler has high polarity. On the other hand, the hydrocarbon rubbers e.g. natural rubber is nonpolar. Thus, the conventional silica is not compatible with those hydrocarbon rubbers (Rahman and Padavettan, 2012). The problem arises as the filler particles are highly aggregated due to greater filler and filler interactions,

resulting in a lower dispersion of filler particle within the rubber matrix and poor filler-rubber adhesion leading to the poor mechanical properties of natural rubber composites (Prasertsri and Rattanasom, 2012; Luo et al., 2013; Santos et al., 2014).

The compatibility between silica and NR matrix can be improved by many approaches. Firstly, it is silica surface treatment (Kickelbick, 2003). This method is conducted by chemical modification of silica surface with organofunctional groups such as alcohol polyoxyethylene ether (AEO) and silane coupling agent (Zheng et al., 2017). Modification of silica surface with silane coupling agents is one of the most effective techniques. The second method is NR matrix modification (Xu et al., 2015). This method is similar to silica surface treatment but reversely by the modification of natural rubber molecular chains to enhance the affinity between the organic and inorganic phases. The example of the modification of NR matrix is epoxidized natural rubber (ENR) which is conducted by the addition of oxygen atom in to NR molecular chain to form epoxides functional group. The last method which is very simple and practically is adding a compatibilizer into NR compound in mixing state. Compatibilizers used in silica/NR composites are ENR, silane coupling agent and NR grafted with chemical functionalities. (Ismail et al., 2002; Murakami et al., 2003; Ismail et al., 2001). Silane coupling agents are mostly used as a compatibilizer to improve compatibility of silica/NR composites. Silane coupling agents ( $\text{Si}(\text{OR})_3\text{R}'$ ) have the ability to bond inorganic materials such as silica into natural rubber. In general, the  $\text{Si}(\text{OR})_3$  portion of the silane-coupling agents reacts with the inorganic reinforcement, while the organofunctional group ( $\text{R}'$ ) reacts with the NR matrix leads to increase the adhesion between silica and NR matrix. The use of silane coupling agents can reduce compound

viscosity and significantly increase modulus, tensile strength, and abrasion resistance of the composites (Sengloyluan et al., 2013; Ismail et al., 2001).

## 1.2 Research objectives

The aims of this research are followed:

- (i) To study the chemical composition, chemical structure and morphology of sugarcane bagasse ash and extracted silica nanoparticles from sugarcane bagasse ash.
- (ii) To study the effect of drying techniques on particle size, particle size distribution and surface properties of prepared silica nanoparticles.
- (iii) To investigate the effect of silica nanoparticle contents and silane coupling agent on cure characteristics, Mooney viscosity, mechanical properties, abrasion resistance, crosslink density and morphology of silica nanoparticles/NR composites.

## 1.3 Scope and limitations of the study

Chemical composition of SBA obtained from Khonburi Power Plant Co., Ltd, was analyzed using wavelength dispersive X-ray fluorescence spectrometer (XRF, PAN analysis, Axios) to investigate silica and other metal oxide contents. X-ray diffractometer (Bruker, D2 PHASER) was used to investigate chemical structure of SBA and silica nanoparticles in the range of  $2\theta = 10-80^\circ$ .

The silica extraction process was performed by refluxing sugarcane bagasse ash with 1 M HCl at 100 °C for 4 h to remove dirt and metal oxides impurity (Ghorbani et al., 2015). Then the solution was cool down to room temperature and filtered. The remaining solid portion was washed with distill water until pH 7 was obtained then filtered and dried in a vacuum oven at 120 °C for 6 h to remove moisture. The acid

leached sugarcane bagasse ash was then dispersed and vigorous stirring in 50 ml of 3M sodium hydroxide (NaOH) for 4 h at 80 °C to produce sodium silicate solution (Norsuraya et al., 2016). The suspension was then filtered in order to remove solid residue. The filtrate solution was sodium silicate supernatant that was used as a precursor to produce silica nanoparticles.

The prepared sodium silicate 10 ml was added in to 20 ml of distill water. Then, the diluted sodium silicate solution was added drop-wise into the ethanol/ammonia mixture in ratio 30:90 ml. Then, the solution was aged for 1 h to form silica gel. Then, it was centrifuged and washed with distilled water (Zulfiqar et al., 2017). Finally, the silica gel was dried under heat drying (HD) in vacuum oven overnight or freeze dry (FD) in deep vacuum overnight to study the effect of different drying techniques on surface properties and particle size distribution of silica nanoparticles.

Particle size of silica nanoparticles was measured by laser diffraction particle size distribution analyzer (Malvern, Zetasizer-zs). Morphology of the samples was examined by scanning electron microscope (SEM, JEOL, JSM-6010LV) and transmission electron microscopy (TEM, FEI: TECNAI G2 20). Specific surface area, pore diameter, pore volume and pore diameter of purified silica nanoparticles were evaluated using nitrogen adsorption-desorption analysis (BELSORP-mini II). FTIR spectrum of silica nanoparticles was performed in the attenuated total reflection mode (ATR) at resolution of 4 cm<sup>-1</sup> in the range of 400-4000 cm<sup>-1</sup> using Fourier transform infrared spectrometer (FTIR, Bruker, T27/Hyp2000) to investigate chemical structure of silica nanoparticles.

Silica nanoparticles from sugarcane bagasse ash were used as a reinforcing filler in NR composites. The effects of silica nanoparticle content and silane coupling agent



on cure characteristics, Mooney viscosity, mechanical properties, abrasion resistance and morphology of NR composites were studied. Maximum torque (MH), minimum torque (ML), scorch time ( $t_{s1}$ ) and cure time ( $t_{90}$ ) of NR and NR composites were investigated with a moving die rheometer (MDR, GOTECH/GT-M200F) at 150 °C.

Tensile and tear properties of NR and NR composites were tested according to ASTM D412 and ASTM D624, respectively using a universal testing machine (UTM, INSTRON/5565). Hardness of NR and NR composites was determined according to ASTM D2240 using a shore A durometer (Bar Eiss, Type BS61 II). Abrasion resistance of NR and NR composites was evaluated as volume loss ( $\text{mm}^3$ ) according to ASTM D 5963.

Tensile fractured surfaces of NR and NR composites were examined using a scanning electron microscope (SEM, Nikon/Neoscope, JCM-5000) at 10 keV. The samples were coated with gold before examination. Moreover, crosslink density of NR and NR composites were investigated on the basis of rapid solvent-swelling measurements. Based on the mechanical and cure characteristics of silica nanoparticles/NR composites, the optimum content of silica nanoparticles in NR composites was selected to further study the effect of silane coupling agent on cure characteristics, Mooney viscosity, mechanical properties, abrasion resistance, crosslink density and morphology of NR composites.



## CHAPTER II

### LITERATURE REVIEW

Large quantity of sugarcane bagasse ash is found in Thailand especially in electricity power production factory or Bio-Power station. Office of the Cane and Sugar Board in Thailand reported the production of sugarcane in 2014/2015 was 105.96 million tons/year. After juice extraction, the sugarcane bagasse amount 27.55 million tons/year was allowed for Bio-Power production process. Followed Cordeiro method, about 0.62% by mass of the sugar cane remained as ash after combustion processes (Cordeiro et al., 2010). So, the amount of bagasse ash was around 660,000 tons/year in Thailand and considered as industrial wastes. Generally, the destination of bio-mass ash generated from the sugar industry is the disposal in landfills or used as fertilizer in the plantations. These practices have caused problems to public health and unwanted environmental impact mainly associated with soil and water (Sales and Lima, 2010). So, the industrial wastes need to be disposed properly, otherwise it may cause a major environmental sustainable issue. One of the possible way to solve this problem is using sugarcane bagasse ash as a new source of silica production for use in rubber industry. Many researches have been carried out to study the chemical composition of sugarcane bagasse ash to optimize the utilization of this solid residue into valuable product for various applications such as in pozzolanic material in concrete product or rubber composites (Chusilp et al., 2009; Huabcharoen et al., 2017).

## 2.1 Silica nanoparticles

Silica nanoparticles, also called silicon dioxide nanoparticles ( $\text{SiO}_2$ , SNPs) is a chemical compound that contains two most abundant elements in earth's crust i.e. oxygen and silicon. Silica nanoparticles have been received much attention for various industries such as pharmaceutical industry, food industry, cosmetic industry as well as rubber industry due to their well-defined order structure, high specific surface area and high thermal stability (Yong-Taeg et al., 2002; Jafarzadeh et al., 2009; Rahman and Padavettan, 2012). Silica nanoparticles are one of the reinforcing fillers widely used in polymer composites. It not only improves mechanical and thermal properties of composites but also reduces rolling resistance in vulcanized rubber when compared to the traditional carbon black. The surface of silica nanoparticles is covered by silanol groups (-Si-OH) that are very high polar and considerably chemically active. The schematic of surface structure of silica nanoparticles is shown in Figure 2.1 This feature leads to low compatibility with hydrocarbon rubbers, and hence weak filler-rubber interaction.

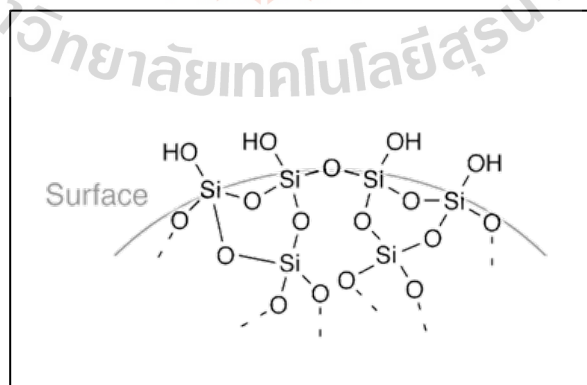


**Figure 2.1** The schematic of surface structure of silica nanoparticles

(Source: <https://commons.wikimedia.org>)

Normally, sol-gel process is a proper route to synthesis silica nanoparticles due to its ability to form high purity and homogenous products at proper conditions. Tetraethyl orthosilicate (TEOS) is commonly used as a precursor in alkaline medium to produce silica nanoparticles. Particle size, particle size distribution and surface properties of silica nanoparticles prepared from TEOS are highly depended on experimental conditions that affect rate of hydrolysis and condensation reactions such as the type and concentration of alkoxides, catalyst's nature and concentration, aging time and drying method, etc (Jafarzadeh et al., 2009). In addition, sodium silicate is another alternative precursor for synthesis of silica nanoparticles. Sodium silicate offers typical advantages over TEOS including refined and uniform particle size along with the high concentration of silica nanoparticles. Extensive researchers have carried out to extract sodium silicate from sugarcane bagasse ash (SBA) for use as a precursor to produce silica nanoparticles (Affandi et al., 2009; Norsuraya et al., 2016; Huabcharoen et al., 2017). Sugarcane bagasse contains high silicon content and abundant availability in agriculture country.

## **2.2 Preparation and characterization of silica nanoparticles from sugarcane bagasse ash**

Sugarcane bagasse ash is industrial waste occurred after burning sugarcane bagasse as a fuel for use in the sugarcane industry or in Bio-Power station. After sugarcane is milled for juice extraction in sugar production processing, the bagasse retrieved from crops is roughly 27-28 dry weight % of plant biomass. It is a highly heterogeneous material that composes of 20-30% lignin, 40-45% cellulose and 30-35% hemicellulose (Cordeiro et al., 2010). Its composition makes it a promising feedstock

for generation of bio-fuel production or bio-power for use in sugar production process. The ash as wastes by-product is obtained. Many researchers have studied the chemical composition of the sugarcane bagasse ash in order to find approaches for retrieving the utility from this waste such as using as a component in plywood, as a reinforcing filler in plastic or rubber product. Although bagasse ash can be applied in various products, the economic value is not high as compared to the value of the element ingredient in the bagasse ash. Sugarcane bagasse ash is an interesting waste to produce sodium silicate due to its high silica content as shown in Table 2.1. The deposition of silica in the sugarcane bagasse ash is influenced by the quantity and availability of silicon in soil. The root system plays the important role in absorbing silicic acid from the soil to the shoots and deposited it as amorphous silica (Norsuraya, 2016). The silica contents in sugarcane bagasse ash from different sources are tabulated in Table 2.1.

**Table 2.1** Silica content in sugarcane bagasse ash from different sources.

Sugarcane sources	Silica content (%)	References
Thailand	68.0-75.0	Kanking et al., 2011
India	72.0	Hariharan and Sivakumar, 2013
Brazil	70.0-90.0	Santos et al., 2014
Indonesia	50.4	Affandi et al., 2009
Malaysia	53.1	Norsuraya et al., 2016

Based on the previous literature, the extraction process of silica from sugarcane bagasse ash is not widely agreed and still open for discussion among rubber scientists and technologists (Huabcharoen et al., 2017). However, many researchers have reported that the alkaline extraction is the proper route to extract the silica from sugarcane

bagasse ash (Huabcharoen et al., 2017; Norsuraya et al., 2016; Worathanakul et al., 2009). Moreover, the acid leaching process also helps to remove some metal oxides from sugarcane bagasse ash. While the alkaline extraction process can dissolve silica in sugarcane bagasse ash to form sodium silicate which is an alternative precursor to produce silica nanoparticles.

Affandi, Setyawan, Winardi, Purwanto and Balgis (2009) reported the silica content from sugarcane bagasse ash determined using an X-ray fluorescent (XRF) method. The silica content of the bagasse ash was 50.36% and the main impurities were  $K_2O$  (19.34%),  $Fe_2O_3$  (18.78%) and  $CaO$  (8.81%). After treatment of bagasse ash using 1 M of HCl to remove the carbon residue, silica content was increased to 91.8 wt% and amount of metal oxides was reduced.

Worathanakul, Payubnop and Muangpet (2009) extracted silica from sugarcane bagasse ash by pretreated sugarcane bagasse ash with HCl at 100 °C for 2 h before heat treatment at 600, 700 and 800 °C. The silica content increased with increasing temperature because impurities such as metal oxides in bagasse ash were eliminated at high temperature. After acid treatment, XRF result showed that silica content increased from 75.14 to 89.04%.

Kanking, Thongsang, Sombatsompop, Sirisinha and Wimolmala (2011) investigated chemical composition of sugarcane bagasse ash from bio-mass power plant station in Nakhonsawan, Lopburi and Suphanburi provinces in Thailand. The result from XRF revealed that the sugarcane bagasse ash from Nakhonsawan and Suphanburi contained 75% of silica as a major component while sugarcane bagasse ash from Lopburi had 68% of silica. Moreover, various metal oxides were found in sugarcane bagasse ash. FTIR spectrum of sugarcane bagasse ash showed strong peak at 3427-3434

$\text{cm}^{-1}$  and  $1090\text{-}1091\text{ cm}^{-1}$  which were characteristics of silanol and siloxane group, respectively. FTIR spectrum of sugarcane bagasse ash was similar to precipitate silica.

Hariharan and Sivakumar (2013) studied the chemical composition of sugarcane bagasse ash obtained from electric power production factory in India. Sugarcane bagasse ash was cleaned, dried and calcined through a heating rate of  $300\text{ }^{\circ}\text{C}/\text{h}$  and then held at  $650\text{ }^{\circ}\text{C}$  for 2 h. The result from XRF indicated that silica content 72% was obtained. FTIR spectrum of silica showed large broad band at  $3440\text{ cm}^{-1}$  and strong intense band at  $1100\text{ cm}^{-1}$  assigned to the presence of OH stretching of silanol groups and siloxane Si-O-Si vibration at silica surface, respectively.

Harish, Arumugam and Ponnusami (2015) extracted silica from bagasse ash. The bagasse was burnt in a furnace at  $300\text{ }^{\circ}\text{C}$ . Silica was extracted by alkali treatment. The solution was kept in a hot water bath for 3 h. After the process, the solution was filtered to remove the ash residue. The filtrate consisted of sodium silicate which was subsequently used for silica gel preparation. Finally, the obtained sodium silicate solutions were titrated against 1N HCl and the pH was monitored. The pH was maintained between 7 and 10 during silica gel formation process. After the titration, the solution was kept for aging up to 24 h to form a gel like substance. The gel was further washed with distilled water and dried silica gel was obtained. XRF result revealed that silica content of 52.3% was obtained after the extraction process. The silica gels prepared from the filtrates of bagasse ash had very less impurities and high silica content.

Manzano, Begum and Noorliyana (2015) extracted silica from sugarcane bagasse ash. Firstly, the bagasse ash was treated with 3 M of HCl at  $100\text{ }^{\circ}\text{C}$  for 2 h with constant stirring. Acid treatment was used to remove metal oxides in the bagasse ash.

Then, the product was then filtered, washed with distilled water and dried. After that, the treated bagasse was treated in furnace at 600, 700 and 800 °C for 3 h. After processing, the bagasse ash was analyzed by XRF. The results indicated that silica contents were 67.325, 76.541 and 89.125% when the temperatures were 600, 700 and 800 °C, respectively. Moreover, high temperature helped to eliminate impurities in bagasse ash.

Mokhtar and Tajuddin (2016) prepared nanosilica from sugarcane bagasse ash by precipitation method. Sugarcane bagasse samples were stirred in NaOH solution and boiled for 3 h. The solution was filtered and the residue was washed with boiling water. The filtrate was allowed to cool down to room temperature and H<sub>2</sub>SO<sub>4</sub> was added until pH 2 and then added NH<sub>4</sub>OH until pH 8.5. Then, the filtrate was dried at 120 °C for 12 h. After that, nanosilica was refluxed with HCl for 4 h and then washed with deionized water to make it acid free. After that, the nanosilica sample was dissolved in NaOH by stirring continuously for 10 h on a magnetic stirrer. Then H<sub>2</sub>SO<sub>4</sub> was added to adjust pH in the range of 7.5-8.5. The precipitated nanosilica was washed repeatedly with warm deionized water until the filtrate became completely alkali free. The deionized water was used time after time for washing process. The nanosilica was dried at 50 °C for 48 h in an oven. The image of nanosilica analyzed using Field Emission Scanning Electron Microscopy (FESEM) revealed rough surface resulted in the high surface area. The result from energy-dispersion X-ray analysis (EDX) showed that nanosilica contained the elements of Si, O, C, Mg, K and Au.

Norsuraya, Fazlena and Norhasyimi (2016) studied the chemical composition of sugarcane bagasse ash after combustion at 1000 °C for 4 h. The ash was analyzed for silica composition using XRF. The chemical compositions of the sugarcane bagasse ash



were Si, S, Mg, P, Fe, Mn, Ca, K and Al. Silica content of sugarcane bagasse ash was 53.10%.

Norsuraya, Norhasyimi and Fazlena (2017) extracted sodium silicate from sugarcane bagasse ash for using as a precursor to synthesis santa barbara amorphous-15 (SBA-15). HCl was introduced during the silica extraction process to improve its purity. Chemical compositions of the sugarcane bagasse ash were Si, S, Mg, P, Fe, Mn, Ca, K and Al. The amount of SiO<sub>2</sub> presented in the raw sugarcane bagasse ash was 53.10% while after acid treatment silica composition in sample was increased to 88.13%. This was because the acid treatment method removed the impurities from the sugarcane bagasse ash. FTIR pattern of extracted sodium silicate showed a similar spectrum to the commercial pattern of sodium silicate.

Rahmat, Hamzah, Sahiron, Mazlan and Zahari (2016) characterized sodium silicate derived from sugarcane bagasse ash. Sugarcane bagasse was burnt at different temperatures of 600, 800 and 1000 °C for 2 h and 4 h and then washed using hydrochloric acid to remove metallic ions and impurities. The chemical composition of bagasse ash was characterized using XRF. The result indicated that sugarcane bagasse ash at 1000 °C for 4 h using acid washing method gave the highest composition of silica which was 88.13%. Then, the ash with the highest silica composition was extracted using 3M of sodium hydroxide solution. During the process, sodium hydroxide was bonded with silicate to form sodium silicate (Na<sub>2</sub>SiO<sub>2</sub>) and water (H<sub>2</sub>O).

Alves, Reis, Rovani, and Fungaro (2017) synthesized bio-silica from sugarcane bagasse ash using alkaline extraction followed by acid precipitation. The result from XRF revealed that, the major component of sugarcane bagasse ash was silica (81.60%). This indicated that this material was suitable to use as a new source of silica. The metal



oxides impurities such as MgO, P<sub>2</sub>O<sub>5</sub>, TiO<sub>2</sub>, SO<sub>3</sub>, MnO, Ta<sub>2</sub>O<sub>5</sub>, and As<sub>2</sub>O<sub>3</sub> were found. After the extraction process, the produced bio-silica had high purity above 99% and free of MgO, P<sub>2</sub>O<sub>5</sub>, TiO<sub>2</sub>, SO<sub>3</sub>, MnO, Ta<sub>2</sub>O<sub>5</sub>, and As<sub>2</sub>O<sub>3</sub>.

Huabcharoen, Wimonmala, Markpin and Sombatsompop (2017) studied the purification and characterization of silica particles from sugarcane bagasse ash obtained from Mitr Phol Sugar Co., Ltd in Thailand. XRF result revealed that the main components of sugarcane bagasse ash were silica (77.2%) and various kinds of metal oxide. After purification of sugarcane bagasse ash with HCl and HCl/ammonium fluoride (NH<sub>4</sub>F), silica content increased to 90.6% and 97.0%, respectively. This was because HCl was capable of removing metal oxides while NH<sub>4</sub>F dissolved the silica in bagasse ash to form fluorosilicate ([NH<sub>4</sub>]<sub>2</sub>·SiF<sub>6</sub>) complex compounds, which were precipitated by NH<sub>4</sub>OH solution to finally obtained purified silica.

Mohd, Wee and Azmi (2017) synthesized silica nanoparticles using sugarcane bagasse. The sugarcane bagasse was soaked in distilled water for overnight. Then, it was washed for several times and dried in an oven at temperature of 90 °C. 1N HCl was added to the sample to remove metallic impurities. Sample was filtered to remove metallic ions in the sample and dried again in an oven with temperature of 90 °C. The sugarcane bagasse was immersed in 1M NaOH solution to form sodium silicate solution. Sodium silicate solution was precipitated with nitric acid until pH 8, followed by the addition of 20 ml ethanol. Then, the precipitate was collected and heated in a furnace with temperature 600 °C for 30 min. to obtain silica nanoparticles. Infrared (IR) spectra showed the vibration peak of Si-O-Si, which was silica characteristics. Amorphous silica nanoparticles with spherical morphology with an average size of 30

nm, and specific surface area of  $111 \text{ m}^2\text{g}^{-1}$  were successfully synthesized. XRD patterns showed the amorphous nature of silica nanoparticles.

### **2.3 The effect of drying techniques on surface properties and particles size of silica nanoparticles**

Properties of silica nanoparticles prepared via sol-gel process are highly depended on experimental parameters and conditions that affect rate of hydrolysis and condensation reactions such as the type and concentration of alkoxides, time of aging and drying method etc. Drying is a simple process which involves the transition of fluid to solid leading to the formation of solid materials. It is the important step in the production of silica nanoparticles process. Collision and coalescence of the primary particles are the main factors of agglomeration in a silica nanoparticles system. In addition, the intense ageing process that occurs during the drying of sol can lead to complex agglomeration behavior arising from polycondensation reactions (Hench and West, 1990). So, a careful controlled drying process leads to the formation of well-dispersed and non-agglomeration of silica nanoparticles. The strength of agglomerates is highly depended on the solubility of the nanoparticles (Kwon and Messing, 1997). Rahman and Padavettan (2012) reported that the strength of water-dispersed agglomerated of silica nanoparticles was found almost three times higher compared to the ethanol dispersed agglomerates due to the presence of moisture. In aqueous system, the agglomeration behavior was caused by condensation reactions at the interparticle contacts during the drying process. In addition, Brownian motion, hydrodynamic effect, and capillary drag during the drying process can also contribute to the agglomeration

behavior. Thus, agglomeration of nanoparticles during drying process could be effectively reduced by using ethanol as the suspension medium.

Rahman, Vejayakumaran, Sipaut, Ismail and Chee (2008) described the effect of alcohol dehydration (AD), freeze drying (FD), and oven drying (OD) techniques on the particles size, size distribution, and agglomeration of silica nanoparticles produced from TEOS by sol-gel process. The results revealed that the alcohol-dehydration technique effectively removed the water and excess reactants from the silica suspension compared with freeze dry and oven dry techniques. Moreover, oven drying technique led to the formation of dense islands due to intense interparticle interactions and capillary force that created by evaporating water. The agglomerate was highest in the oven drying samples and least in the alcohol-dehydration samples.

Jafarzadeh, Rahman and Sipaut (2009) studied the effect of different drying techniques on particle size, particle size distribution and surface properties of silica nanoparticles prepared from TEOS. Particles size of silica nanoparticles prepared with heat drying and freeze-drying technique showed insignificant difference. The specific surface area, micropore area, average pore diameter and micropore volume of nanoparticles produced from FD were higher than of HD drying techniques. This may be because in freeze dry technique, a slow removal of water or other solvents through sublimation process under vacuum reduced the capillary forces resulting in a minimal shrinkage and preserving a high surface area and porosity of the particles.

Sarawade, Kim, Hilonga, Quang and Kim (2011) studied the effect of different drying techniques on properties of silica gel prepared from an aqueous sodium silicate solution by precipitation process. The oven drying (OD), microwave drying (MD) and spray drying (SD) techniques were used. SD technique provided the highest BET

specific surface area, and a lower in case of MD and OD techniques, respectively. Moreover, the cumulative pore volume and average pore diameters obtained from SD sample were much greater than the samples dried by OD and MD techniques. This was attributed to less drying shrinkage during the SD technique which was uniformly heated the wet-gel silica slurry. In contrast, the drying shrinkage occurring in the OD and MD techniques could be relatively high. Hence, the drying shrinkage reduced the total pore volume and pore diameter. Therefore, the total pore volume and BET specific surface area were reduced in the case of OD samples. The moisture content observed from the SD sample was relatively less than those of the samples dried by the OD and MD techniques. This indicated that the SD technique effectively removed water molecules in less time and at a lower temperature than the OD or MD techniques.

Duraes, Ochoa, Rocha, Patricio, Duarte, Redondo and Portugal (2012) studied the effect of different heating rates for the supercritical fluids drying (SFD) on density and porosity properties of silica aerogel. The result revealed that at the lower heating rate ( $\sim 80^\circ\text{C}/\text{h}$ ) silica aerogel with very low bulk density, high porosity, high surface area was obtained compared to silica aerogel with the higher heating rate ( $\sim 360^\circ\text{C}/\text{h}$ ). This may be because slow elimination of water led to lower drying shrinkage of sample resulting in low bulk density, high porosity and high surface area of silica aerogel.

Satha, Atamnia and Despetis (2013) studied the effect of different drying techniques including alcohol supercritical drying and  $\text{CO}_2$  supercritical drying on properties of silica aerogel. Surface area of aerogels obtained from  $\text{CO}_2$  supercritical drying was higher than that aerogels from alcoholic supercritical drying. The decrease in surface area of silica aerogel was related to the solubility of silica at high temperature and high pressure in alcohol supercritical drying process.

## 2.4 Properties of silica reinforcing natural rubber composites

Silica is used as a non-black reinforcing filler in natural rubber composites for a decade because it has high specific surface area and performance to improve the mechanical properties of the rubber composites, especially tensile properties, tear properties and hardness. In 1951, the first commercial silica product was marketed under the trade-name of Ultra-sil VN3 in Europe. Silica was initially used in light-colored or transparent articles, e.g. shoe soles. Precipitated silica was also used in small amounts in tire treads for commercial vehicles to improve tear propagation resistance. In 1990s, the European tire manufacturer Michelin introduced passenger car tires with treads formulated by incorporating silica as reinforcing filler instead of conventional carbon black. The tires with silica-filled tire tread compounds were claimed as “Green Tires” due to their lower rolling resistance and heat build-up, when compared with conventional tires with treads filled with carbon black.

Chuayjuljit, Eiumnoh and Potiyaraj (2001) studied cure characteristics and mechanical properties of NR and NR reinforced with silica. Scorch time and cure time of silica reinforced NR composites were higher than unreinforced NR because silica had an ability to absorb activators used in the compound thus prolonging the scorch time and cure time. In term of mechanical properties, such as tensile strength, tear strength and hardness, NR reinforcing with silica showed better overall mechanical properties when compared with unreinforced NR due to reinforcing effect of silica.

Arayapranee, Na-Ranong and Rempel (2005) studied cure characteristics and mechanical properties of natural rubber reinforced with silica. Cure time of silica/NR composites increased with increasing silica content. This was commonly explained by the silica structure which can absorb some accelerators into the porous structure, thus

slowing down the vulcanization process. Silica filled NR composites gave the highest tensile strength compared to NR composites. The tensile strength of the filled natural rubber increased with filler loading until a maximum level reached at 30 phr and then the property started to decrease with increasing filler loading due to the agglomeration of filler.

Mathew and Narayanankutty (2010) studied mechanical properties of NR composites reinforced with silica nanoparticles. The minimum torque increased with silica nanoparticles loading due to a better dispersion of the filler particles in the matrix. Scorch time of the composites increased linearly with the silica nanoparticles content. The delay of the cure reaction was attributed to the possible interaction of the silica with the accelerators, making it unavailable for cure reaction. Tensile strength of the composites was dropped at low content of silica nanoparticles and then tended to regain at higher silica content. The initial drop at lower levels of reinforcing fillers was a result of dilution effect in a strain-crystallization of NR matrix. The addition of silica nanoparticles improved abrasion resistance of the composites.

Thongpin, Sripethdee and Rodsantiea (2011) investigated cure characteristics and mechanical properties of NR filled with in-situ silica gel (Si-Gel). The silica contents were 5, 10, 15, 20, 25, 30, 35 and 40 phr. They reported that scorch time and cure time increased with the content of Si-Gel. This was because the absorption of vulcanizing accelerator by silica led to slow curing reaction. The presence of Si-Gel also obstructed flow of the rubber compound. Minimum and maximum torques increased with Si-Gel content. At low contents of Si-Gel ( $\leq 20$  phr), the vulcanization was retarded due to high porosity and polarity of Si-Gel, resulting in lower crosslink density. This would result in low modulus at 100% elongation, tensile strength, and

elongation at break of the composites. However, at higher contents of Si-Gel (>20 phr), the tensile properties increased with Si-Gel content and the properties were slightly higher than lower Si-gel case due to effect of interconnection between natural rubber molecular chain and Si-Gel cluster.

Prasertsri and Rattanasom (2012) studied cure characteristics and mechanical properties of NR filled with fumed silica (FSi) and precipitated silica (PSi) via latex system. They found that scorch time of both silica-filled NR gradually reduced with increasing silica loading while cure time was not significantly affected. This shorter scorch time may result from the effect of the moisture-treated silanol groups on silica surfaces and the hydrolysis of nitrogen-sulfur bonds of accelerators (TBBS and MBT), resulting in faster onset of crosslinking. Moreover, tensile strength of the composites increased with increasing silica loading up to 20 phr. Then, it decreased when the silica content reached to 30 phr. It was likely that larger aggregates were formed and acted as defects when the silica content was high. Tensile strength of FSi/NR composite was higher than Psi/NR composite. This was ascribed to the greater reinforcing ability of FSi that had higher specific surface area.

Lay, Azura, Othman, Tezuka and Pen (2013) reported the effect of nanosilica on cure characteristics and mechanical properties of nanosilica/NR composites. Maximum torque of composite increased with nanosilica content due to the improvement of stiffness of natural rubber. Minimum torque of composites decreased with increasing nanosilica due to the disturbance of very fine particles size of nanosilica and the reduction of entanglement of NR matrix by polarity of silica surface. Tensile strength, M100 and M300 of the composites increased with nanosilica content due to good dispersion of nanosilica in NR matrix.



Luo, Feng, Wang, Yi, Qiu, Lx and Peng (2013) reported the effect of silica loading on mechanical properties of NR composite. Tensile strength of the composites turned out to increase first, and then slowly decreased. Maximum tensile strength was obtained at silica loading 0.5 wt%. The enhancement of tensile strength was attributed to better dispersion silica in NR matrix, which was in reasonable agreement with the morphological property from SEM observation. Increasing silica content gradually decreased the tensile strength because the site of silica aggregation was easy to concentrate stress and led to breaking of the sample. The flexibility of the composite was reduced which was confirmed by decreasing elongation at break.

Santos, Agostini, Cabrera, Reis, Ruiz, Budenberg, Teixeira and Job (2014) studied cure characteristics and mechanical properties of NR composites reinforced with sugarcane bagasse ash (SBA) containing 70-90% of amorphous silica. With increasing amount of sugarcane bagasse ash, minimum torque and maximum torque of the composites also increased, while the scorch time and cure time were reduced. The increase in the minimum torque was directly related to the increasing viscosity by the addition of the filler. Moreover, modulus as well as the strength at break of the composites increased with adding 10-40 phr of sugarcane bagasse ash due to the high degree of interfacial adhesion between filler-polymer. SEM images of the surface of the SBA/NR composites showed homogeneity, i.e. surfaces without imperfections as well as the natural rubber covering the SBA particles. Increasing amount of SBA particles to 50 phr increased the filler-filler interactions (aggregates) promoting poor filler dispersion in NR matrix. This led to a reduction of the mechanical properties of the composites.



Huabcharoen, Wimonmala, Markpin and Sombatsompop (2017) reported the effect of silica from sugarcane bagasse ash on cure characteristic and mechanical properties of NR composites. Silica content had no effect on scorch time of the composites. However, cure time of silica/NR composites appeared to be decreased with increasing silica content. This was because the silica from bagasse ash contained metal oxides which could act as co-activators to reduce the cure time. Hardness and tensile modulus increased when the silica content was increased. This was due to the naturally high rigidity of the silica. The tensile strength of the composites increased at a silica content of 15 phr, and then it progressively declined at higher silica loadings. The increase in tensile strength at lower silica suggested there was a higher reinforcing level due to good dispersion of silica in the NR matrix. The decreases in tensile strength of the composite at higher dosages of silica was generally expected because of the poor silica dispersion in the NR matrix and high filler-filler interactions.

## **2.5 Compatibility improvement of silica/NR composites**

One of the important aspects of silica filled natural rubber composites is the ability to attain homogenous silica dispersion within natural rubber matrix, which determines the overall properties of the composites. The high polarity at silica surface leads to incompatible with hydrocarbon chain of natural rubber matrix. Agglomeration of silica particles is formed thus poor overall mechanical properties of the composites are obtained. Many researchers have studied the improvement of compatibility between silica and natural rubber matrix using many methods such as natural rubber matrix modification, silica surface modification and adding the compatibilizer.

### 2.5.1 NR matrix modification

Epoxidized natural rubber (ENR) is a chemical modified form of natural rubber. As the NR is epoxidized, its chemical and physical properties change depended on degree of epoxidation. When the degree of epoxidation is increased the rubber becomes more polar. ENR can interact with hydroxyl groups on the silica surfaces. This may be made ENR more compatible to silica than NR. Consequently, two grades of ENR, ENR-25 and ENR-50 with 25 and 50% mole of epoxidation, respectively have attained commercial importance. It has been reported that the mechanical properties of silica-filled ENR were higher than those of silica-filled NR. This was due to improved interaction between the ENR and silica surface via hydrogen bonds (Wang et al., 2012). Luo, Wang, Zhong, He, Li and Peng (2011) investigated cure characteristics and mechanical properties of silica/ENR composites. Both cure time and scorch time of ENR/silica composites increased with increasing amount of silica. This was attributed to the interaction of silica and accelerator. Silica with high surface area could adsorb accelerators, which reduced the accelerator reactivity and then retarded the cure process. Modulus at 100% and 300% elongation went up with increasing silica amount. The different trend appeared in terms of tensile strength. The tensile strength of the composites increased with increasing silica amount and reached the peak with adding 10 phr silica and then decreased with the silica more than 10 phr. At high content of silica (20 and 30 phr), the filler-filler interaction was dominant. SEM result revealed silica aggregations at 20 and 30 phr of silica.

Sarkawi, Aziz, Rahim, Ghani and Kamaruddin (2016) studied cure characteristics and mechanical properties of silica/ENR composites. Silica/ENR composites showed shorter scorch time and cure time compared with silica/NR

composites. The interaction of epoxy group of ENR with silanol groups decreased the silanol groups at silica surface. This also led to less of accelerators and other compounding ingredients to interact with silanol group of silica and resulted in the faster cure of the compound. Moreover, the interaction of ENR and silica came from hydrogen bonding between the silanol groups of silica with epoxide group in ENR. The stronger interactions between ENR and silica derived from bonding of silica with ring opening of ENR resulted in the improvement of silica dispersion in ENR and good mechanical properties of the composites.

### 2.5.2 Silica surface modification

Chemical modification of silica surface is main routes to obtain homogenous filler distribution in NR matrix. Modification of silica surface with silane is one of the most effective techniques. Silane ( $\text{Si}(\text{OR})_3\text{R}'$ ) has the ability to bond inorganic materials such as silica into natural rubber. In general, the  $\text{Si}(\text{OR})_3$  portion of the silane reacts with the inorganic reinforcement, while the organofunctional group ( $\text{R}'$ ) reacts with the NR matrix. The silica surface modifications with silane enhance the compatibility between the silica and natural rubber phases and at the same time improve the dispersion of silica particles within the natural rubber matrix.

Theppradit, Prasassarakich and Poompradub (2014) modified silica surface with different three organosilane modifiers including methyltriethoxysilane (MTES), vinyltriethoxysilane (VTES) and aminopropyltrimethoxysilane (APTMS). The selected organosilane modifier was added into the stirred solution and the sol-gel reaction was allowed to continue for 20 h with stirring. Thereafter, the modified silica particles were separated by filtration and then mixed in NR. Scorch time and cure time of unmodified silica/NR composites had longer than those modified silica/NR

composites. This was because the abundant level of the acidic silanol groups on the silica surface rapidly trapped the curing agents leading to a retarded vulcanization reaction. After modification of the silica surface, the substituted groups on the surface silanol groups of silica reduced the number of silanol groups and so decreased scorch time and cure time in the curing process. The modified silica particles improved the mechanical properties of the NR composites compared to unmodified silica. This could be explained by the better level of dispersion in the rubbery matrix leading to a higher efficiency of external load transfer within the filled vulcanizate, as well as a stronger interfacial interaction between the rubber and fillers.

Zheng, Han, Ye, Wu, Wu, Wang and Zhang (2017) modified silica particle with 3-mercaptopropyl-ethoxy-di (tridecyl-pentamethoxy)-silane (Si-747), which is a silane with long arms. Tensile strength and modulus of the modified silica/NR composites were higher than those of the unmodified silica/NR composite. The Si-747 could react with rubber by the mercaptopropyl group therefore it could function as a “coupling bridge” which was a typical chemical interaction between silica and rubber.

### **2.5.3 Addition of compatibilizer**

A compatibilizer, interfacial modifier or coupling agent is added into the incompatible polymer composites to enhance the compatibility between filler and polymer matrix. The compatibilizer attends at the interface during blending and plays the roles of reducing the interfacial tension and strengthening interfacial adhesion resulting the improvement of the physical and mechanical properties of the composites. Silane coupling agent, NR grafted with chemical functionalities and epoxidized natural

rubber are used to improve the compatibility between silica and NR (Ismail et al., 2002; Murakami et al., 2003; Ismail et al., 2001).

Xu, Jia, Luo, Jia and Peng (2015) studied mechanical and morphological properties of silica/NR composites using epoxidized natural rubber with 25% epoxidation (ENR-25) as an interfacial modifier. ENR-25 contents were 1, 3, 5 and 10 phr. Modulus at 300% elongation and tensile strength of the composites were enhanced with increasing ENR-25 content. Tear strength appeared a maximum value at 3 phr of ENR-25 content. It meant that the mechanical properties of silica/NR composites improved by adding ENR-25 with appropriate contents. ENR as an interfacial modifier promoted the dispersion of silica in NR matrix and improved interfacial adhesion between silica and rubber. SEM images of tensile fractured surface of the composites showed that the dispersion of silica significantly improved and the particle sizes became smaller in rubber matrix with the addition of ENR-25. However, when the content of ENR-25 exceed 3 phr, the phase separation between NR and ENR was observed with an ENR-25 particle about 3-4  $\mu\text{m}$  in NR matrix, which deteriorated the final performance of the composites.

Sengloyuan, Sahakaro, Dierkes and Noordermeer (2013) investigated the effect of epoxidized natural rubber as a compatibilizer on cure characteristics and mechanical properties of silica/NR composites. ENR consisting of 10, 38 and 51 mole % of epoxidation were used in a range of 2.5-15.0 phr. Scorch time and cure time of the compounds were prolonged when ENR contents and mole% of epoxidation were increased. This might be due to the high polarities of ENR and silica which interfered the vulcanization. Even though part of the silanol groups were assumed to interact with epoxide groups, the remaining free silanol groups as well as free epoxide groups

possibly formed hydrogen bonds with polar accelerators, causing accelerator adsorption on the polar surface. In addition, due to the polarity difference between NR and ENR, the more polar curatives migrated into the ENR phase which caused a delay of the vulcanization reaction in the NR matrix. The use of ENR-10 showed no positive effect on the tensile strength of the silica/NR, but the addition of ENR-38 and ENR-51 enhanced the tensile strength compared to the compound without compatibilizer. ENR-51 gave a higher tensile strength of the composites than ENR-38. With increasing ENR content, tensile strength of the composites increased to a maximum where thereafter the property dropped. The optimum value was observed at 7.5 phr for ENR-51 and 12.5 phr for ENR-38. The results supported the proposition that the epoxide functional groups improved silica–rubber interaction in the compounds.

Sengloyluan, Sahakaro, Dierkes and Noordermeer (2013) studied cure characteristics and mechanical properties of silica/NR composites with addition of bis-(3-triethoxysilyl-propyl) tetrasulfide (TESPT) as a compatibilizer. The result revealed that silica/NR composite with TESPT showed shorter scorch time and cure time than silica/NR composite without TESPT. TESPT itself can act as sulfur donor thus scorch time and cure time were reduced. Silica/NR composite with TESPT showed higher tensile strength than silica/NR composite without TESPT due to good silica dispersion and silica-to-rubber bonding via the silane molecule.

Katueangnan, Tulyapitak, Saetung, Soontaranon and Nithi-uthai (2016) comparatively studied cure characteristics and mechanical properties of silica/NR composites with different interface modifiers; i.e. TESPT and hydroxyl telechelic natural rubber (HTNR). Silica/NR/TESPT composite had shorter scorch time and cure time than silica/NR composite. For silica-filled NR composites, silanol groups

on silica surface can interact with accelerators resulting in longer scorch time and cure time. For the silica/NR/TESPT composite, the ethoxy groups of silane were firstly hydrolyzed to form a hydroxyl group which underwent condensation reaction with silanol groups on silica surface resulting in less adsorption of accelerator. Therefore, shorter scorch and cure time of silica/NR/TESPT were obtained. For silica/NR/HTNR composite, cure properties were insignificantly changed with the addition of HTNR. Tensile strength of silica/NR/TESPT composite was greater than silica/NR and silica/NR/HTNR composite because of higher crosslink density and rubber-filler interactions.

Sengloyluan, Sahakaro, Dierkes and Noordermeer (2016) studied the effect of different types of silane coupling agent on properties of silica/NR composites. The silane coupling agents included bis (triethoxysilylpropyl) tetrasulfide (TESPT) and 3-Octanoylthio1-propyltriethoxysilane (NXT). Scorch time of the silica/NR composite without silane was longer than those of the silica/NR composites with TESPT and NXT due to the polar character of the silica surface that adsorbed the polar curatives and resulted in cure retardation as well as a lower vulcanization efficiency. In contrast, the composite with NXT gave a longer scorch time than the composite with TESPT due to the carboxylic blocking groups in the NXT structure. Silica/NR/TESPT composite showed the highest modulus at 100% elongation and tensile strength because TESPT might donate some of its sulfur to the compound to implicitly raise the amount of free sulfur and consequently gave extra crosslinking.



# CHAPTER III

## METHODOLOGY

### 3.1 MATERIALS

Sugarcane bagasse ash (SBA) was supplied from Khonburi Power Plant Co., Ltd. subordinated to Khonburi Sugar Public Co., Ltd. Chemicals used in silica extraction from sugarcane bagasse ash were hydrochloric acid (Carlo Erba Reagents), sodium hydroxide (Carlo Erba Reagents), ammonia (Carlo Erba Reagents) and ethanol (Carlo Erba Reagents) from Italmar (Thailand) Co., Ltd. Natural rubber (NR, STR XL) was obtained from Natural Art and Technology Co., Ltd. Bis[3-(triethoxysilyl) propyl] tetrasulfide (Si-69) was supplied from PI Industry Co., Ltd. Commercial sodium silicate (Ajax Finechem) was obtained from Thai Poly Chemicals Co., Ltd. Other ingredients used to vulcanize natural rubber were stearic acid, zinc oxide, N-cyclohexyl-2-benzothiazole-2-sulfenamide (CBS) and sulfur supplied from PI Industry Co., Ltd.

### 3.2 EXPERIMENTAL

#### 3.2.1 Preparation of silica nanoparticles from sugarcane bagasse ash

##### 3.2.1.1 Leaching sugarcane bagasse ash with acid

The collected 100 g of SBA was refluxed with hydrochloric acid (HCl) at 100 °C for 4 h to remove dirt and metal oxides. The concentration of acids was 1 M. Then, the solution was filtered using filter paper (Whatman No.41). The remaining solid portion was washed with distill water until pH 7 was obtained and then filtered and dried in a vacuum oven at 120 °C for 6 h to remove moisture. The leaching



process of sugarcane bagasse ash is shown in Figure 3.1.

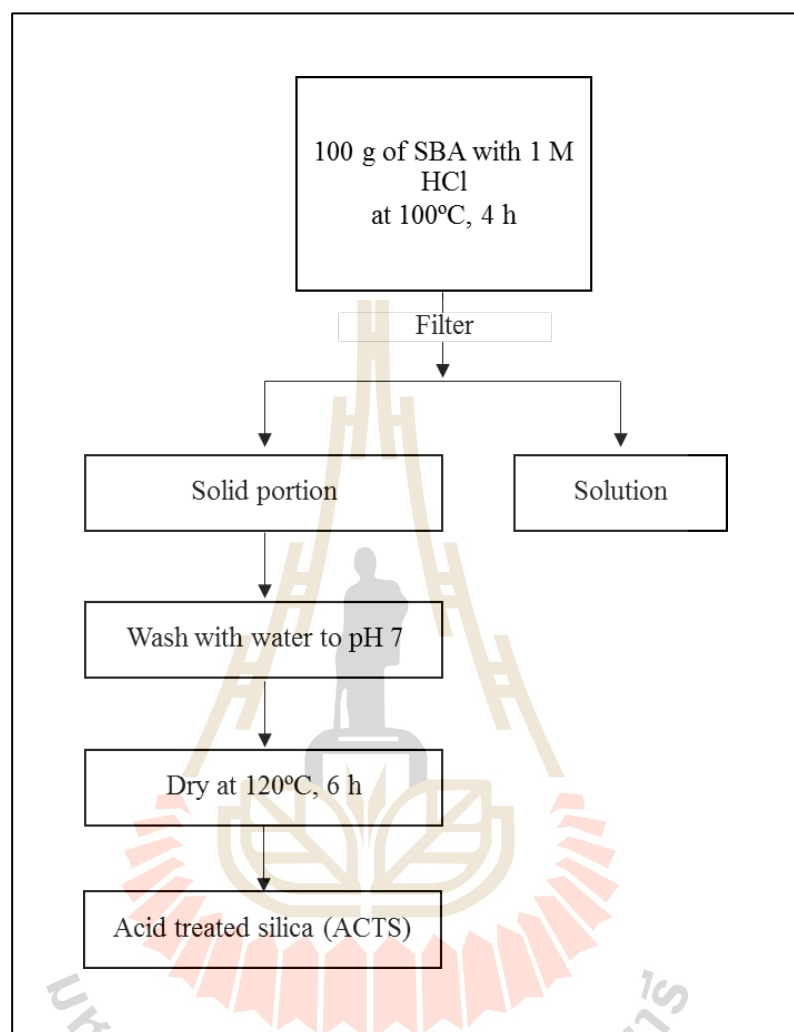


**Figure 3.1** Leaching process of sugarcane bagasse ash

### 3.2.1.2 Extraction of sodium silicate from acid treated sugarcane bagasse ash

The acid leached sugarcane bagasse ash was dispersed in 50 ml of 3 M sodium hydroxide (NaOH) for 4 h at 80 °C and vigorous stirring was applied to produce sodium silicate solution. The reaction is shown in Equation 3.1.

The suspension was then filtered through a filter paper Whatman No. 41 in order to remove solid residue. The filtrate solution was silica supernatant that was continuously used as a precursor to prepare silica nanoparticles. FTIR spectrum of extracted sodium silicate was compared with commercial sodium silicate. The extraction of sodium silicate from sugarcane bagasse ash is shown in Figure 3.2.

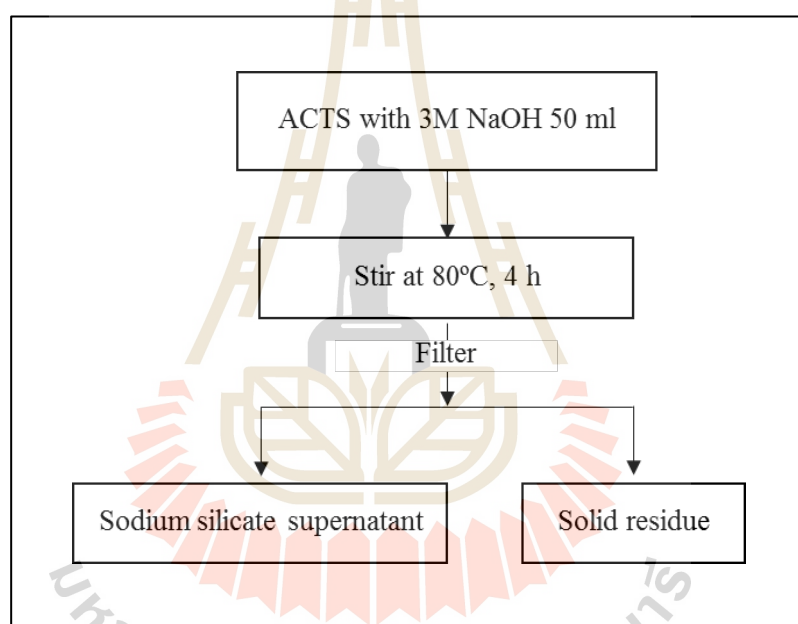


**Figure 3.2** Extraction process of sodium silicate from sugarcane bagasse ash

### 3.2.1.3 Preparation of silica nanoparticles from extracted sodium silicate

The extracted sodium silicate 10 ml was added in to 20 ml of distilled water. Then, the diluted sodium silicate solution was added drop-wise into the ethanol/ammonia mixture in ratio 30:90 ml. Then, the solution was aged for 1 h to

form silica gel. Then, it was centrifuged and washed with distilled water (Zulfiqar et al., 2017). Finally, the silica gel was dried under heat drying (HD) in vacuum oven overnight or freeze drying (FD) in deep vacuum overnight to study the effect of different drying techniques on surface properties and particle size distribution of silica nanoparticles. The preparation process of silica nanoparticles is shown in Figure 3.3. Prepared silica nanoparticles and sugarcane bagasse ash are shown in Figure 3.4.

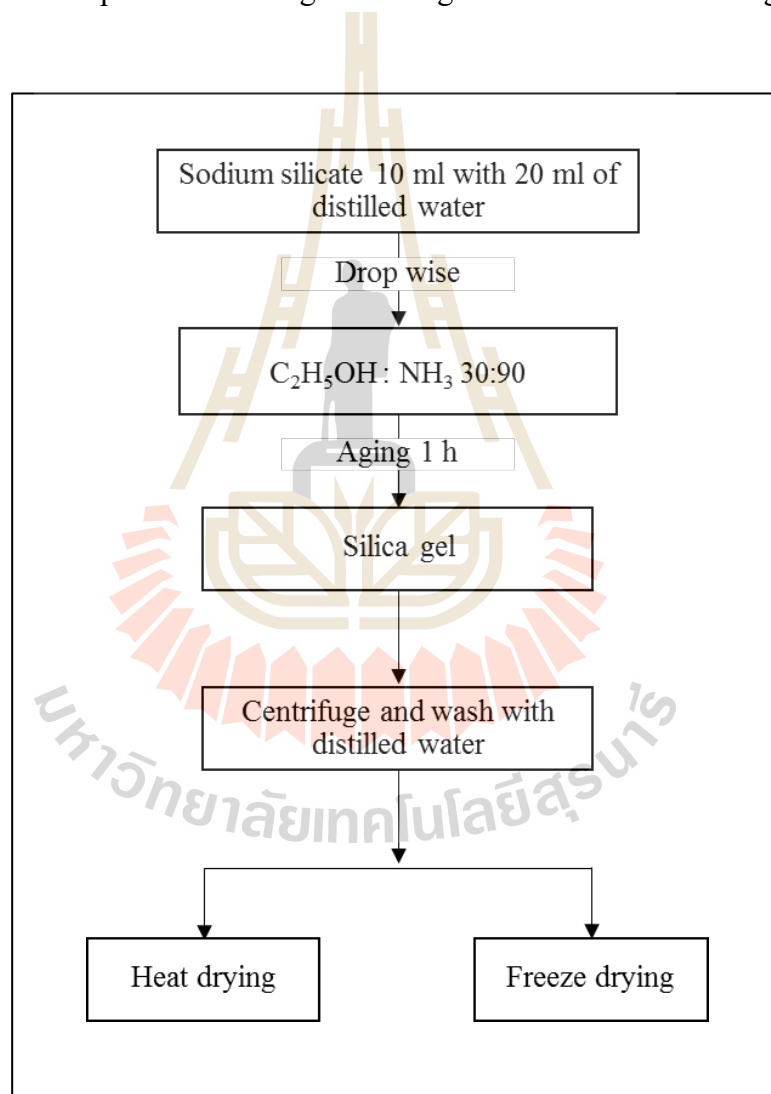


**Figure 3.3** Preparation process of silica nanoparticles from sodium silicate

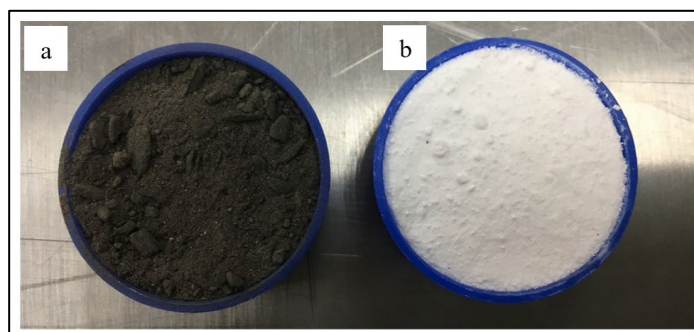


**Figure 3.4** (a) Sugarcane bagasse ash and (b) Silica nanoparticles

### **3.2.2 Characterization of sugarcane bagasse ash, sodium silicate and silica nanoparticles from sugarcane bagasse ash**

The chemical compositions of SBA and purified silica nanoparticles were analyzed using wavelength dispersive X-ray fluorescence spectrometer (XRF, PAN analysis, Axios).

X-ray diffraction patterns of SBA and silica nanoparticles were obtained from X-ray diffractometer (Bruker, D2 PHASER) in the range of  $2\theta = 10-80^\circ$ .

FTIR spectra of sodium silicate and silica nanoparticles were performed in the attenuated total reflection mode (ATR) at resolution of  $4\text{ cm}^{-1}$  in the range  $400-4000\text{ cm}^{-1}$  using Fourier transform infrared spectrometer (FTIR, Bruker, T27/Hyp2000).

Particle size of silica nanoparticles was measured using a laser diffraction particle size distribution analyzer (Malvern, Zetasizer-zs).

Morphology of silica nanoparticles was examined by scanning electron microscope (SEM, JEOL, JSM-6010LV) at 5 keV and transmission electron microscopy (TEM, FEI: TECNAI G2 20). In TEM sample preparation, the suspension of silica nanoparticles was prepared by diluting silica nanoparticles with ethanol and



### 3.2.4 Characterization of NR and NR composites

#### 3.2.4.1 Cure characteristics

Maximum torque (MH), minimum torque (ML), scorch time ( $t_{s1}$ ) and cure time ( $t_{90}$ ) of NR and NR composites were investigated using a moving die rheometer (MDR, GOTECH/GT-M200F) at 150 °C according to ASTM D 5289.

#### 3.2.4.2 Mooney viscosity

The Mooney viscosities ML (1+4) at 100 °C of the compounds were determined using a Mooney viscometer (MonTech, MV 3000 Basic) based on ASTM D 1646

#### 3.2.4.3 Mechanical properties

Tensile properties of NR and NR composites were tested according to ASTM D 412 using a universal testing machine (UTM, INSTRON/5565) with a load cell of 15 kN, a crosshead speed of 500 mm/min and a gauge length of 33 mm. Modulus at 100% elongation, modulus at 300% elongation, tensile strength and elongation at break of NR and NR composites were measured. Tensile test specimen of the composites is shown in Figure 3.5.

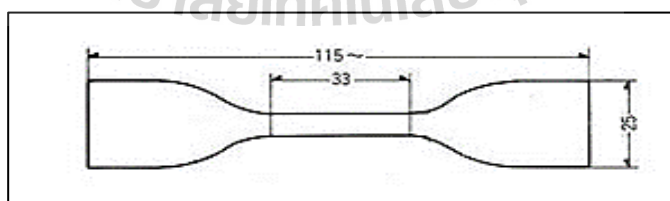


**Figure 3.5** Tensile test specimen. (Source: <https://compass.astm.org>)

Tear properties of NR and NR composites were tested according to ASTM D 624 using a universal testing machine (UTM, INSTRON/5565)

with a load cell of 5 kN at a crosshead speed of 500 mm/min. Tear test specimen of the composites is shown in Figure 3.6.

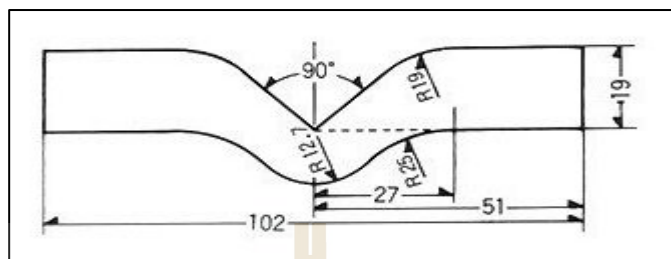


**Figure 3.6** Tear test specimen (Source: <https://compass.astm.org>)

Hardness of NR and NR composites were determined according to ASTM D 2240 using a shore A durometer (Bar Eiss, Type BS61 II).

#### 3.2.4.4 Abrasion resistance

Abrasion test was conducted according to ASTM D 5963 using Abrasion tester (Bareiss). The abrasion resistance was expressed as volume loss ( $\text{mm}^3$ )

#### 3.2.4.5 Morphology

Tensile fractured surfaces of NR and NR composites were examined using a scanning electron microscope (SEM, Nikon/Neoscope, JCM-5000) at 10 keV. The samples were coated with gold before examination.

#### 3.2.4.6 Crosslink density

Crosslink density ( $V_c$ ) of the NR and NR composites were estimated according to ASTM D 6814. The samples were swollen in toluene at room temperature for 72 h until equilibrium swelling was reached. The Flory-Rehner equation was used for calculation of crosslinking density as follows (Flory, 1953):

$$V_e = \frac{\ln(1 - V_r) + V_r + X_1 V_r^2}{V_1 [V_r^{1/3} - (\frac{V_r}{2})]} \quad (3.2)$$

Where;  $V_e$  is effective number of chains in a real network per unit volume.

$X_1$  is polymer-solvent interaction parameter ( $X_1$  is 0.391 for toluene).  $V_1$  is molecular volume of solvent ( $V_1$  is 106.2 for toluene).  $V_r$  is volume fraction of polymer in swollen network in equilibrium with pure solvent and calculated as follows:

$$V_r = \frac{\frac{\text{Weight of dry rubber} / \text{density of rubber}}{\text{Density of dry rubber}} + \frac{\text{Weight of solvent absorbed by sample}}{\text{Density of solvent}}}{\text{Density of dry rubber} + \text{Density of solvent}} \quad (3.3)$$



## CHAPTER IV

### RESULTS AND DISCUSSION

#### 4.1 Characterization of sodium silicate from sugarcane bagasse ash

##### 4.1.1 Chemical structure

FTIR spectra of commercial sodium silicate and extracted sodium silicate from SBA are illustrated in Figure 4.1. The peak at wavenumber  $980\text{ cm}^{-1}$  was characteristic of Si-O-Si stretching. Both spectra showed peak at  $1640\text{ cm}^{-1}$  which was attributed to H-O-H stretching vibration due to water adsorption of the samples. Broad peak around  $2500\text{-}3000\text{ cm}^{-1}$  confirmed the presence of hydroxyl group in the sample (Ghorbani et al., 2015, Norsuraya et al., 2016).

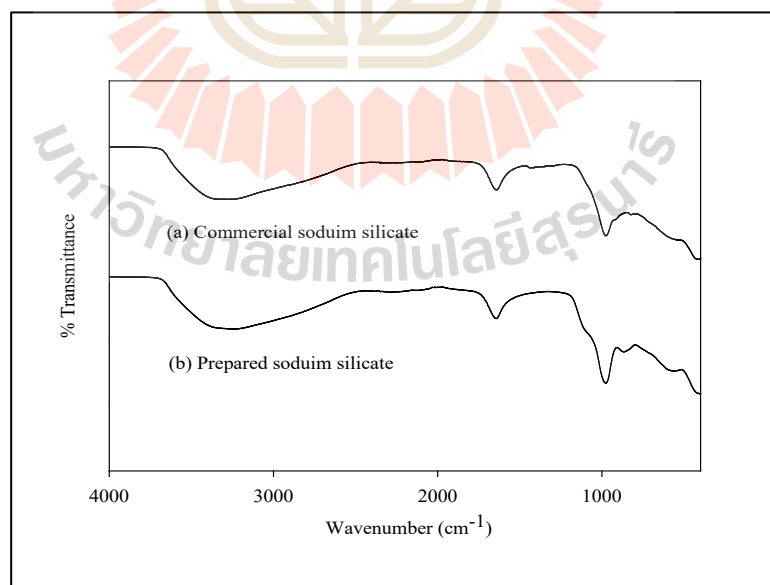


**Figure 4.1** FTIR spectra of commercial sodium silicate and prepared sodium silicate

## 4.2 Effect of drying techniques on properties of silica nanoparticles

### 4.2.1 Chemical structure

FTIR spectra of FD-silica nanoparticles and HD-silica nanoparticles are illustrated in Figure 4.2. FTIR spectrum of FD-silica nanoparticles showed essentially similar pattern with HD-silica nanoparticles. Basically, the vibration signal at  $1091\text{ cm}^{-1}$  represented the asymmetric vibration of Si-O-Si. Peak at  $800\text{ cm}^{-1}$  was the symmetric stretching vibration of Si-O-Si. Peak at  $467\text{ cm}^{-1}$  was assigned to the bending vibration of Si-O-Si. Moreover, peak at  $950\text{ cm}^{-1}$  confirmed the presence of hydroxyl group in the sample. (Ghorbani et al., 2015; Geetha et al., 2016). Mohd et al., (2017) prepared silica nanoparticles from sugarcane bagasse and found similar result.

XRD diffraction patterns of SBA, HD-silica nanoparticle and FD-silica nanoparticle are shown in Figure 4.3. The XRD patterns of FD-silica nanoparticle and HD-silica nanoparticle showed same broad peak in the range of  $15\text{-}30^\circ$  and centered at  $23^\circ$  attributed to amorphous phase of silica. FD-silica nanoparticle and HD-silica nanoparticle did not have any peaks represented the existing of crystalline structure. However, SBA presented peaks that are mainly characteristics of mineral phases including quartz ( $21^\circ$ ,  $26^\circ$ ,  $42^\circ$ ), cristobalite ( $24^\circ$ ), potassium carbonate ( $31^\circ$ ,  $37^\circ$ ,  $57^\circ$ ), calcium phosphate ( $25^\circ$ ), hematite ( $40^\circ$ ) (Schettino and Holanda 2015).

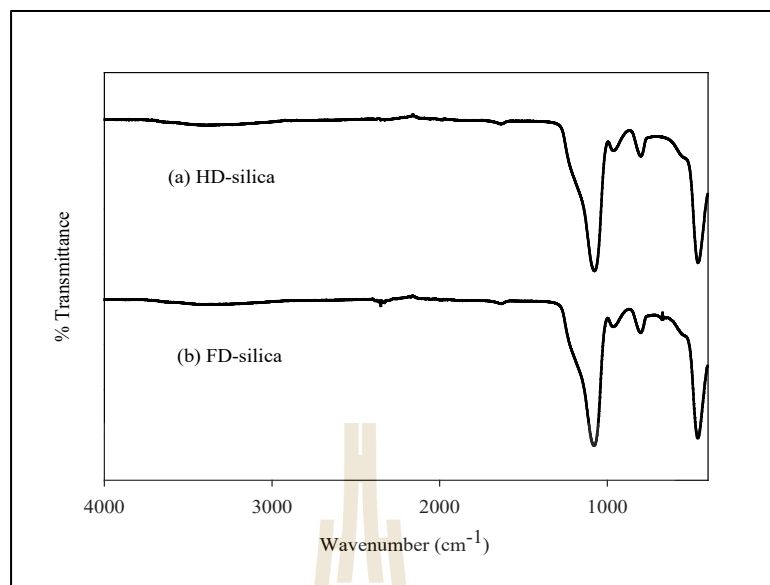


**Figure 4.2** FTIR spectra of HD-silica nanoparticles and FD-silica nanoparticles

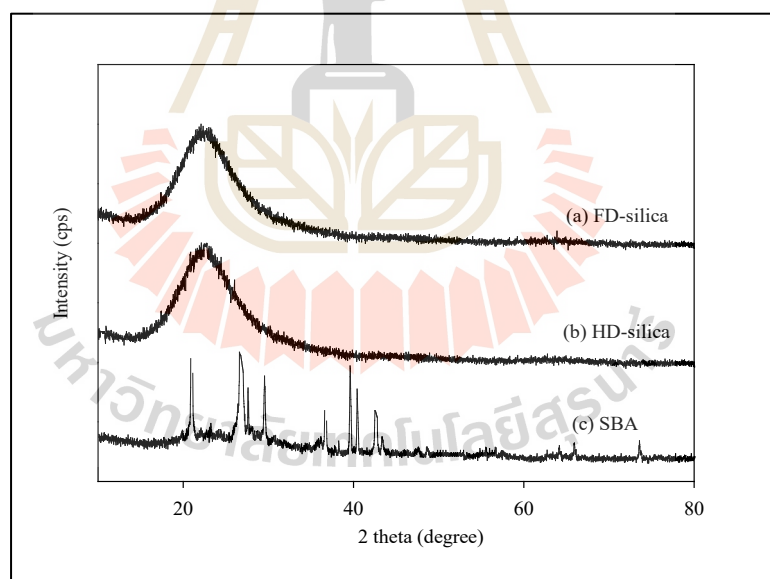


**Figure 4.3** XRD diffraction patterns of FD-silica nanoparticles, HD-silica nanoparticles and SBA

#### 4.2.2 Chemical composition

Chemical compositions of SBA, FD-silica nanoparticle and HD-silica nanoparticle are listed in Table 4.1. The sugarcane bagasse ash contained 67.5% of SiO<sub>2</sub> and major metal oxide impurities were K<sub>2</sub>O, Fe<sub>2</sub>O<sub>3</sub>, CaO and TiO<sub>2</sub> with 14.7%, 8.3%, 5.3% and 0.8%, respectively. On the other hand, silica purities of 95.1% and 96.0% were obtained after using freeze dry and heat dry process, respectively. This indicated that the extraction process was useful for removing metallic impurities and resulted in improved purity of silica. The drying techniques had insignificant effect on the impurity of the prepared silica nanoparticles. Huabcharoen et al., (2017) reported that the acid leaching process removed some metal oxides from sugarcane bagasse ash. While the alkaline extraction process dissolved silica in sugarcane bagasse ash to form sodium silicate. This led to increased purity of the silica (Affandi et al., 2009; Alves et al., 2017; Huabcharoen et al., 2017).

**Table 4.1** Chemical composition of SBA and prepared silica nanoparticles

Compound	SBA (%)	FD-silica (%)	HD-silica (%)
SiO <sub>2</sub>	67.5 ± 2.1	95.1 ± 3.4	96.0 ± 3.2
CaO	5.3 ± 0.6	0.3 ± 0.3	0.3 ± 0.2
TiO <sub>2</sub>	0.8 ± 0.2	0.1 ± 0.1	0.2 ± 0.3
K <sub>2</sub> O	14.7 ± 0.6	0.2 ± 0.2	0.2 ± 0.1
Fe <sub>2</sub> O <sub>3</sub>	8.3 ± 0.7	0.5 ± 0.3	0.3 ± 0.1

#### 4.2.3 Surface properties

The specific surface area, pore area and pore volume of FD-silica nanoparticle were significantly higher than that of HD-silica nanoparticle as shown in

Table 4.2. This may be because in freeze dry technique, water or other solvents were slowly removed through sublimation process under vacuum. This led to reduction of capillary forces and thermal tension resulting in minimal shrinkage, high specific surface area and high porosity at surface of the particles (Jafarzadeh et al., 2009). On the other hand, heat dry process decreased in gel volume due to the loss of liquid by evaporation through the silica pores by rapid removal of the water from the pores which caused blistering, shrinkage and shriveling of silica gel (Jafarzadeh et al., 2009). However, freeze dry technique presented the structure of materials without shrinkage of the gel structure (Chen and Wang 2007; Jafarzadeh et al., 2009). Rahman et al. (2008) reported that the heat dry of silica gel resulted in the formation of dense islands due to intense interparticle interactions and capillary force that created by evaporating water.

**Table 4.2** Surface properties and particle size of prepared silica nanoparticles

Properties	FD-silica	HD-silica
Surface area ( $\text{m}^2\text{g}^{-1}$ )	156	70
Pore area ( $\text{m}^2\text{g}^{-1}$ )	125.89	74.91
Pore volume ( $\text{cm}^3\text{g}^{-1}$ )	1.35	0.68
Mean pore diameter (nm)	35.25	39.09
Average particle size (nm)	$91.06 \pm 10.00$	$92.12 \pm 10.00$

#### 4.2.4 Particle size and particles size distribution

Both of drying techniques provided silica nanoparticles in size range  $90 \pm 10$  nm. Particle size and particle size distribution of silica nanoparticles prepared from these two drying techniques were insignificantly different as shown in Figure 4.4. Jafarzadeh et al. (2009) reported that particles size and particle size distribution of silica

nanoparticles prepared via sol-gel process were very sensitive towards the experimental conditions that affected the rate of hydrolysis and condensation reactions, e.g., the type and concentration of starting materials, catalyst's nature and concentration, nature of solvent, temperature, time of reaction, aging and drying method. However, in this study, drying technique exhibited no influence on particles size and particle size distribution of silica nanoparticles prepared from SBA.

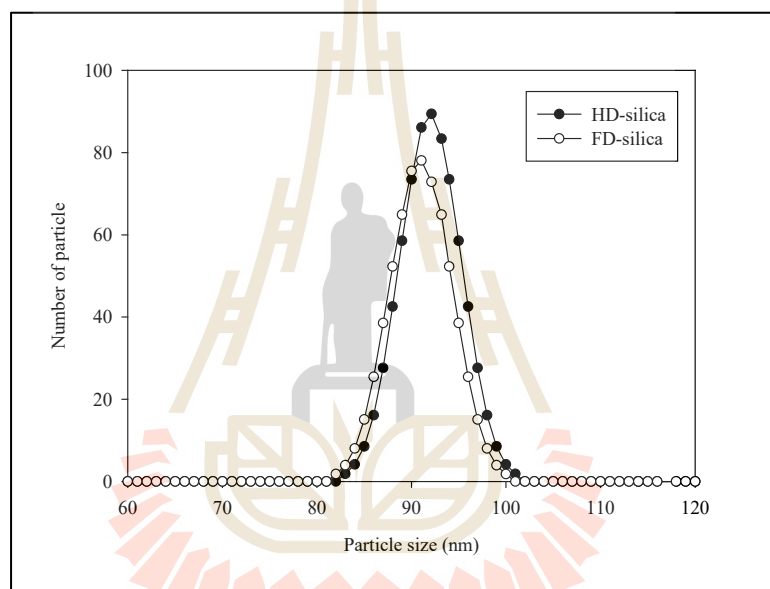


**Figure 4.4** Particle size distribution of FD-silica nanoparticles and HD-silica nanoparticles

#### 4.2.5 Morphology

SEM images of FD-silica nanoparticles and HD-silica nanoparticles at a magnification of 50000X are displayed in Figure 4.5. Silica nanoparticles did not show clear boundaries as they were in agglomerate. Due to the nonconductive nature of silica,

the charges quickly accumulated on the powder surfaces even after gold sputtering caused agglomeration of particles (Lu and Hsieh, 2012).

From Figure 4.6, the agglomerated form of silica nanoparticles was observed. Silica nanoparticles had particle size range in 10-20 nm which was smaller than the result from the particles size analyzer. This may be because in TEM sample preparation process, silica agglomerates were dispersed in ethanol solution and vibrated with ultrasonic wave. This process led to good dispersion of silica agglomerates.

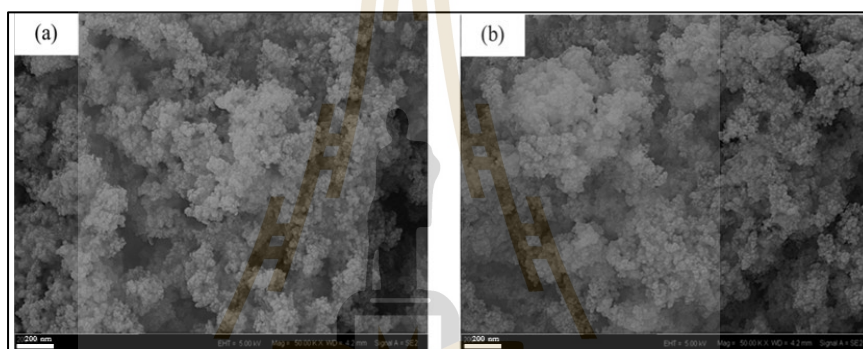


**Figure 4.5** SEM images at 50000X magnification of FD-silica nanoparticles and HD-silica nanoparticles

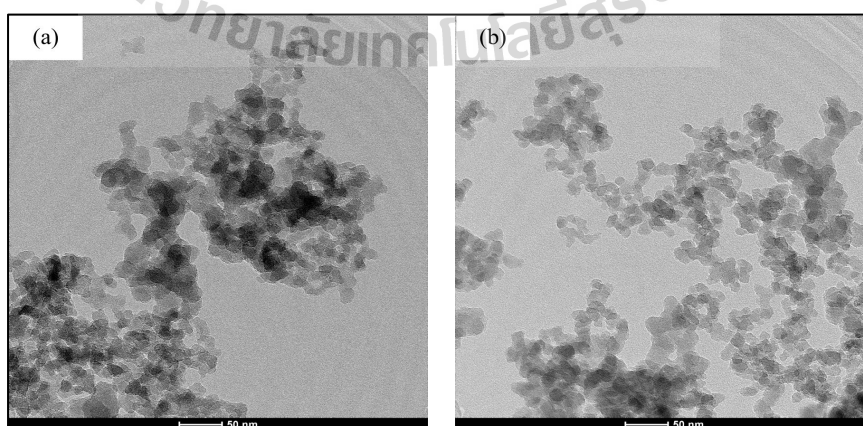


**Figure 4.6** TEM images of FD-silica nanoparticles and HD-silica nanoparticles



## 4.3 Effect of silica nanoparticle content on properties of silica nanoparticles/NR composites

### 4.3.1 Cure characteristics and Mooney viscosity

From MDR results, maximum torque (MH) measures stiffness in the rubber compound while minimum torque (ML) indicates the initial viscosity of rubber compounds. MH, ML, scorch time ( $t_{s1}$ ), and cure time ( $t_{90}$ ) of NR, NR composites filled with FD-silica and HD-silica are listed in Table 4.3.

Maximum torque and minimum torque of NR and NR composites are displayed in Figure 4.7. The incorporation of both FD-silica nanoparticle and HD-silica nanoparticle into NR matrix increased MH and ML of composites and further increased with increasing nanoparticle content. This may be due to an increase stiffness of the composites and a reduction of the deformation of NR molecules. FD-silica/NR composites showed higher MH and ML than HD-silica/NR composite because of high specific surface area of FD-silica leading to high filler-matrix interaction. Santos et al. (2014) reported the MH and ML of NR composites reinforced with sugarcane bagasse ash containing 70-90% of amorphous silica enhanced with sugarcane bagasse ash content due to increased viscosity and stiffness of composites. Scorch time and cure time of NR and NR composites filled with silica nanoparticles are shown in Figure 4.8. The incorporation of both silica nanoparticles into NR matrix led to longer scorch time and cure time compared to NR. With increasing silica content, longer scorch time and cure time of NR composites were found due to the disturbance in vulcanization process of silica nanoparticles. The silanol group at silica surface can interact with accelerator and activators leading to delay scorch time and cure time of NR composites (Pongdong et al., 2015). FD-silica/NR composites showed longer scorch time and cure time than



those of HD-silica/NR composites. This may be due to higher specific surface area of FD-silica surface resulted in high active surface and high absorption of chemicals in vulcanization process (Chuayjuljit et al., 2001). Thongpin et al. (2011) also observed the similar result that scorch time and cure time of Si-Gel/NR composites increased with Si-Gel content due to the absorption of vulcanizing accelerator by silica leading to slow curing reaction. However, different result was reported by Prasertsri and Rattanasom (2012). They found that scorch time of silica filled NR gradually reduced with increasing silica loading due to the effect of the moisture-treated silanol groups on silica surfaces and the hydrolysis of nitrogen-sulfur bonds of accelerators (TBBS and MBT) resulting in faster onset of crosslinking.

Mooney viscosities of NR and NR composites filled with silica nanoparticle are shown in Figure 4.9. NR composites showed higher viscosity than NR. The viscosity of silica nanoparticles/NR composites increased with silica nanoparticles content. This was attributed to the hydrodynamic effect of the filler aggregates that can obstruct the flow (Ansarifar and nuhawan, 2000). FD-silica/NR composites showed higher viscosity than HD-silica/NR composites due to high specific surface area of FD-silica leading to high filler-matrix interaction.

**Table 4.3** Cure characteristics and Mooney viscosity of NR and NR composites filled with FD-silica and HD-silica.

Formulation	Mooney viscosity (MU)	MH (dN-m)	ML (dN-m)	Time (min)	
				t <sub>s1</sub>	t <sub>90</sub>
NR	10.29	20.03	5.27	6.49	18.52
1 FD-silica/NR	18.04	33.49	12.90	9.27	19.54
1 HD-silica/NR	17.28	30.49	9.93	6.93	18.46
3 FD-silica/NR	20.10	36.50	12.96	10.16	19.91
3 HD-silica/NR	19.89	33.69	10.35	7.16	19.13
5 FD-silica/NR	22.11	36.69	15.35	12.28	20.45
5 HD-silica/NR	20.83	35.29	13.17	9.28	20.00
10 FD-silica/NR	26.28	38.35	17.15	14.44	21.33
10 HD-silica/NR	23.88	37.35	16.02	12.44	20.13

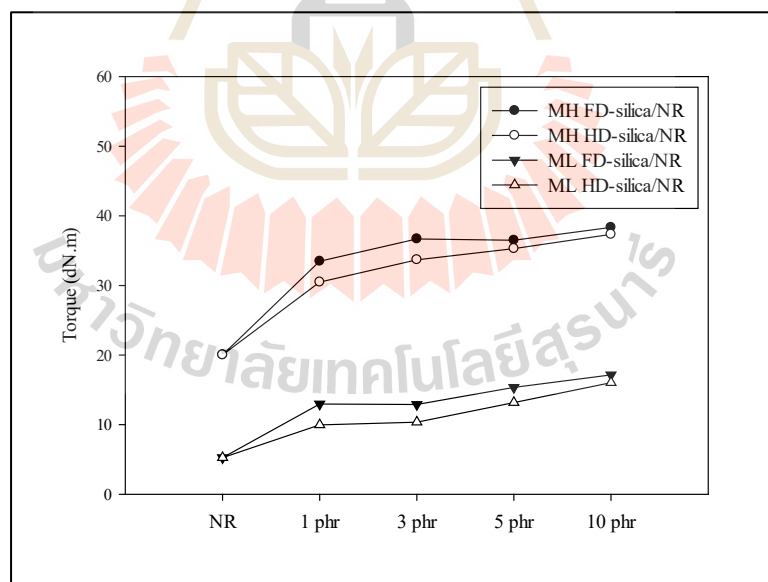


**Figure 4.7** Effect of silica nanoparticle content on maximum torque and minimum torque of NR composites

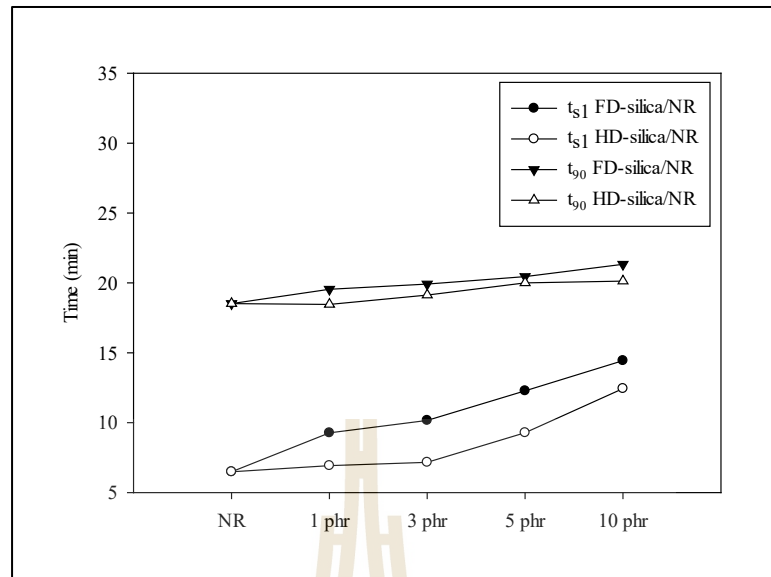


**Figure 4.8** Effect of silica nanoparticle content on scorch time and cure time of NR composites

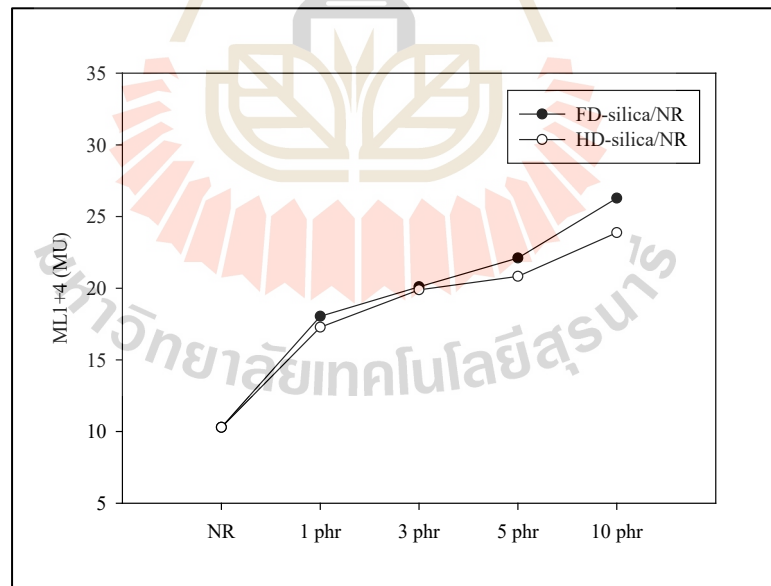


**Figure 4.9** Effect of silica nanoparticle content on Mooney viscosity of NR composites

### 4.3.2 Mechanical properties

Mechanical properties of NR and NR composites filled with FD-silica and HD-silica are listed in Table 4.4.

#### 4.3.2.1 Tensile properties

Modulus at 100% elongation (M100) and modulus at 300% elongation (M300) of NR and NR composites filled with FD-silica and HD-silica are shown in Figure 4.10 and Figure 4.11, respectively. As expected, M100 and M300 of NR composites continuously increased with increasing silica content. This may be because silica nanoparticles reduced the elasticity of NR molecular chain leading to increased stiffness of composites (Sarkawi and Aziz, 2003). A reduction of elongation at break of NR composites was found as shown in Figure 4.12. FD-silica/NR composites showed higher M100, M300 and elongation at break than HD-silica/NR composites because FD-silica had higher specific surface area and high porosity than HD-silica leading to high filler-matrix interaction of the composites. Huabcharoen et al. (2017) also reported that tensile modulus of silica/NR composites was increased while elongation at break was decreased with increasing silica content due to the naturally high rigidity of the silica particles.

Tensile strength of NR and NR composites are shown in Figure 4.13. The incorporation of silica nanoparticles at contents of 1, 3 and 5 phr resulted in improved tensile strength of NR composites. Whereas, at 10 phr of silica nanoparticles, tensile strength of FD-silica/NR and HD-silica composites were reduced due to the filler-filler interaction between segregated networks. This led to prevention of molecular diffusion between the natural rubber chains. On the other hand, at low content of silica, silica nanoparticles well dispersed in natural rubber matrix resulted in

the formation of thin filler network around NR chains. Crosslinks between NR chains along with diffusion across NR led to reinforcement. Arayapranee et al. (2005) reported that tensile strength of silica filled natural rubber increased with filler loading until a maximum level reached at 30 phr and then the tensile strength started to decrease with increasing filler loading due to the agglomeration of filler.

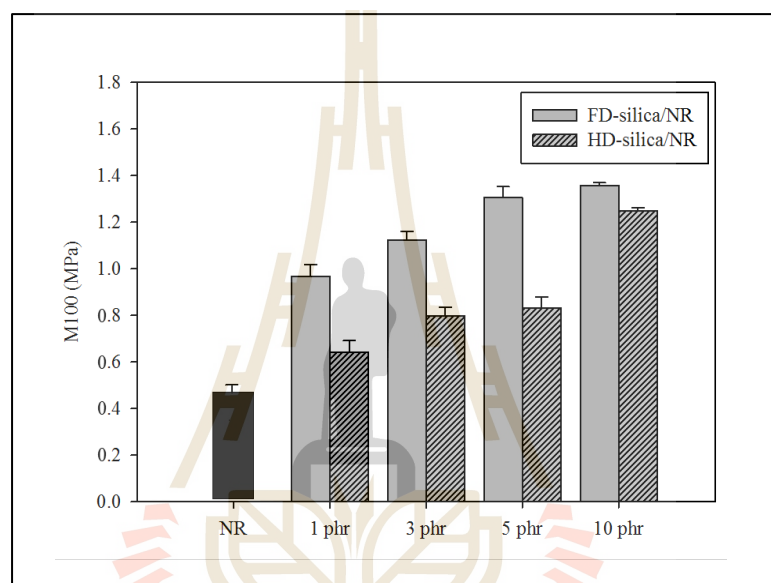


**Figure 4.10** Effect of silica nanoparticle content on modulus at 100% elongation of NR composites

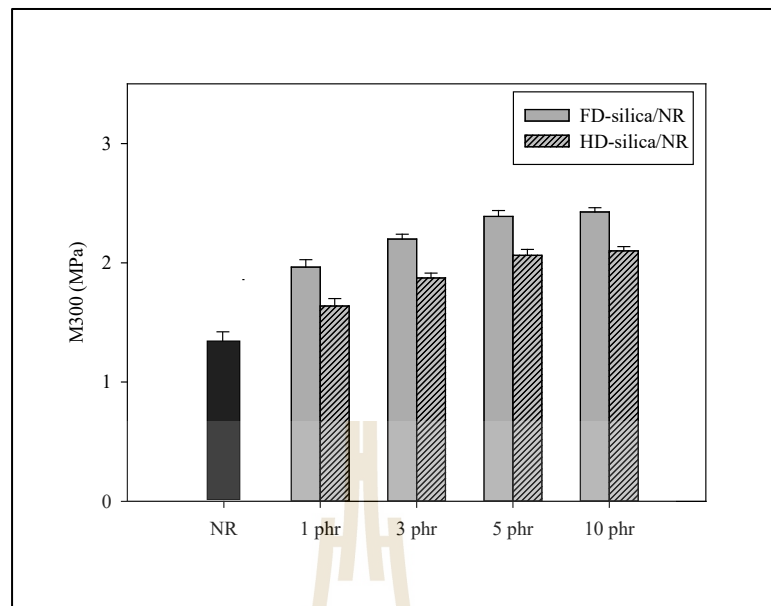


**Figure 4.11** Effect of silica nanoparticle content on modulus at 300% elongation of NR composites

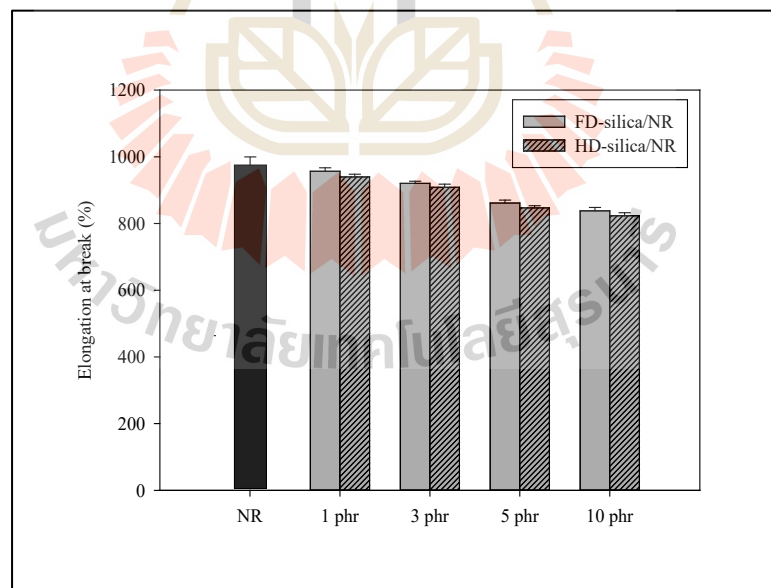


**Figure 4.12** Effect of silica nanoparticle content on elongation at break of NR composites

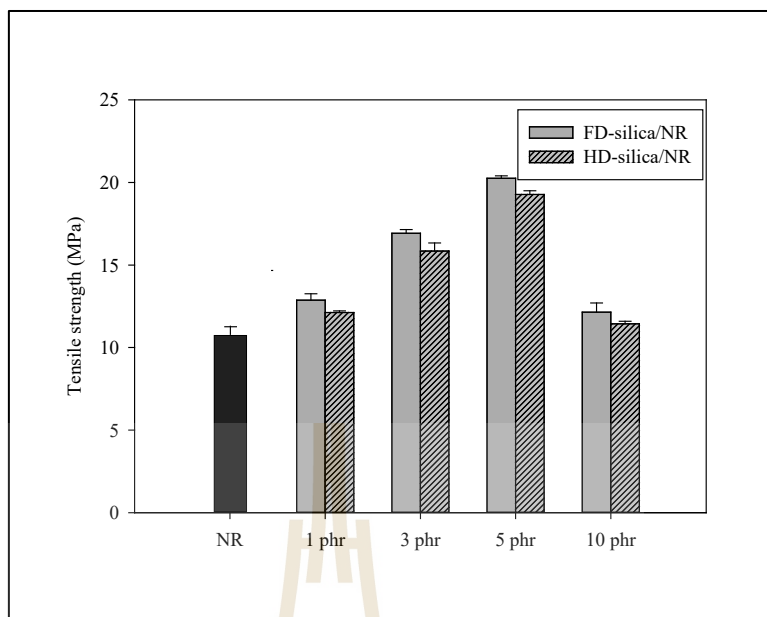


**Figure 4.13** Effect of silica nanoparticle content on tensile strength of NR composites

#### 4.3.2.2 Tear properties

Tear strength of NR and NR composites filled with FD-silica and HD-silica are shown in Figure 4.14. The incorporation of silica nanoparticles at content of 1, 3 and 5 phr improved tear strength of NR composites. However, with adding 10 phr of silica nanoparticles tear strength of the composites insignificantly changed. At low content of silica, silica nanoparticles well dispersed in natural rubber matrix leading to the formation of thin filler network around NR chains. Crosslinks between NR chains along with diffusion across NR led to reinforcement. (Francis et al., 2007; Arun et al., 2010). FD-silica/NR composites showed higher tear strength than HD-silica/NR composites due to high interaction between FD-silica and NR.

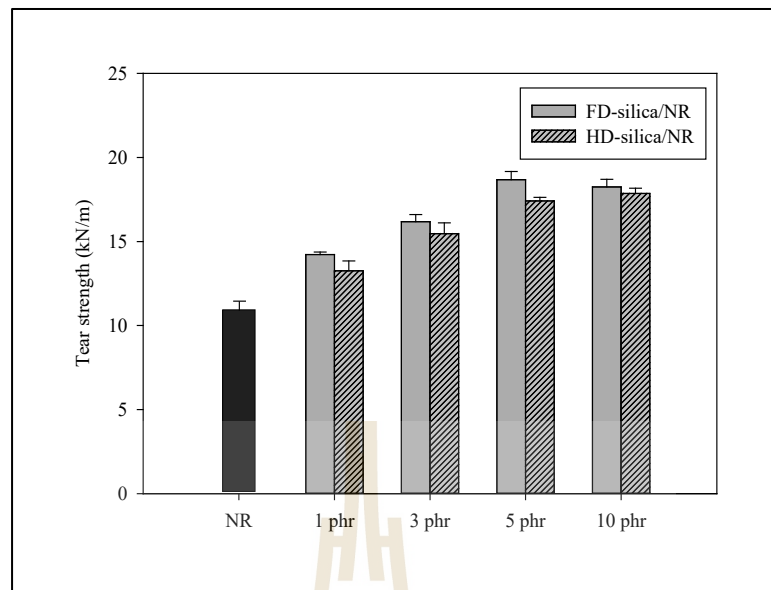


**Figure 4.14** Effect of silica nanoparticle content on tear strength of NR composites

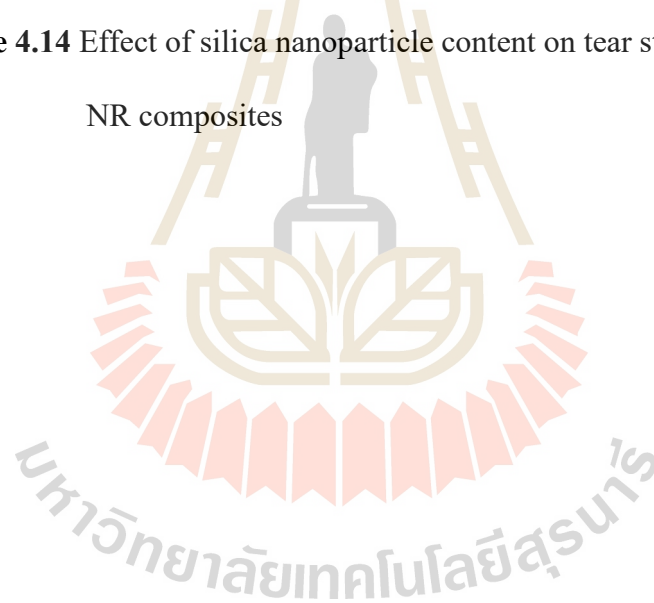




**Table 4.4** Mechanical properties of NR and NR composites filled with FD-silica and HD-silica

<b>Formulation</b>	<b>M100 (MPa)</b>	<b>M300 (MPa)</b>	<b>Tensile strength (MPa)</b>	<b>Elongation at break (%)</b>	<b>Hardness (Shore A)</b>	<b>Tear strength (kN/m)</b>
NR	0.48±0.05	1.35±0.08	10.73±0.54	987.15±15.23	33.78±1.14	10.97±0.12
1 FD-silica/NR	0.97±0.05	1.96±0.06	12.88±0.38	956.51±10.60	40.92±1.30	14.23±0.15
1 HD-silica/NR	0.64±0.05	1.64±0.06	12.12±0.10	939.57±8.30	38.00±0.30	13.26±0.59
3 FD-silica/NR	1.12±0.04	2.20±0.04	16.92±0.23	920.55±6.30	42.85±1.02	16.18±0.42
3 HD-silica/NR	0.80±0.04	1.87±0.04	15.84±0.50	908.60±9.50	40.85±1.11	15.47±0.64
5 FD-silica/NR	1.31±0.05	2.39±0.05	20.25±0.15	861.61±8.80	47.80±1.14	18.68±0.49
5 HD-silica/NR	0.83±0.05	2.06±0.05	19.27±0.23	846.92±6.50	45.80±0.50	17.42±0.21
10 FD-silica/NR	1.36±0.01	2.42±0.04	12.14±0.56	838.12±10.10	49.55±1.28	18.25±0.45
10 HD-silica/NR	1.25±0.01	2.10±0.04	11.45±0.15	823.25±9.00	48.00±1.28	18.24±0.31

#### 4.3.2.3 Hardness

Hardness of NR composites continuously increased with increasing silica content as shown in Figure 4.15. This was because silica nanoparticles increased stiffness of composites (Sarkawi and Aziz 2003). FD-silica/NR composites showed higher hardness than HD-silica/NR composites due to higher specific surface area and high porosity of FD-silica leading to high filler-matrix interaction of the composites.

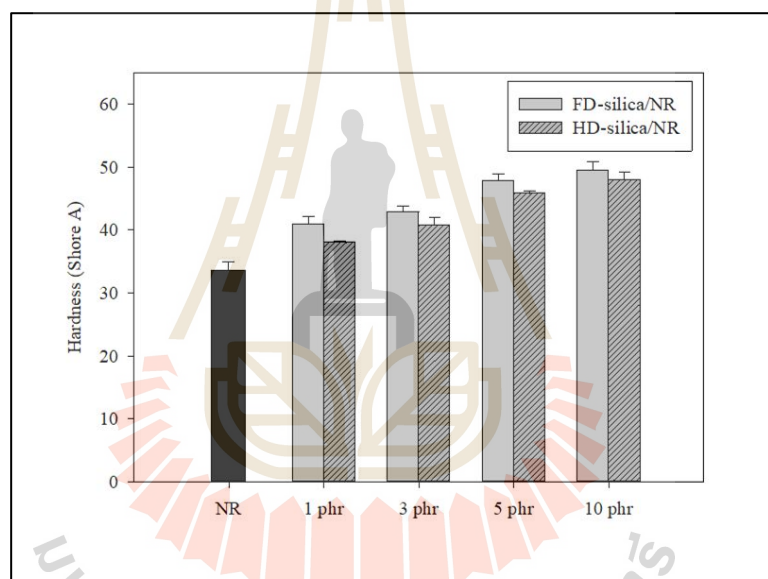


**Figure 4.15** Effect of silica nanoparticle content on hardness of NR composites

#### 4.3.3 Abrasion resistance

Abrasion resistance of material is the ability to resist mechanical rubbing or erosion. Abrasion resistance of NR and NR composites in term of volume loss (%) is displayed in Figure 4.16. The result revealed that at 1 and 3 phr of silica nanoparticles, the composites exhibited lower volume loss compared to NR due to high rubber-filler interaction and good dispersion of silica nanoparticles in NR matrix (Mathew and

Narayanankutty 2010). In the case of 5 and 10 phr of silica nanoparticles, volume loss of the composites was higher than that of NR due to silica agglomeration. (Tangudom et al., 2012). FD-silica/NR composites showed lower volume loss compared to HD-silica/NR composites due to higher specific surface area of FD-silica.

**Table 4.5** Volume loss and crosslink density of NR and NR composites filled with FD-silica and HD-silica

<b>Formulation</b>	<b>Volume loss (%)</b>	<b>Crosslink density (<math>\times 10^{-3}</math> mol/cm<sup>3</sup>)</b>
NR	110.04±0.20	5.16±0.06
1 FD-silica/NR	100.13±0.49	7.07±0.06
1 HD-silica/NR	102.86±0.65	6.69±0.06
3 FD-silica/NR	98.12±0.36	10.48±0.04
3 HD-silica/NR	101.12±0.42	9.33±0.04
5 FD-silica/NR	136.06±0.47	12.78±0.05
5 HD-silica/NR	139.55±0.76	9.96±0.05
10 FD-silica/NR	145.05±0.51	6.48±0.04
10 HD-silica/NR	152.07±0.75	5.96±0.04

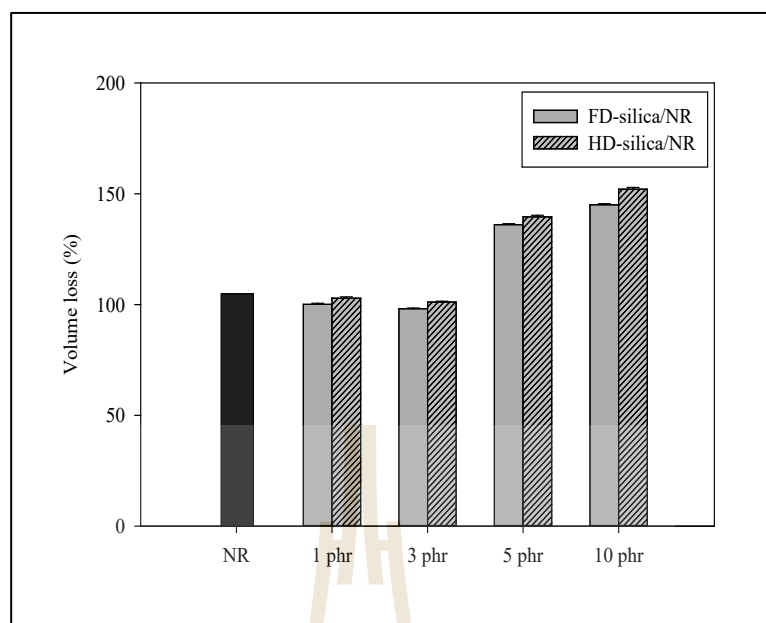


**Figure 4.16** Effect of silica nanoparticle content on volume loss of NR composites

#### 4.3.4 Crosslink density

Crosslink density of NR and NR composites with different silica nanoparticle contents is represented in Figure 4.17. Mechanical properties of rubber vulcanizate e.g. modulus and hardness are directly proportional to crosslink density of the composites (Sae-oui et al., 2006). From Figure 4.17 crosslink density of the composites increased with increasing silica nanoparticle content up to 5 phr and decreased at 10 phr of silica nanoparticles. FD-silica/NR composites showed higher crosslink density than HD-silica/NR composites due to high ability of dispersion of silica nanoparticles in NR matrix. Crosslink density of the composites reduced at high silica nanoparticle content because the filler-filler interaction between segregated networks led to prevent molecular diffusion between the natural rubber chains. However, Thongpin et al., (2011) reported that the increasing Si-Gel content resulted in

decreased crosslink density of NR composites. This was because high polarity and high porosity of Si-Gel retarded the vulcanization process.

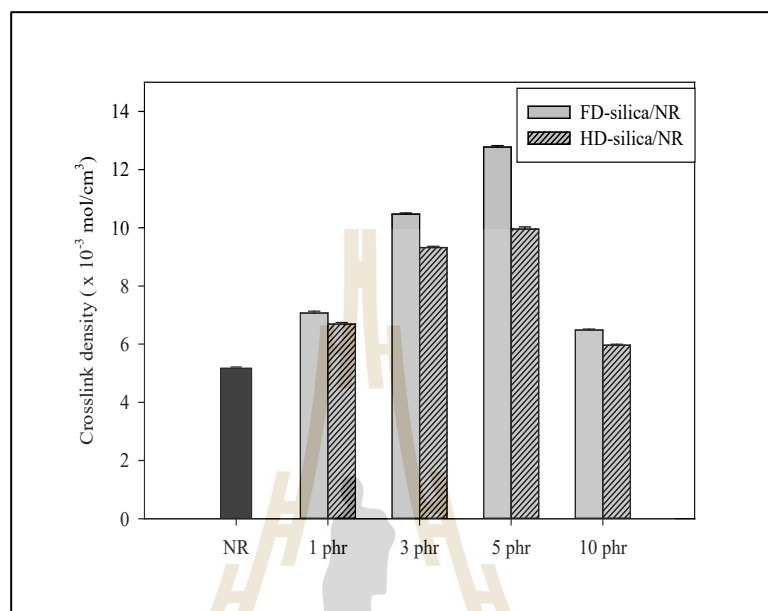


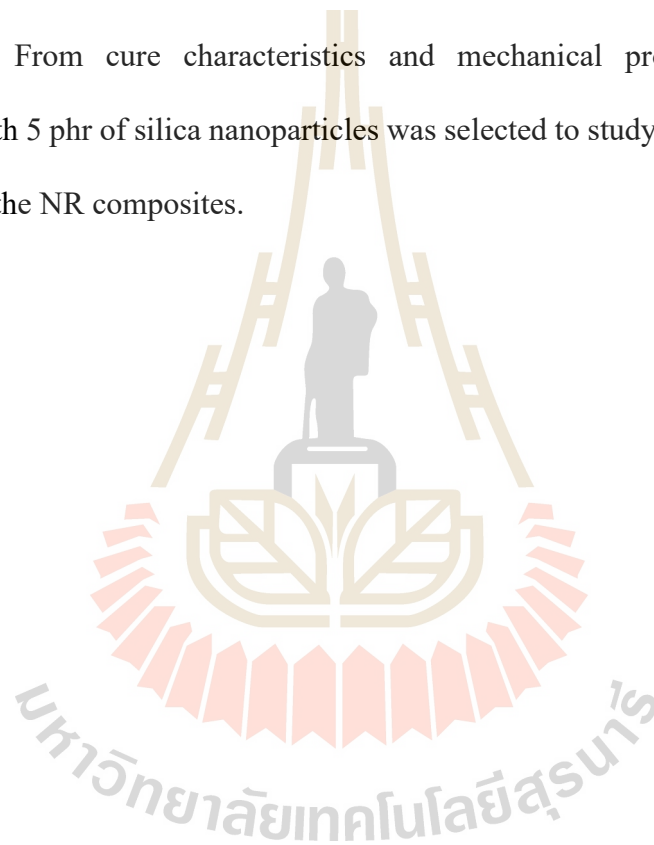
**Figure 4.17** Effect of silica nanoparticle content on crosslink density of NR composites

#### 4.3.5 Morphology

Tensile fractured surface of NR and NR composites are shown in Figure 4.18. The fractured surface of NR showed smooth surface. Filler dispersion significantly affects the performance and rubber-filler interaction of rubber composites. The good dispersion of filler in rubber matrix result in the enhancement of mechanical properties of rubber composites (Roy et al., 2019). With the addition of 1, 3 and 5 phr of silica nanoparticles into NR matrix, roughly and many layer surfaces were observed due to good dispersion of nanoparticles in NR (Bailly et al., 2010; Lay et al., 2013). This was corresponding with the improvement in tensile strength and tear strength of

the composites. Good dispersion of silica in rubber matrix led to high interaction between silica and rubber (Yin et al., 2013). Agglomerate formation was found in NR composite filled with 10 phr of FD-silica nanoparticles and HD-silica nanoparticles due to high filler-filler interaction. Moreover, the smooth surface with micropores was found in NR composite filled with 10 phr of FD-silica nanoparticles and HD-silica nanoparticles.

From cure characteristics and mechanical properties results, NR composite with 5 phr of silica nanoparticles was selected to study effect of Si-69 on the properties of the NR composites.



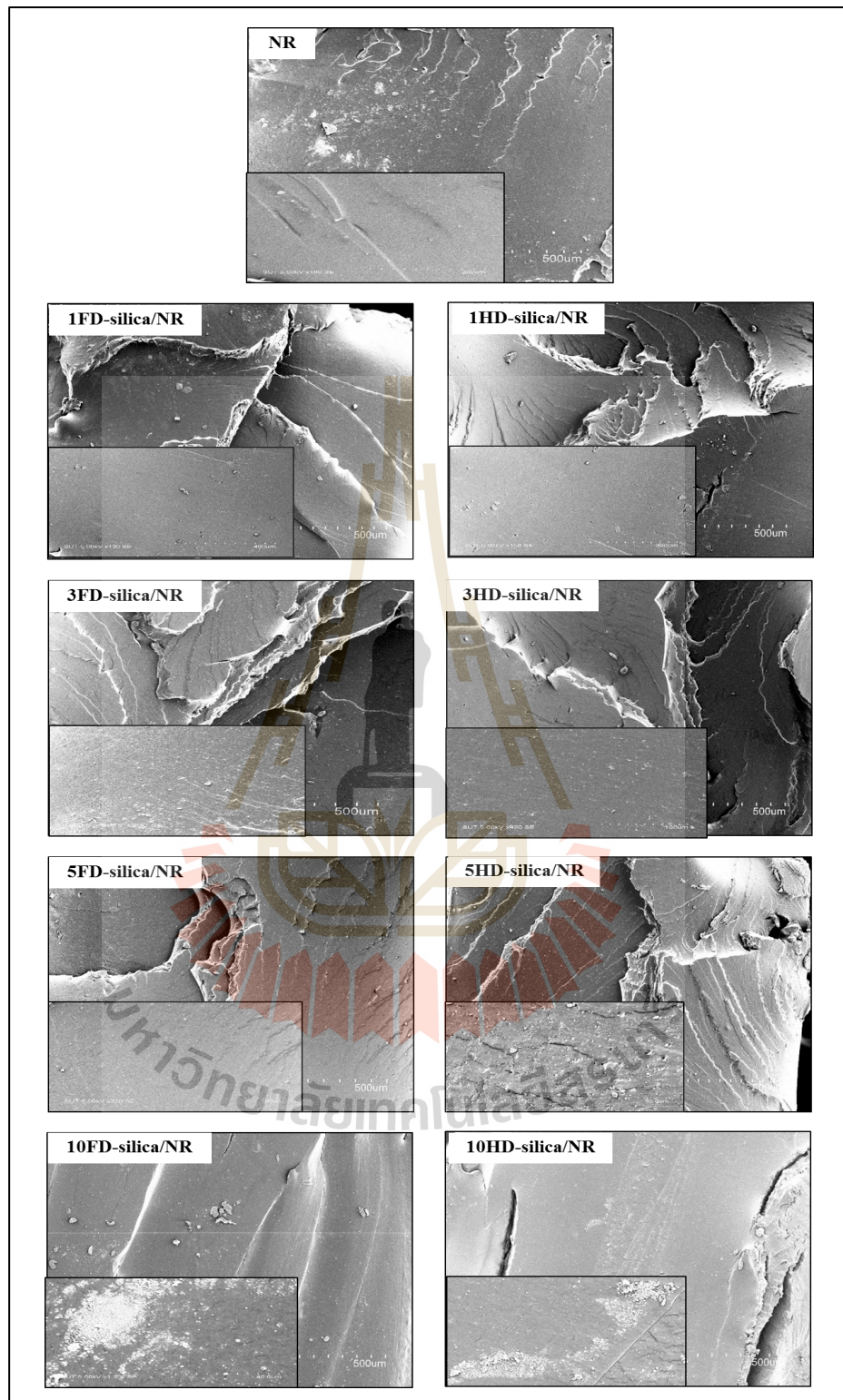


**Figure 4.18** SEM images of tensile fractured surface at 100X and 10000X of NR and NR composites



## 4.4 Effect of Si-69 on properties of silica nanoparticles/NR composites

### 4.4.1 Cure characteristics and Mooney viscosity

Maximum torque, minimum torque, scorch time and cure time of NR and NR composites with and without Si-69 are listed in Table 4.5. Maximum torque and minimum torque of NR and NR composites are displayed in Figure 4.19. The incorporation of Si-69 increased MH and ML of the composites due to improved compatibility between silica nanoparticles and NR matrix and good dispersion of silica nanoparticles in NR matrix. Si-69 possesses two functionally active end groups which can chemically react with both silica and rubber. The hydrolysable alkoxy group can react with silanol group on silica surface to form stable siloxane linkages. The other end group is organo-functional group can participate in sulfur vulcanization leading to chemical linkage with the rubber (Sae-Oui et al., 2005). Their salinization mechanism resulted in improve dispersion of silica nanoparticles in NR matrix (Reuvekamp et al., 2002; Ten Brinke et al., 2003; Sae-Oui et al., 2005). FD-silica/NR/Si-69 composite showed higher MH and ML than HD-silica/NR/Si-69 composite because of high specific surface area of FD-silica leading to high filler-matrix interaction. Adding Si-69 led to decrease in scorch time and cure time of NR composites as shown in Figure 4.20. Katueangngan et al. (2016) reported that the ethoxy groups of Si-69 were hydrolyzed to form a hydroxyl group which underwent condensation reaction with silanol groups on silica surface resulting in less adsorption of accelerator. Thus, shorter scorch and cure time of silica/NR/Si-69 composite were found. FD-silica/NR/Si-69 composite showed longer scorch time and cure time than those of HD-silica/NR/Si-69 composite. This may



be due to higher specific surface area of FD-silica surface resulted in high active surface and high absorption of chemicals in vulcanization process.

Mooney viscosity of NR and NR composites filled with silica nanoparticles are shown in Figures 4.21. As expected, the silica nanoparticles/NR composites without Si-69 showed higher Mooney viscosity compared to silica nanoparticles/NR composites with Si-69 because of the strong filler-filler interactions via hydrogen bonding of the silanol groups on the silica surfaces. This resulted in poor dispersion and large agglomerates of silica nanoparticles (Choi 2001). The incorporation of Si-69 improved silica dispersion in NR matrix, consequently, the Mooney viscosity of the composites was reduced (Choi 2001). FD silica/NR/Si-69 composite showed insignificant difference in Mooney viscosity when compared to HD silica/NR/Si-69 composite.

**Table 4.6** Cure characteristics and Mooney viscosity of NR and NR composites filled with FD-silica and HD-silica with and without Si-69.

Formulation	Mooney viscosity (MU)	MH (dN-m)	ML (dN-m)	Time (min)	
				t <sub>s1</sub>	t <sub>90</sub>
NR	10.29	20.03	5.27	6.49	18.52
5 FD-silica/NR	22.11	36.50	15.35	12.28	20.45
5 HD-silica/NR	20.83	35.29	13.17	9.28	20.00
5 FD-silica/NR/Si-69	17.17	38.53	16.47	9.13	18.17
5 HD-silica/NR/Si-69	16.90	37.17	15.43	9.16	17.56

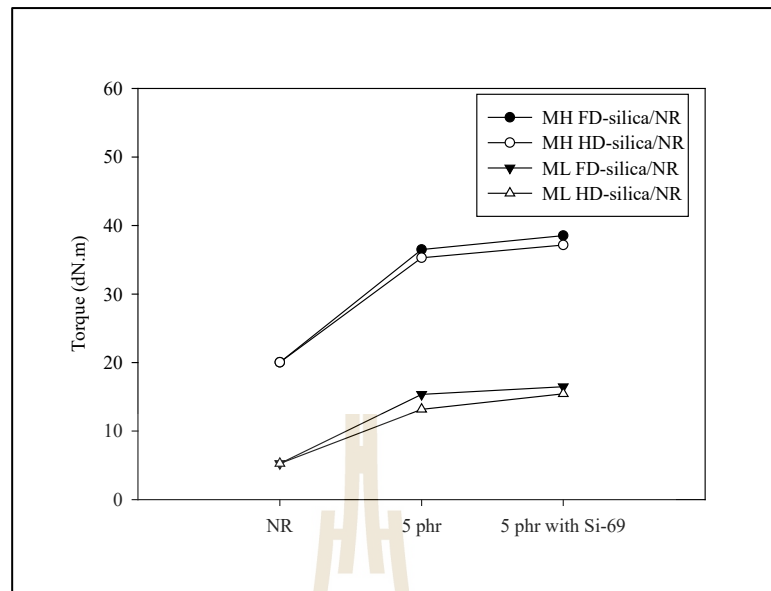


**Figure 4.19** Effect of Si-69 on maximum torque and minimum torque of NR composites filled with FD-silica and HD-silica

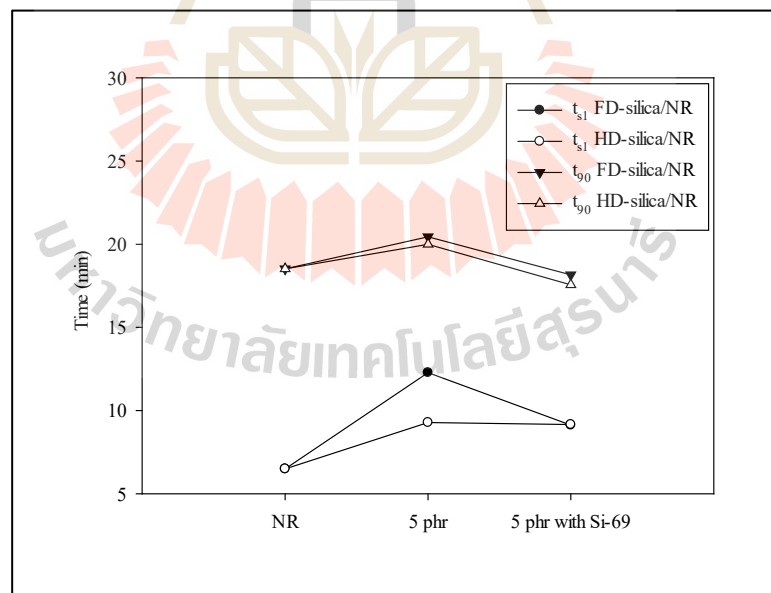


**Figure 4.20** Effect of Si-69 on scorch time and cure time of NR composites filled with FD-silica and HD-silica

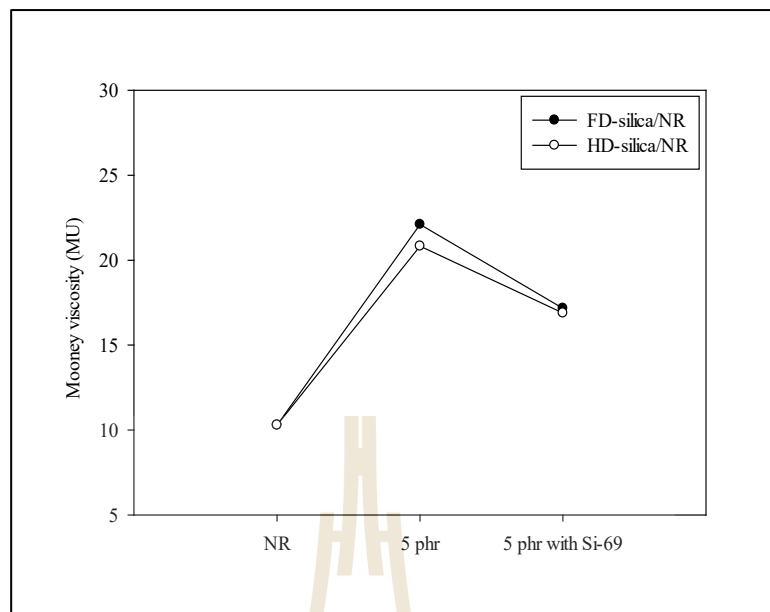


**Figure 4.21** Effect of Si-69 on Mooney viscosity of NR composites filled with FD-silica and HD-silica

#### 4.4.2 Mechanical properties

##### 4.4.2.1 Tensile properties

Modulus at 100% elongation, modulus at 300% elongation and tensile strength of NR and silica nanoparticles/NR composites with and without Si-69 are shown in Figure 4.22, 4.23 and 4.25, respectively. M100, M300 and tensile strength of silica nanoparticles/NR composites increased with the presence of Si-69 due to the improvement of the compatibility between silica nanoparticles and natural rubber. The hydrolysable alkoxy group of Si-69 can react with silanol group on silica surface to form stable siloxane linkages. Moreover, the organo-functional group of Si-69 can participate in sulfur vulcanization leading to chemical linkage with the rubber (Sae-Oui et al., 2005). The salinization mechanism resulted in improved adhesion and dispersion of silica nanoparticles in NR matrix. However, Si-69 showed insignificant effect on

elongation at break of the composites as shown in Figure 4.24. Sengloyluan et al. (2013) reported that the addition of Si-69 into silica/NR composites improved modulus and tensile strength of the composites because the silica/NR composites with Si-69 had a good silica dispersion and silica-to-rubber bonding via the silane molecule. FD-silica/NR/Si-69 composite showed higher M100, M300, tensile strength, and elongation at break than HD-silica/NR/Si-69 composite because FD-silica had higher specific surface area and high porosity than HD-silica leading to high filler-matrix interaction of the composites.

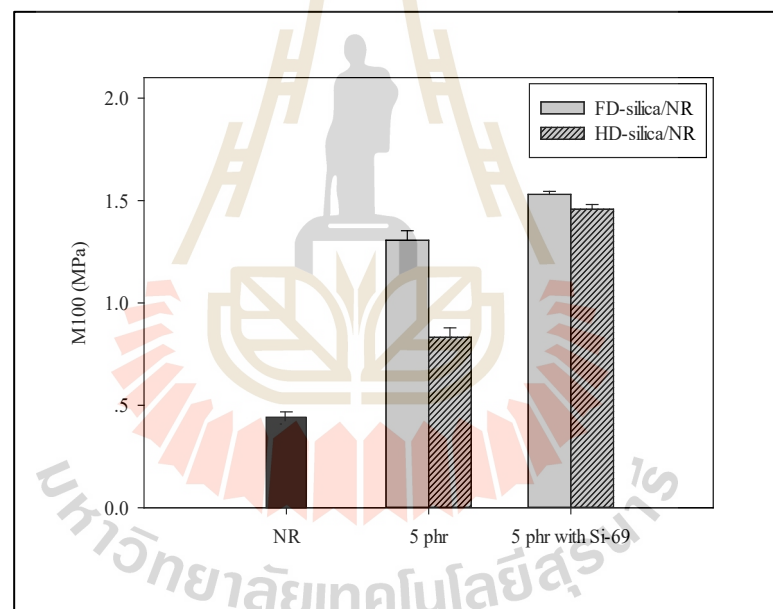


**Figure 4.22** Effect of Si-69 on modulus at 100% elongation of NR composites filled with FD-silica and HD-silica

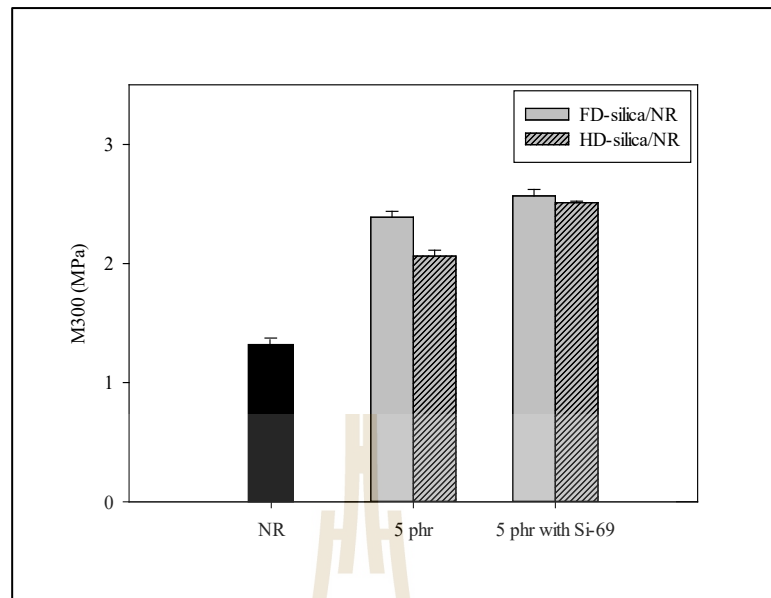


**Figure 4.23** Effect of Si-69 on modulus at 300% elongation of NR composites filled with FD-silica and HD-silica

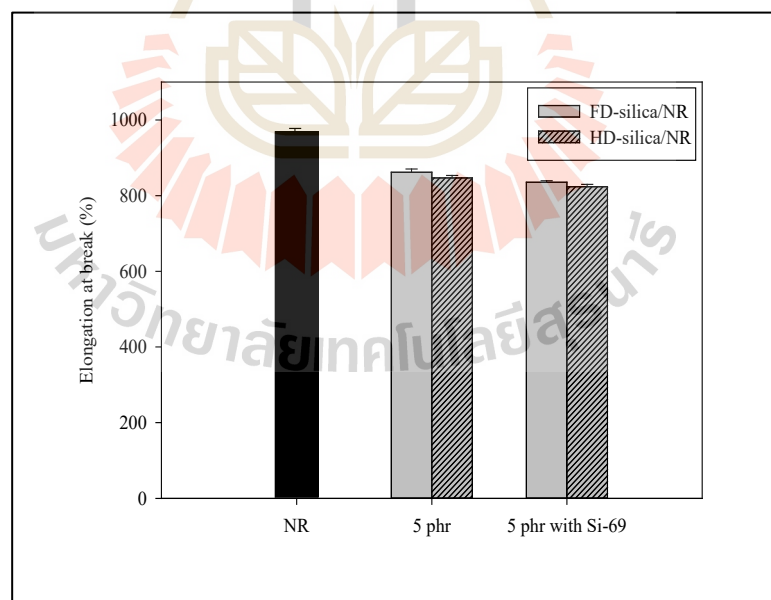


**Figure 4.24** Effect of Si-69 on elongation at break of NR composites filled with FD-silica and HD-silica

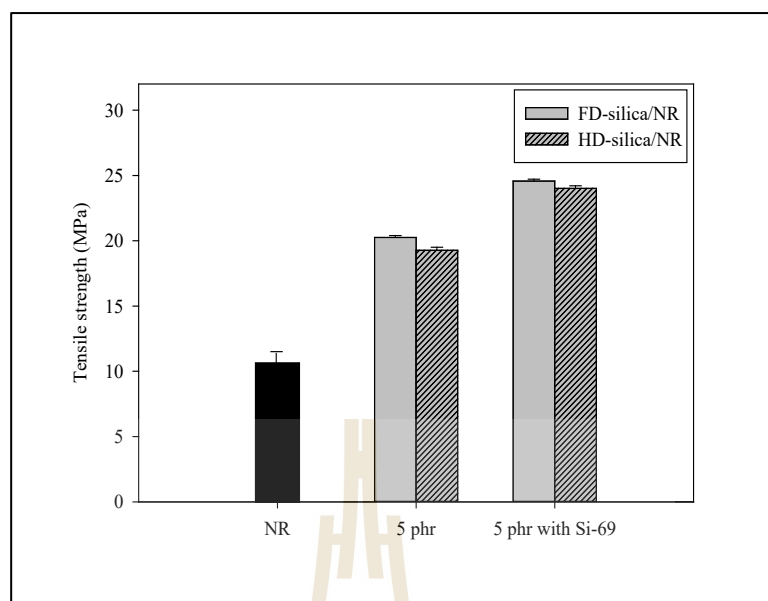


**Figure 4.25** Effect of Si-69 on tensile strength of NR composites filled with FD-silica and HD-silica

#### 4.4.2.2 Tear properties

Tear strength of NR composites was affected by filler-rubber adhesion, particle size, and surface area of the filler (Ishak and Bakar, 1995). The addition of Si-69 increased tear strength of silica nanoparticles/NR composites as shown in Figure 4.26. This was because the incorporation of Si-69 improved the compatibility of silica and natural rubber (Sae-oui et al., 2005, Rahman and Padavettan 2012). FD-silica/NR/Si-69 composites showed higher tear strength than HD-silica/NR/Si-69 composites due to high interaction between FD-silica and NR.

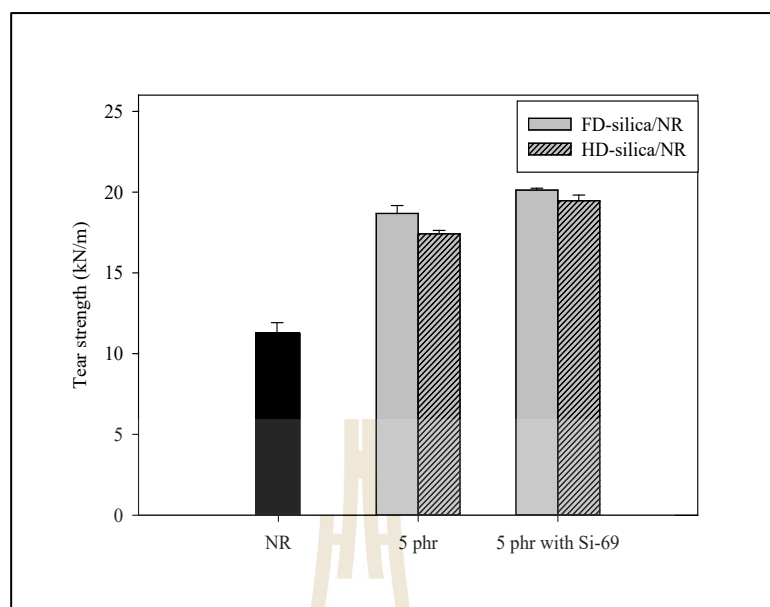


**Figure 4.26** Effect of Si-69 on tear strength of NR composites filled with FD-silica and HD-silica

#### 4.4.2.3 Hardness

Hardness of NR and silica nanoparticles/NR composites with and without Si-69 are shown in Figure 4.27. Hardness of silica nanoparticles/NR composites increased with the incorporation of Si-69 because of improved compatibility of silica and natural rubber. FD-silica/NR/Si-69 composite showed higher hardness than HD-silica/NR/Si-69 composite due to higher specific surface area and high porosity of FD-silica leading to high filler-matrix interaction of the composites.

**Table 4.7** Mechanical properties of NR and NR composites filled with FD-silica and HD-silica with and without Si-69

<b>Formulation</b>	<b>M100 (MPa)</b>	<b>M300 (MPa)</b>	<b>Tensile strength (MPa)</b>	<b>Elongation at break (%)</b>	<b>Hardness (Shore A)</b>	<b>Tear strength (kN/m)</b>
NR	0.48±0.05	1.35±0.08	10.73±0.54	987.15±15.24	33.78±1.14	10.97±0.12
5 FD-silica/NR	1.31±0.05	2.39±0.05	20.25±0.15	861.61±8.80	47.80±1.14	18.68±0.49
5 HD-silica/NR	0.83±0.05	2.06±0.05	19.27±0.23	846.92±6.50	45.80±0.50	17.42±0.21
5 FD-silica/NR/Si-69	1.53±0.02	2.57±0.05	24.57±0.15	835.23±4.23	52.00±0.96	20.12±0.12
5 HD-silica/NR/Si-69	1.46±0.02	2.51±0.01	24.01±0.2	823.56±6.12	50.00±1.21	19.47±0.35





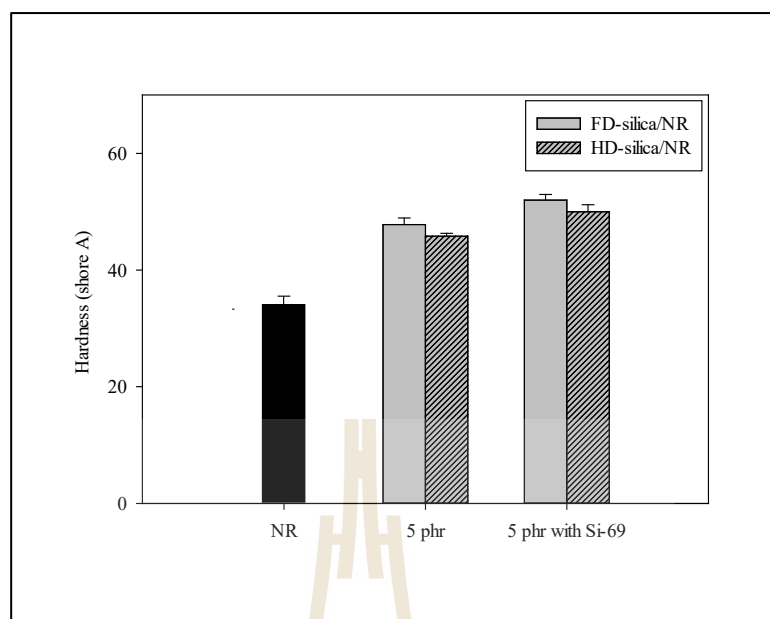


**Figure 4.27** Effect of Si-69 on hardness of NR composites filled with FD-silica and HD-silica

#### 4.4.3 Abrasion resistance

Volume loss of NR and silica nanoparticles/NR composites with and without Si-69 are shown in Figure 4.28. The composites with Si-69 showed less volume loss after abrasion test compared to silica nanoparticles/NR composites without Si-69. This was attributed to high interaction between silica nanoparticles and NR chains with the addition of Si-69. FD-silica/NR/Si-69 composite showed lower volume loss compared to HD-silica/NR/Si-69 composite due to higher specific surface area of FD-silica.

**Table 4.8** Volume loss and crosslink density of NR and NR composites filled with FD-silica and HD-silica with and without Si-69

Formulation	Volume loss (%)	Crosslink density ( $\times 10^{-3}$ mol/cm <sup>3</sup> )
NR	110.04±0.20	5.16±0.06
5 FD-silica/NR	136.06±0.47	12.78±0.05
5 HD-silica/NR	139.55±0.76	9.96±0.05
5 FD-silica/NR with Si-69	117.82±0.12	28.83±0.05
5 HD-silica/NR with Si-69	125.53±0.45	32.08±0.05

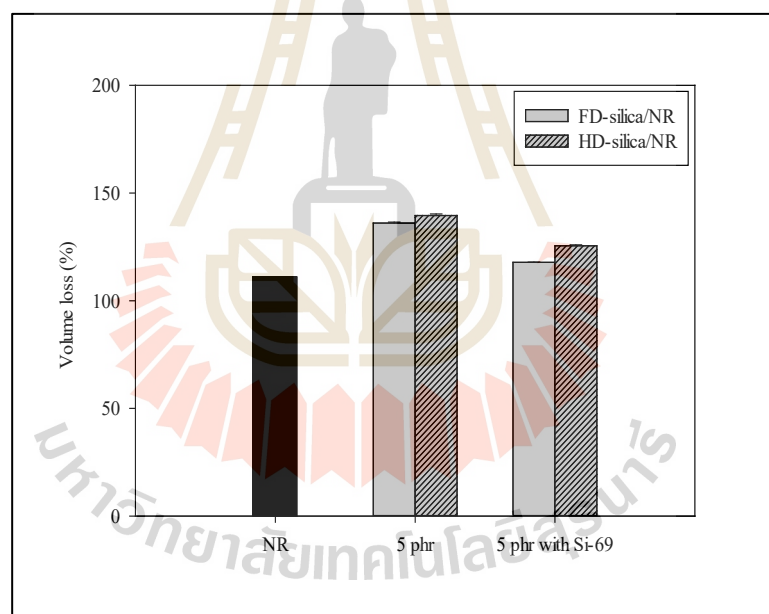


**Figure 4.28** Effect of Si-69 on volume loss of NR composites filled with FD-silica and HD-silica

#### 4.4.4 Crosslink density

The addition of Si-69 increased crosslink density of NR composites as shown in Figure 4.29. Si-69 might donate some of its sulfur to the compound to

implicitly raise the amount of free sulfur and consequently gave extra crosslinking (Sengloyluan et al., 2016). Thus, the results of M100, M300 and of the composites showed the same trend as the crosslink density results.

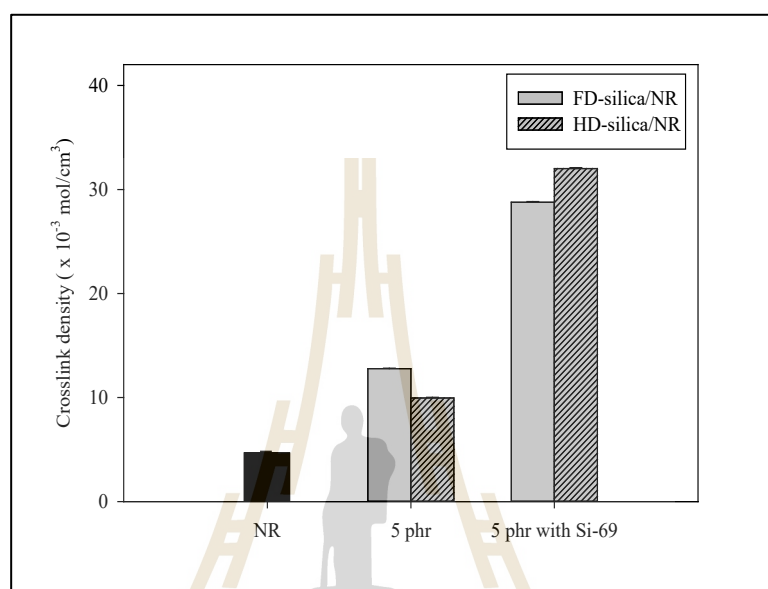


**Figure 4.29** Effect of Si-69 on crosslink density of NR composites filled with FD-silica and HD-silica

#### 4.4.5 Morphology

SEM images of the tensile fractured surface of NR and silica nanoparticles/NR composites with and without Si-69 are shown in Figure 4.30. Silica nanoparticles/NR composites without Si-69 had similar failure surfaces. However, Si-69 improved adhesion between silica nanoparticles and NR resulted in uniform distribution of silica nanoparticles, adhesive surface causing further enhancement in filler-rubber interaction (Alkadasi, 2006).

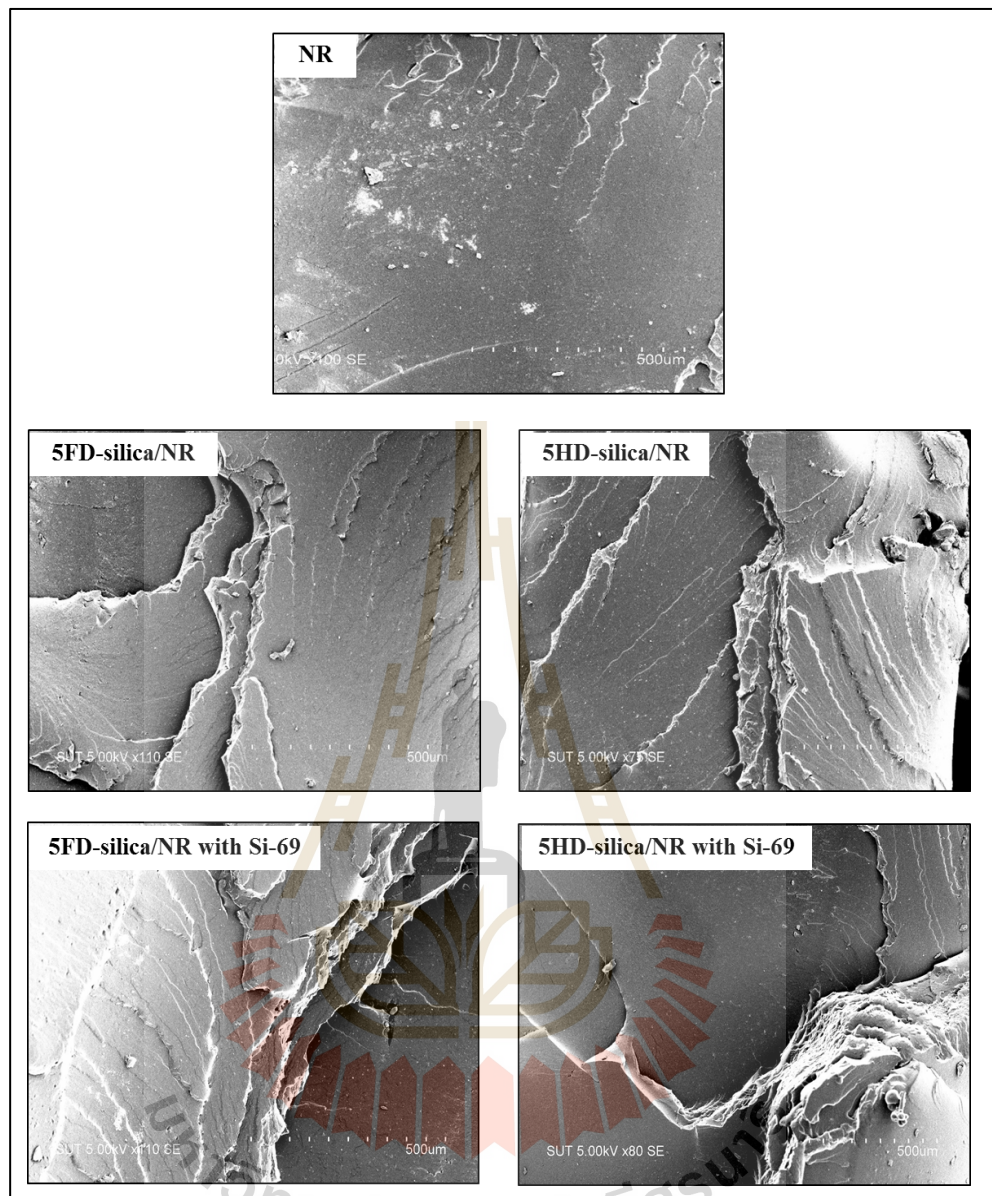


**Figure 4.30** SEM images at 100X of NR and NR composites filled with FD-silica and HD-silica with and without Si-69

# CHAPTER V

## CONCLUSIONS

### 5.1 Conclusions

Silica nanoparticles in the size range of  $90 \pm 10$  nm were successfully prepared from sugarcane bagasse ash in alkaline medium. FTIR spectra of prepared silica nanoparticles represented the absorption band at wavenumber 1091, 800 and  $467\text{ cm}^{-1}$  which confirmed silica characteristics. Silica nanoparticles with 98.8% and 98.5% purity were obtained from freeze dry and heat dry techniques, respectively. XRD diffraction patterns of FD-silica and HD-silica showed same broad peak in the range of  $15\text{-}30^\circ$  and centered at  $23^\circ$  attributed to amorphous structure of silica. Freeze drying technique provided silica nanoparticles with higher specific surface area and porosity than conventional heat drying technique due to slow removal of water through sublimation process.

The incorporation of both FD-silica and HD-silica nanoparticles into NR matrix increased MH and ML of the composites. MH and ML of the composites increased with increasing silica nanoparticle content due to an increment of stiffness of the composites and a reduction of the deformation of NR molecules. FD-silica/NR composites showed higher MH and ML compared to HD-silica/NR composites because of higher specific surface area of FD-silica leading to high filler-matrix interaction. Scorch time and cure time of NR composites increased with increasing silica nanoparticle content due to the

adsorption of accelerator in vulcanization process by silica surface. FD-silica/NR composites provided longer scorch time and cure time compared to HD-silica/NR composites due to higher specific surface area of FD-silica nanoparticles. This resulted in higher active surface and high absorption of chemicals in vulcanization process. Mooney viscosity of silica nanoparticles/NR composites increased with silica nanoparticle content. This was attributed to the hydrodynamic effect of the filler aggregates that obstructed the flow.

M100, M300 and hardness of NR composites were increased with increasing silica nanoparticle content while elongation at break was decreased. Tensile strength and tear strength of NR composites increased with silica nanoparticle content and tended to reduce at high silica nanoparticle content due to agglomerate formation of silica. Volume loss of the composites decreased at 1 and 3 phr of silica nanoparticle content and tended to increase at 5 and 10 phr of silica nanoparticle content due to silica agglomeration. Crosslink density of the composites increased with increasing silica nanoparticle loading and tended to decrease at silica nanoparticle of 10 phr. FD-silica/NR showed higher crosslink density compared to HD-silica/NR composites due to better ability of dispersion of FD-silica in NR matrix.

The fractured surface of NR showed smooth surface. With the addition of 1, 3 and 5 phr of silica nanoparticles into NR matrix, roughly and many layer surfaces were observed due to the strong interfacial adhesion between NR chains and silica nanoparticles. Agglomerate formation and micropores were found in NR composites filled with 10 phr of silica nanoparticles due to high filler-filler interaction which corresponded to a decrease in tensile strength.

The incorporation of Si-69 in to NR composites increased MH and ML of composites due to the improved compatibility between silica nanoparticles and NR matrix. FD-silica/NR/Si-69 composite showed higher MH and ML than HD-silica/NR/Si-69 composite due to high specific surface area of FD-silica. Scorch time and cure time of NR composites were reduced with adding Si-69. The ethoxy group of Si-69 was hydrolyzed to form a hydroxyl group which underwent condensation reaction with silanol groups on silica surface resulting in less adsorption of accelerator. The incorporation of Si-69 led to improved silica dispersion in NR matrix thus Mooney viscosity of the composites reduced.

M100, M300, tensile strength, hardness and tear strength of silica nanoparticles/NR composites were improved with the presence of Si-69. This was because the incorporation of Si-69 enhanced the compatibility of silica and natural rubber. Si-69 showed insignificant effect on elongation at break of the composites. FD-silica/NR/Si-69 composite showed higher M100, M300 tensile strength, hardness and tear strength than those of HD-silica/NR/Si-69 composite due to high surface area of FD-silica leading to high interaction between silica surface and NR matrix. The composites with Si-69 showed less of volume loss after abrasion test compared to silica nanoparticles/NR composites without Si-69. This was due to improved interaction between silica nanoparticles and NR chains. FD-silica/NR/Si-69 composites showed lower volume loss compared to HD-silica/NR/Si-69 composites due to higher specific surface area of FD-silica.

The addition of Si-69 increased crosslink density of NR composites. This was because Si-69 raised amount of free sulfur and gave extra crosslink. Si-69 improved



adhesion between silica nanoparticles and NR resulted in uniform distribution of silica nanoparticles and high filler-rubber interaction.





## REFERENCES

- Affandi, S., Setyawan, H., Winardi, S., Purwanto, A., and Balgis, R. (2009). A facile method for production of high-purity silica xerogels from bagasse ash. **Advanced Powder Technology**. 20(5): 468-472.
- Ahmed, K., Nizami, S. S., and Riza, N. Z. (2014). Reinforcement of natural rubber hybrid composites based on marble sludge/silica and marble sludge/rice husk derived silica. **Journal of Advanced Research**. 5(2):165-173.
- Alay, S. O., Dare, E. O., Ayinde, W. B., Bamigbose, J., Ayedun, P. A., and Osinkolu, G. A. (2012). Development of ordered and disordered macroporous silica from bagasse ash. **African Journal of Pure and Applied Chemistry**. 6(1): 10-14.
- Alkadasi, N. A. (2006). Effect of silane coupling agent on the mechanical properties of flyash-filled natural rubber. **Journal of Rubber Research**. 9(2): 96-107.
- Alves, R. H., Reis, T. V. d. S., Rovani, S., and Fungaro, D. A. (2017). Green synthesis and characterization of biosilica produced from sugarcane waste ash. **Journal of Chemistry**. 2017: 1-9.
- Ansarifar, M. A., and Nijhawan, R. (2000). Effects of silane on properties of silica filled natural rubber compounds. **Journal of Rubber Research**. 3(3): 169-184.
- Arayapranee, W., Na-Ranong, N., and Rempel, G. L. (2005). Application of rice husk ash as fillers in the natural rubber industry. **Journal of Applied Polymer Science**. 98(1): 34-41.

- Arun, K. J., Francis, P. J., and Joseph, R. (2010). Mechanical properties of nr latex-nano silica composites. **Journal of Optoelectronics and Advanced Materials**. 4(10): 1520-1525.
- Bailly, M., Kontopoulou, M., and El Mabrouk, K. (2010). Effect of polymer/filler interactions on the structure and rheological properties of ethylene-octene copolymer/nanosilica composites. **Polymer**. 51(23): 5506-5515.
- Chen, G., and Wang, W. (2007). Role of freeze drying in nanotechnology. **Drying Technology**. 25(1): 29-35.
- Choi, S. S. (2001). Improvement of properties of silica-filled styrene-butadiene rubber compounds using acrylonitrile-butadiene rubber. **Journal of Applied Polymer Science**. 79(6): 1127-1133.
- Chuayjuljit, S., Eiumnoh, S., and Potiyaraj, P. (2001). Using silica from rice husk as a reinforcing filler in natural rubber. **Journal of Scientific Research Chulalongkorn University**. 26(2): 127-138.
- Chusilp, N., Jaturapitakkul, C., and Kiattikomol, K. (2009). Utilization of bagasse ash as a pozzolanic material in concrete. **Construction and Building Materials**. 23(11): 3352-3358.
- Cordeiro, G., Toledo Filho, R., and Fairbairn, E. M. R. (2010). Ultrafine sugar cane bagasse ash: high potential pozzolanic material for tropical countries. **Ibracon Structures and Materials Journal**. 3(1): 50-58.
- Faizul, C. P., Abdullah, C., and Fazlul, B. (2013). Review of extraction of silica from agricultural wastes using acid leaching treatment. **Advanced Materials Research**. 626: 997-1000.

- Flory, P. J. (1953). **Principles of Polymer Chemistry**. New York: Cornell University Press.
- Francis, L. F., Grunlan, J. C., Sun, J., and Gerberich, W. W. (2007). Conductive coatings and composites from latex-based dispersions. **Colloids and Surfaces A: Physicochemical and Engineering Aspects**. 311(1-3): 48-54.
- Geetha, D., Ananthiand A., and Ramesh PS. (2016). Preparation and characterization of silica material from rice husk ash-an economically viable method. **Journal of Pure and Applied Physics**. 4 (3): 20-26
- Ghorbani, F., Sanati, A. M., and Maleki, M. (2015). Production of silica nanoparticles from rice husk as agricultural waste by environmental friendly technique. **Environmental Studies of Persian Gulf**. 2(1): 56-65.
- Hariharan, V., and Sivakumar, G. (2013). Studies on synthesized nanosilica obtained from bagasse ash. **International Journal of Chemical Technology and Research**. 5(2): 1263-1266.
- Hench, L. L., and West, J. K. (1990). The sol-gel process. **Chemical Reviews**. 90(1): 33-72.
- Harish, P. R., Aru, A., and Ponnusami, V. (2015). Recovery of silica from various low cost precursors for the synthesis of silica gel. **Scholar Research Library**. 7(6): 208-213.
- Huabcharoen, P., Wimolmala, E., Markpin, T., and Sombatsompop, N. (2017). Purification and characterization of silica from sugarcane bagasse ash as a reinforcing filler in natural rubber composites. **BioResources**. 12(1): 1228-1245.

- Ishak, Z. M., and Bakar, A. A. (1995). An investigation on the potential of rice husk ash as fillers for epoxidized natural rubber (ENR). **European Polymer Journal**. 31(3): 259-269.
- Ismail, H., Mega, L., and Khalil, H. P. S. A. (2001). Effect of a silane coupling agent on the properties of white rice husk ash-polypropylene/natural rubber composites. **Polymer International**. 50(5): 606-611.
- Ismail, H., Edyham, M. R., and Wirjosentono, B. (2002). Bamboo fibre filled natural rubber composites: the effects of filler loading and bonding agent. **Polymer Testing**. 21(2): 139-144.
- Jafarzadeh, M., Rahman, I. A., and Sipaut, C. S. (2009). Synthesis of silica nanoparticles by modified sol-gel process: the effect of mixing modes of the reactants and drying techniques. **Journal of Sol-Gel Science and Technology**. 50(3): 328-336.
- Kanking, S., Thongsang, S., Sombatsompop, N., Sirisinha, C., and Wimolmala, E. (2011). Influences of bagasse ash source and silica content in bagasse ash on cure and mechanical properties of natural rubber composite. In **49<sup>th</sup> Kasetsart University Annual Conference** (pp. 89-95). Bangkok, Thailand.
- Katueangnan, K., Tulyapitak, T., Saetung, A., Soontaranon, S., and Nithi-uthai, N. (2016). Renewable interfacial modifier for silica filled natural rubber compound. **Procedia Chemistry**. 19: 447-454.
- Kickelbick, G. (2003). Concepts for the incorporation of inorganic building blocks into organic polymers on a nanoscale. **Progress in Polymer Science**. 28(1): 83-114.

- Kwon S. and Messing G. L., (1997). The effect of particle solubility on the strength of nanocrystalline agglomerates: boehmite. **Nanostructured Materials**. 8(4): 399-418.
- Lay, M., Azura, A. R., Othman, N., Tezuka, Y., and Pen, C. (2013). Effect of nanosilica fillers on the cure characteristics and mechanical properties of natural rubber composites. **Advanced Materials Research**. 626: 818-822.
- Lu, P., and Hsieh, Y. L. (2012). Highly pure amorphous silica nano-disks from rice straw. **Powder Technology**. 225: 149-155.
- Luo, Y. Y., Wang, Y. Q., Zhong, J. P., He, C. Z., Li, Y. Z., and Peng, Z. (2011). Interaction between fumed-silica and epoxidized natural rubber. **Journal of Inorganic and Organometallic Polymers and Materials**. 21(4): 777-783.
- Luo, Y., Feng, C., Wang, Q., Yi, Z., Qiu, Q., Lx, K., and Peng, Z. (2013). Preparation and characterization of natural rubber/silica nanocomposites using rule of similarity in latex. **Journal of Wuhan University of Technology-Mater**. 28(5): 997-1002.
- Manzano, I. R. L., Begum, N., and Noorliyana (2015). A silica extraction from sugarcane bagasse as green corrosion inhibitor. **Asian Transactions on Basic & Applied Sciences**. 5(5): 1-3
- Mathew, L., and Narayanankutty, S. K. (2010). Synthesis, characterisation and performance of nanosilica as filler in natural rubber compounds. **Journal of Rubber Research**. 13(1): 27-43.

- Mokhtar, H., and Tajuddin, R. M. (2016). The effect of nanosilica extracted from sugarcane bagasse on formulation of flat sheet nanofiltration membrane. **International Journal of Chemical Engineering and Applications**. 7(5): 323-326.
- Mohd, N. K., Wee, N. N. A. N., and Azmi, A. A. (2017). Green synthesis of silica nanoparticles using sugarcane bagasse. In **AIP Conference Proceedings**. (pp. 1-7). AIP Publishing.
- Murakami, K., Iio, S., Ikeda, Y., Ito, H., Tosaka, M., and Kohjiya, S. (2003). Effect of silane- coupling agent on natural rubber filled with silica generated in situ. **Journal of Materials Science**. 38(7): 1447-1455.
- Norsuraya, S., Fazlena, H., and Norhasyimi, R. (2016). Sugarcane bagasse as a renewable source of silica to synthesize santa barbara amorphous-15 (SBA-15). **Procedia Engineering**. 148: 839-846.
- Norsuraya, S., Norhasyimi, R., Fazlena, H. (2017). Characterization of sodium silicate derived from sugarcane bagasse ash. **Malaysian Journal of Analytical Sciences**. 21(2): 512-517.
- Prasertsri, S., and Rattanasom, N. (2012). Fumed and precipitated silica reinforced natural rubber composites prepared from latex system: mechanical and dynamic properties. **Polymer Testing**. 31(5): 593-605.
- Pongdong, W., Nakason, C., Kummerlöwe, C., and Vennemann, N. (2015). Influence of filler from a renewable resource and silane coupling agent on the properties of epoxidized natural rubber vulcanizates. **Journal of Chemistry**. 2015: 1-15.

- Rahman, I. A., Vejayakumaran, P., Sipaut, C. S., Ismail, J., and Chee, C. K. (2008). Effect of the drying techniques on the morphology of silica nanoparticles synthesized via sol-gel process. **Ceramics International**. 34(8): 2059-2066.
- Rahman, I. A., and Padavettan, V. (2012). Synthesis of silica nanoparticles by sol-gel: size-dependent properties, surface modification, and applications in silica-polymer nanocomposites-a review. **Journal of Nanomaterials**. 2012:1-15
- Rahmat, N., Hamzah, F., Sahiron, N., Mazlan, M., and Zahari, M. M. (2016). Sodium silicate as source of silica for synthesis of mesoporous SBA-15. In **IOP Conference Series: Materials Science and Engineering** (pp. 1-9). IOP Publishing.
- Rani, K. M., Palanisamy, P. N., and Sivakumar, P. (2014). Synthesis and characterization of amorphous nanosilica from biomass ash. **International Journal of Advanced Technology in Engineering and Science**. 2(10): 71-76.
- Rattanasom, N., Saowapark, T., and Deeprasertkul, C. (2007). Reinforcement of natural rubber with silica/carbon black hybrid filler. **Polymer Testing**. 26(3): 369-377.
- Reuvekamp, L. A., Ten Brinke, J. W., Van Swaaij, P. J., and Noordermeer, J. W. (2002). Effects of time and temperature on the reaction of TESPT silane coupling agent during mixing with silica filler and tire rubber. **Rubber chemistry and technology**, 75(2): 187-198.
- Roy, K., Debnath, S. C., and Potiyaraj, P. (2019). A critical review on the utilization of various reinforcement modifiers in filled rubber composites. **Journal of Elastomers & Plastics**. <http://doi.org/10.1177/0095244319835869>.

- Sae-Oui, P., Sirisinha, C., Hatthapanit, K., and Thepsuwan, U. (2005). Comparison of reinforcing efficiency between Si-69 and Si-264 in an efficient vulcanization system. **Polymer Testing**. 24(4): 439-446.
- Sae-Oui, P., Sirisinha, C., Thepsuwan, U., and Hatthapanit, K. (2006). Roles of silane coupling agents on properties of silica-filled polychloroprene. **European Polymer Journal**. 42(3): 479-486.
- Sahiron, N., Rahmat, N., and Hamzah, F. (2017). Characterization of sodium silicate derived from sugarcane bagasse ash. **Malaysian Journal of Analytical Sciences**. 21(2): 512-517.
- Sarkawi, S. S., and Aziz, Y. (2003). Ground rice husk as filler in rubber compounding. **Jurnal Teknologi**. 39: 135-148.
- Sarkawi, S. S., Aziz, A. K. C., Rahim, R. A., Ghani, R. A., and Kamaruddin, A. N. (2016). Properties of epoxidized natural rubber tread compound: the hybrid reinforcing effect of silica and silane system. **Polymers & Polymer Composites**. 24(9): 775-782.
- Santos, R. J. d., Agostini, D. L. d. S., Cabrera, F. C., Reis, E. A. P. d., Ruiz, M. R., Budemberg, E. R., and Job, A. E. (2014). Sugarcane bagasse ash: new filler to natural rubber composite. **Polímeros**. 24: 646-653.
- Sales, A., and Lima, S. A. (2010). Use of Brazilian sugarcane bagasse ash in concrete as sand replacement. **Waste Management**. 30(6): 1114-1122.
- Sarawade, P. B., Kim, J. K., Hilonga, A., Quang, D. V., and Kim, H. T. (2011). Effect of drying technique on the physicochemical properties of sodium silicate-based mesoporous precipitated silica. **Applied Surface Science**. 258(2): 955-961.

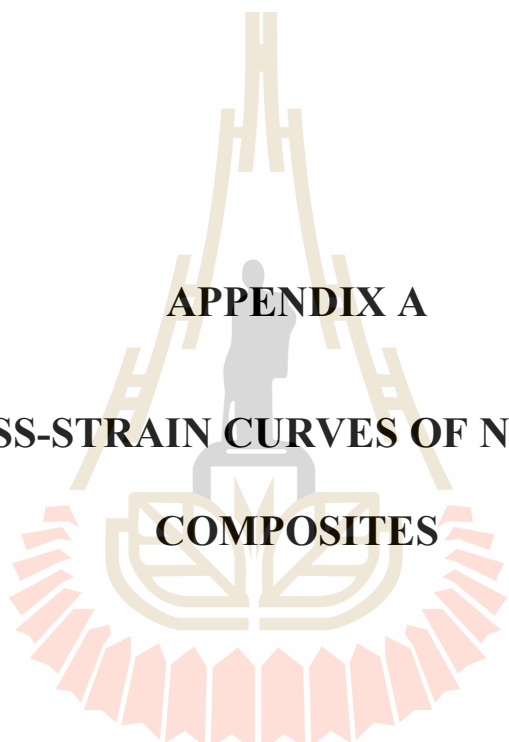


- Satha, H., Atamnia, K., and Despetis, F. (2013). Effect of drying processes on the texture of silica gels. **Journal of Biomaterials and Nanobiotechnology**. 4(1): 17-21.
- Schettino, M. A. S., and Holanda, J. N. F. (2015). Characterization of sugarcane bagasse ash waste for its use in ceramic floor tile. **Procedia Materials Science**. 8: 190-196.
- Sengloyluan, K., Sahakaro, K., K. Dierkes, W., and Noordermeer, J. (2013). Silica-reinforced tire tread compounds compatibilized by using epoxidized natural rubber. **European Polymer Journal**. 51: 69-79.
- Sengloyluan, K. (2015). Silica-reinforced natural rubber: use of natural rubber grafted with chemical functionalities as compatibilizer. [Ph.D. Dissertation]. University of Twente, Enschede, the Netherlands, and Prince of Songkla University, Pattani Campus, Thailand.
- Sengloyluan, K., Sahakaro, K., Dierkes, W. K., and Noordermeer, J. W. M. (2016). Reinforcement efficiency of silica in dependence of different types of silane coupling agents in natural rubber-based tire compounds. **KGK Kautschuk, Gummi, Kunststoffe**, 69(5): 44-53.
- Tangudom, P., Sombatsompop, N., and Thongsang, S. (2012). Cure characteristics and mechanical properties of rubbers filled with silica hybrid filler. **The 4<sup>th</sup> Science Research Conference**. Faculty of Science, Naresuan University, Thailand.
- Ten Brinke, J. W., Debnath, S. C., Reuvekamp, L. A., and Noordermeer, J. W. (2003). Mechanistic aspects of the role of coupling agents in silica-rubber composites. **Composites Science and Technology**, 63(8): 1165-1174.

- Theppradit, T., Prasassarakich, P., and Poompradub, S. (2014). Surface modification of silica particles and its effects on cure and mechanical properties of the natural rubber composites. **Materials Chemistry and Physics**. 148(3): 940-948.
- Thongpin, C., Sripethdee, C. and Rodsunthia, R. (2011). Cure characteristic, mechanical properties and morphology of in-situ silica-gel/NR composites. **18<sup>TH</sup> International Conference on Composite Materials**. Jeju Island, Korea.
- Wang, Y. Q., Wang, Q. H., Luo, Y. Y., Zhong, J. P., Li, Y. Z., He, C. Z., and Peng, Z. (2012). Role of epoxidized natural rubber in dynamic mechanical properties of NR/ENR/silica composites. **Advanced Materials Research**. 415: 415-419.
- Weichold, O., Tigges, B., Bertmer, M., and Möller, M. (2008). A comparative study on the dispersion stability of monofunctionalized silica nanoparticles made from sodium silicate. **Journal of Colloid and Interface Science**. 324(1-2): 105-109.
- Worathanakul, P., Payubnop, W., and Muangpet, A. (2009). Characterization for post-treatment effect of bagasse ash for silica extraction. **Engineering and Technology**. 56: 360-362.
- Xu, T., Jia, Z., Luo, Y., Jia, D., and Peng, Z. (2015). Interfacial interaction between the epoxidized natural rubber and silica in natural rubber/ silica composites. **Applied Surface Science**. 328: 306-313.
- Yin, C., Zhang, Q., Gu, J., Zheng, J., Gong, G., Liang, T., and Zhang, H. (2013). In situ silica reinforcement of vinyltriethoxysilane-grafted styrene-butadiene rubber by sol-gel process. **Journal of Applied Polymer Science**. 128(4): 2262-2268.
- Zheng, J., Han, D., Ye, X., Wu, X., Wu, Y., Wang, Y., and Zhang, L. (2017). Chemical and physical interaction between silane coupling agent with long arms and silica and its effect on silica/natural rubber composites. **Polymer**. 135: 200-210.

Zulfiqar, U., Subhani, T., and Husain, S. W. (2016). Synthesis of silica nanoparticles from sodium silicate under alkaline conditions. **Journal Sol-Gel Science. Technology**. 77(3): 753-758.





**APPENDIX A**  
**STRESS-STRAIN CURVES OF NR AND NR**  
**COMPOSITES**

มหาวิทยาลัยเทคโนโลยีสุรนารี

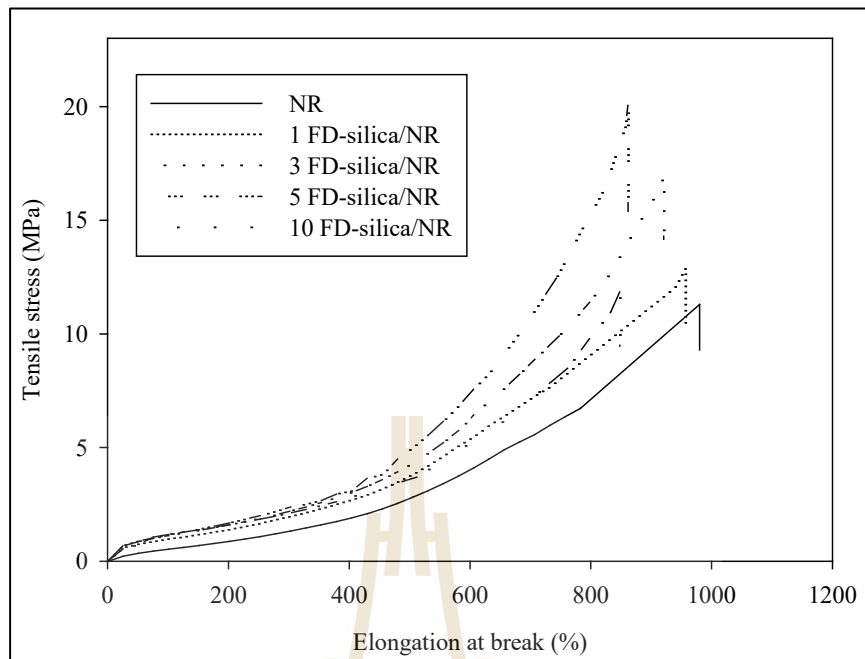


**Figure A.1** Stress-strain curves of NR and FD-silica/NR composites

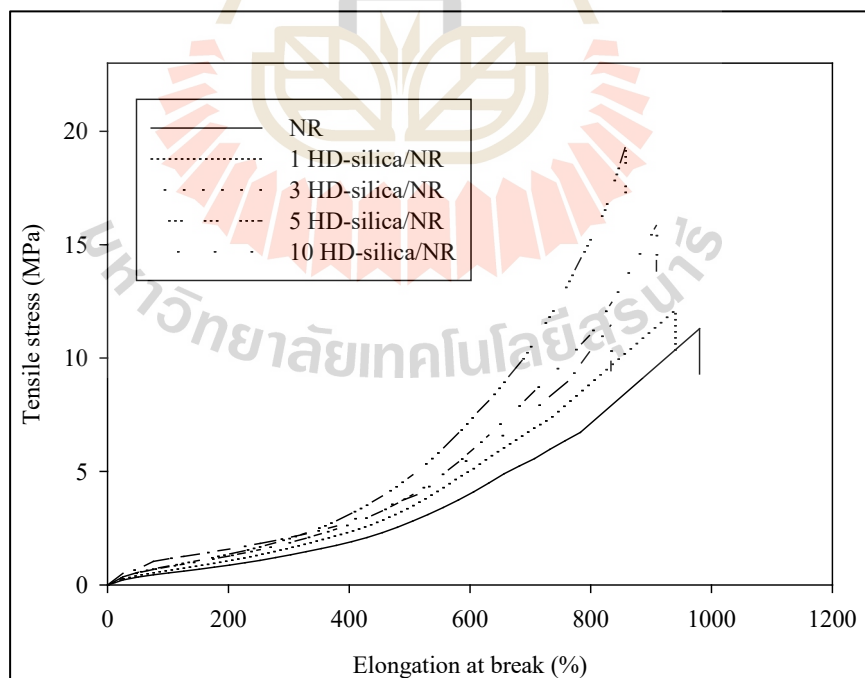


**Figure A.2** Stress-strain curves of NR and HD-silica/NR composites



**APPENDIX B**

**LIST OF PUBLICATION**

มหาวิทยาลัยเทคโนโลยีสุรนารี

## List of Publication

- Boonmee, A., and Jarukumjorn, K. (2019). Preparation and characterization of silica nanoparticles from sugarcane bagasse ash for using as a filler in natural rubber composites. *Polymer Bulletin*.
- Boonmee, A., and Jarukumjorn, K. (2019). Mechanical properties and cure characteristics of silica nanoparticles from sugarcane bagasse ash/natural rubber composites. In *Proceeding of The International Polymer Conference of Thailand*. 13-14 June, 2019. Bangkok, Thailand.
- Boonmee, A., Sabsiroht, P., and Jarukumjorn, K. (2019). Preparation and characterization of rice husk ash for using as a filler in natural rubber. *Materials Today: Proceedings*, 17, 2097-2103.
- Boonmee, A. and Jarukumjorn, K. (2019). Preparation and characterization of silica from sugarcane bagasse ash as filler in natural rubber. *Suranaree Journal of Science and Technology*.



## Preparation and characterization of silica nanoparticles from sugarcane bagasse ash for using as a filler in natural rubber composites

Anupong Boonmee<sup>1</sup> · Kasama Jarukumjorn<sup>1</sup>

Received: 20 February 2019 / Revised: 26 July 2019 / Accepted: 21 August 2019  
 © Springer-Verlag GmbH Germany, part of Springer Nature 2019

### Abstract

Silica nanoparticles from sugarcane bagasse ash (SBA) were prepared from sol–gel process. Particle size, specific surface area, morphology, chemical composition and chemical structure of SBA and prepared silica nanoparticles were characterized. The effect of drying techniques such as freeze drying (FD) and heat drying (HD) on the properties of silica nanoparticles was investigated. High purity of silica nanoparticles in size range of  $90 \pm 10$  nm were successfully prepared. FD provided silica nanoparticles with high specific surface area and high porosity compared to conventional HD. The effect of silica nanoparticle contents on cure characteristics, mechanical properties, and morphology of natural rubber (NR) composites was studied. Scorch time of NR composites was increased with an increase in silica nanoparticle content due to the disturbance of vulcanization process by silica surface. FD-silica/NR composites provided longer scorch time and cure time compared to HD-silica/NR composites due to higher active surface area of FD-silica. Modulus and hardness of NR composites were increased while elongation at break was decreased with an increase in silica nanoparticle content. Tensile strength of the composites increased with silica nanoparticle content and tended to reduce at high silica nanoparticle content. FD-silica/NR composites exhibited better mechanical properties than HD-silica/NR composites due to better filler-rubber interaction.

**Keywords** Silica nanoparticle · Natural rubber · Sugarcane bagasse ash · Composites · Mechanical properties

✉ Kasama Jarukumjorn  
 kasama@sut.ac.th

<sup>1</sup> School of Polymer Engineering, Institute of Engineering, Suranaree University of Technology, Nakhon Ratchasima 30000, Thailand



## Introduction

Natural rubber (NR) is one of the main rubbers and widely used to prepare many rubber compounding products such as automotive tire, gasket and seal, and rubber goods product. NR is a renewable material. It combines excellent and wide range of mechanical and dynamical properties for various applications. Properties and performances of rubber compounds depend mainly on the right compounding ingredient combination, including rubber additives and reinforcing fillers. Different types of reinforcing fillers affect significantly the properties of NR compounds [1, 2].

The introduction of silica nanoparticles into NR matrix as a reinforcing filler has been recently attracted interest because silica nanoparticles play an important role to improve some mechanical properties of natural rubber composites such as tensile strength, hardness and modulus [1]. The properties of silica-filled NR composite are generally depended on silica characteristics such as specific surface area, particle size as well as the ability of dispersion in NR matrix [3, 4].

Sol-gel process is a proper route to synthesis silica nanoparticles due to its ability to form high purity and homogenous products at proper conditions. Tetraethyl orthosilicate (TEOS) is commonly used as a precursor in alkaline medium to produce silica nanoparticles. Particle size, particle size distribution and surface properties of silica nanoparticles prepared from TEOS are highly depended on experimental conditions such as the type and concentration of alkoxides, catalyst's nature and concentration, time of aging and drying method that affect rate of hydrolysis and condensation reactions [5]. Rahman et al. [6] studied the effect of different drying techniques on properties of silica nanoparticles prepared from TEOS. They reported that the alcohol dehydration technique effectively removed the water and excess reactants from the silica suspension compared with freeze dry and oven dry techniques. Moreover, oven drying technique led to the formation of dense islands due to intense interparticle interactions and capillary force created by evaporating water. The agglomerates formation was the highest in the oven drying samples and least in the alcohol dehydration samples.

Sodium silicate is another alternative precursor for synthesis of silica nanoparticles. Sodium silicate offers typical advantages over TEOS including refined and uniform particle size along with the high concentration of silica nanoparticles [7]. Zulfiquar et al. [8] synthesized silica nanoparticles under alkaline conditions using commercial sodium silicate as a precursor. Ammonia/ethanol mixture in ratio 3:1 provided the smallest spherical silica nanoparticles size of  $60 \pm 11$  nm. Moreover, particle size of silica nanoparticles tended to decrease with the decrease in ammonia content and increase in ethanol content.

Extensive researchers have carried out to extract sodium silicate from sugarcane bagasse ash (SBA) for use as a precursor to produce silica particles [9, 10]. Sugarcane bagasse contains high silicon content and abundant availability in agriculture country. The deposition of silica in the sugarcane bagasse is influenced by the quantity and availability of silicon in soil [9]. SBA is waste in sugar industry and by-products from Bio-power station. It needs to be disposed properly;

otherwise, it may cause a major environmental sustainable issue. Using SBA as a source of sodium silicate to produce silica nanoparticles not only provides a solution for waste disposal but also recovers a valuable material from agricultural wastes.

In this study, SBA was used as a precursor to produce silica nanoparticles by sol-gel process. Particle size, surface area, morphology, chemical composition and chemical structure of SBA and prepared silica nanoparticles were characterized. The effect of drying techniques on the properties of silica nanoparticles was studied. Moreover, the influence of silica nanoparticle content on mechanical properties, cure characteristics and morphology of NR composites was described.

## Materials and methods

### Materials

Sugarcane bagasse ash was supplied from Khonburi Power Plant Co., Ltd. subordinated to Khonburi Sugar Public Co., Ltd. Chemicals used in silica preparation were hydrochloric acid (HCl), sodium hydroxide (NaOH), ethanol and ammonia. Natural rubber (NR, STR XL) was purchased from Natural Art and Technology Co., Ltd. Other ingredients used to vulcanize natural rubber were stearic acid, zinc oxide, *N*-cyclohexyl-2-benzothiazole-2-sulfenamide (CBS) and sulfur.

### Preparation of sodium silicate solution

The collected 100 g of SBA was ground and refluxed with 1 mol/l hydrochloric acid (HCl) at 100 °C for 4 h to remove dirt and metal oxides impurity. Then, the solution was cooled down to room temperature and filtered using a filter paper (Whatman No.41). The remaining solid portion was washed with distilled water until pH 7 was obtained, and then filtered and dried in a vacuum oven at 120 °C for 6 h to remove moisture. The acid leached sugarcane bagasse ash was then dispersed and vigorously stirred in 50 ml of 3 mol/l sodium hydroxide (NaOH) for 4 h at 80 °C to produce sodium silicate solution [9]. The suspension was then filtered through a filter paper (Whatman No. 41) in order to remove solid residue. The filtrate solution was sodium silicate supernatant that was used as a precursor to produce silica nanoparticles.

### Preparation of silica nanoparticles

The prepared sodium silicate 10 ml was added into 20 ml of distilled water. Then, the diluted sodium silicate solution was added drop-wise into the ethanol/ammonia mixture in the ratio 30:90 ml [8]. Then, the solution was aged for 1 h to form silica gel. Then, it was centrifuged and washed with distilled water. Finally, the silica gel was dried under heat drying (HD) in vacuum oven over night or freeze dry (FD) in deep vacuum overnight to study the effect of different drying techniques on surface properties and particle size distribution of silica nanoparticles.

### Characterization of silica nanoparticles

Chemical compositions of SBA and silica nanoparticle were analyzed using wavelength dispersive X-ray fluorescence spectrometer (XRF, PAN analysis, Axios). FTIR spectra of the samples were performed in the attenuated total reflection mode (ATR) at resolution of  $4\text{ cm}^{-1}$  in the range  $400\text{--}4000\text{ cm}^{-1}$  using Fourier transform infrared spectrometer (FTIR, Bruker, T27/Hyp2000). X-ray diffraction pattern of SBA and silica nanoparticles were carried out by X-ray diffractometer (Bruker, D2 PHASER) in the range of  $2\theta = 10^\circ\text{--}80^\circ$ . Particle size distribution of silica nanoparticles was measured using a laser diffraction particle size distribution analyzer (Malvern, Zetasizer-zs). Morphology of silica nanoparticles was examined using scanning electron microscope (SEM, JEOL, JSM-6010LV) at 5 keV. Surface properties of silica nanoparticles were characterized using nitrogen adsorption desorption analysis (BELSORP-mini II).

### Preparation of silica nanoparticles/NR composites

Formulations of natural rubber composites are shown in Table 1. The compounds were mixed in an internal mixer (Chareontut) at  $60^\circ\text{C}$ . The filler contents used in this study were 1, 3, 5 and 10 phr. The total mixing time was 25 min. Test specimens were prepared using a compression molding machine (Labtech LP20-B) under a pressure of 150 MPa and a temperature of  $150^\circ\text{C}$ .

### Characterization of NR and NR composites

Cure characteristics of NR and NR composites were investigated using a moving die rheometer (MDR, GOTECH/GT-M200F) at  $150^\circ\text{C}$ . Cure rate index (CRI) of NR and NR composites was calculated by following equation.

$$\text{CRI} = 100 / (\text{cure time} - \text{scorch time}) \quad (1)$$

Tensile and tear properties of NR and NR composites were tested according to ASTM D412 and ASTM D624, respectively, using a universal testing machine (UTM, INSTRON/5565) with a load cell of 5 kN and a crosshead speed of 500 mm/

**Table 1** Formulation of natural rubber compounds

Materials	Content (phr)									
Natural rubber	100	100	100	100	100	100	100	100	100	100
ZnO	5	5	5	5	5	5	5	5	5	5
Stearic acid	2	2	2	2	2	2	2	2	2	2
CBS	1.5	1.5	1.5	1.5	1.5	1.5	1.5	1.5	1.5	1.5
Sulfur	1	1	1	1	1	1	1	1	1	1
FD-silica	–	1	3	5	10	–	–	–	–	–
HD-silica	–	–	–	–	–	1	3	5	10	–



min. Hardness of NR and NR composites was determined using a shore A durometer (Bar Eiss, Type BS61 II) according to ASTM D2240.

Tensile fractured surfaces of NR and NR composites were examined using a scanning electron microscope (SEM, Hitachi S3400 N) at 5 keV. The samples were coated with gold before examination.

## Results and discussion

FTIR spectra of commercial sodium silicate and extracted sodium silicate from SBA are shown in Fig. 1a. The peak at wavenumber of  $980\text{ cm}^{-1}$  represented Si–O–Si asymmetric stretching of siloxane bond in both samples. The peak at  $1640\text{ cm}^{-1}$  was due to the presence of H–O–H stretching vibration which indicated a water absorption of the samples [9]. Broad peak around  $2500\text{--}3600\text{ cm}^{-1}$  was attributed to O–H stretching in both sodium silicate which confirm the presence of hydroxyl group at silica nanoparticles surface and the water absorption in samples [9, 10]. Moreover, sodium silicate from SBA showed peak at  $876\text{ cm}^{-1}$  which represented the  $\text{SiO}_4$  tetrahedron structure in the sample [9]. From Fig. 1b, FD-silica and HD-silica showed essentially similar FTIR spectrum. Basically, the vibration signal at  $1091\text{ cm}^{-1}$  was the asymmetric stretching of Si–O–Si. Peak at  $800\text{ cm}^{-1}$  represented the symmetric stretching of Si–O–Si bond. Peak at  $467\text{ cm}^{-1}$  was assigned to the asymmetric bending of Si–O–Si bond [10–12]. These Si–O–Si stretching and bending were confirmed silica characteristics. Moreover, peak at  $950\text{ cm}^{-1}$  was Si–OH bond stretching of silanol group in the sample [10].

XRD diffraction patterns of SBA, HD-silica and FD-silica are shown in Fig. 2. The XRD pattern of SBA showed many peaks that referred to the crystalline characteristics of residual metal oxides [13]. FD-silica and HD-silica showed same broad peak in the range of  $15^\circ\text{--}30^\circ$  and centered at  $23^\circ$  attributed to amorphous structure of silica [12]. Thus, silica nanoparticles prepared from SBA were purely amorphous type. Amorphous silica nanoparticles have been broadly used in the preparation of

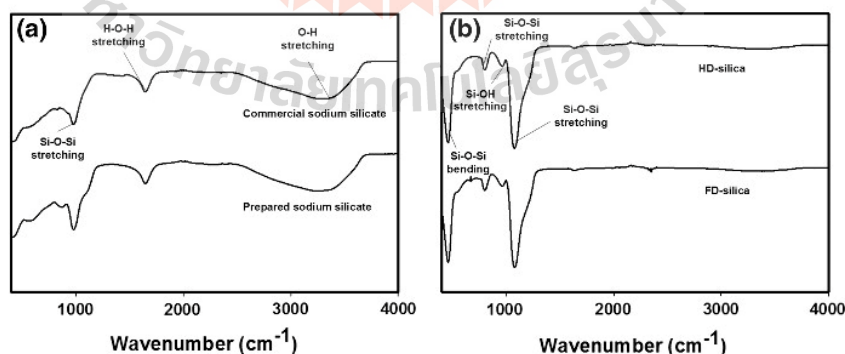


**Fig. 1** FTIR spectra of sodium silicate (a) and silica nanoparticle (b)

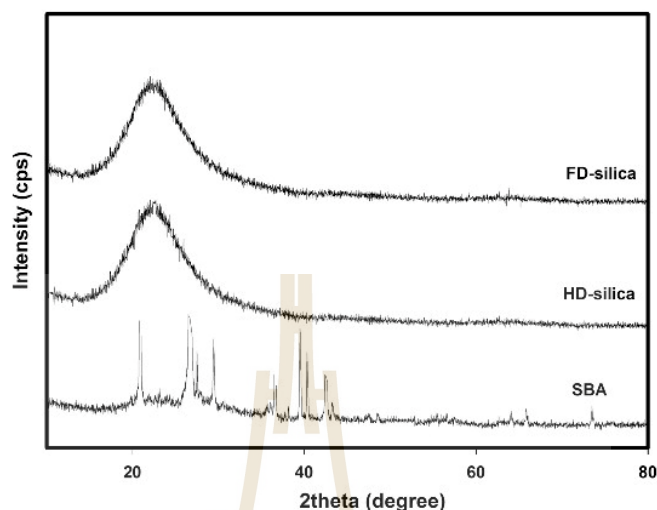


**Fig. 2** X-ray diffraction patterns of SBA, HD-silica and FD-silica

NR composites because amorphous silica nanoparticles were stable in a long time compared to the crystalline silica nanoparticles [11, 14, 15].

Chemical compositions of SBA, FD-silica and HD-silica are listed in Table 2. SBA contained 64.8% of  $\text{SiO}_2$ , and major metal oxide impurities were  $\text{K}_2\text{O}$ ,  $\text{Fe}_2\text{O}_3$ ,  $\text{CaO}$  and  $\text{TiO}_2$  with 15.2%, 8.9%, 5.2% and 0.9%, respectively. After purification process, silica purities of 98.8% and 98.5% were obtained in freeze dry and heat dry process, respectively. This indicated that the processes were useful for removing metallic impurities and resulted in improved purity of silica. As expected, the drying techniques had insignificant effect on the purity of the prepared silica.

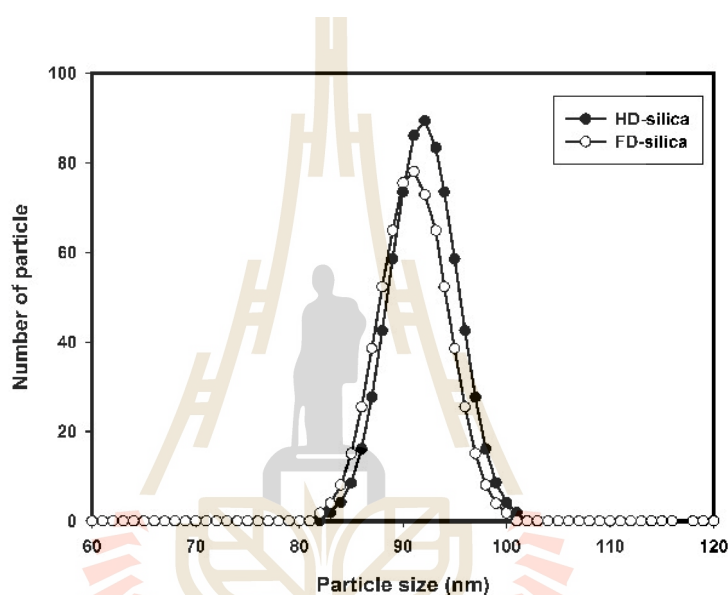
Surface properties and particle size distribution of prepared silica nanoparticles are shown in Table 3 and Fig. 3, respectively. The results revealed that both of drying techniques provided silica nanoparticles in size range of  $90 \pm 10$  nm. Particle size and particle size distribution of silica nanoparticles prepared from these two drying techniques were insignificant difference as shown in Fig. 3. However, FD-silica revealed interesting surface characteristics as shown in Table 3. Specific surface area, pore area and pore volume of FD-silica were

**Table 2** Chemical composition of SBA and prepared silica nanoparticles

Compound	SBA	FD-silica	HD-silica
$\text{SiO}_2$	64.8	98.8	98.5
$\text{CaO}$	5.2	0.4	0.3
$\text{TiO}_2$	0.9	–	0.2
$\text{K}_2\text{O}$	15.2	0.1	0.2
$\text{Fe}_2\text{O}_3$	8.9	0.4	0.4

**Table 3** Surface properties and particle size of prepared silica nanoparticles

Properties	FD-silica	HD-silica
Surface area ( $\text{m}^2 \text{g}^{-1}$ )	156	70
Pore area ( $\text{m}^2 \text{g}^{-1}$ )	125.89	74.91
Pore volume ( $\text{cm}^3 \text{g}^{-1}$ )	1.35	0.68
Mean pore diameter (nm)	35.25	39.09
Average particle size (nm)	$91.06 \pm 10.00$	$92.12 \pm 10.00$

**Fig. 3** Particle size distribution of HD-silica and FD-silica

significantly higher than that of HD-silica. This may be because in freeze dry technique, water or other solvents were slowly removed through sublimation process under vacuum. This led to the reduction in capillary forces and thermal tension resulting in minimal shrinkage, high specific surface area and high porosity at surface of the particles [6]. On the other hand, heat dry process decreased in gel volume due to the loss of liquid by evaporation through the silica pores by rapid removal of the water from the pores which caused blistering, shrinkage and shriveling of silica gel. In addition, freeze dry technique presented the structure of materials without shrinkage of the gel structure [5, 16].

Figure 4 presents SEM images of FD-silica and HD-silica at a magnification of  $50,000\times$ . Silica nanoparticles did not show clear boundaries as they were in agglomerate and amorphous form. Because of the nonconductive nature of silica, the charges quickly accumulated on the silica surfaces even after gold sputtering caused agglomeration of particles [17].

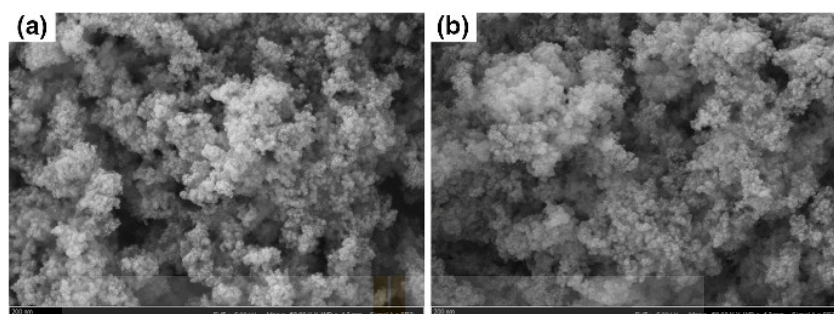


Fig. 4 SEM images at 50,000 $\times$  magnification of HD-silica (a) and FD-silica (b)

### Cure characteristics

Scorch time ( $t_{s1}$ ) and cure time ( $t_{90}$ ) of NR and NR composites are shown in Fig. 5. The incorporation of both silica nanoparticles into NR matrix led to longer scorch time of NR composites. With an increase in silica content, longer scorch time of NR composites was found especially at 5 phr and 10 phr of silica due to the disturbance in vulcanization process of silica nanoparticles. The silanol group at silica surface can interact with accelerator and activator leading to delay scorch time of NR composites [18, 19]. However, silica nanoparticle content showed insignificant effect on cure time of the composites [20]. FD-silica/NR composites showed longer scorch time and cure time than HD-silica/NR composites. This

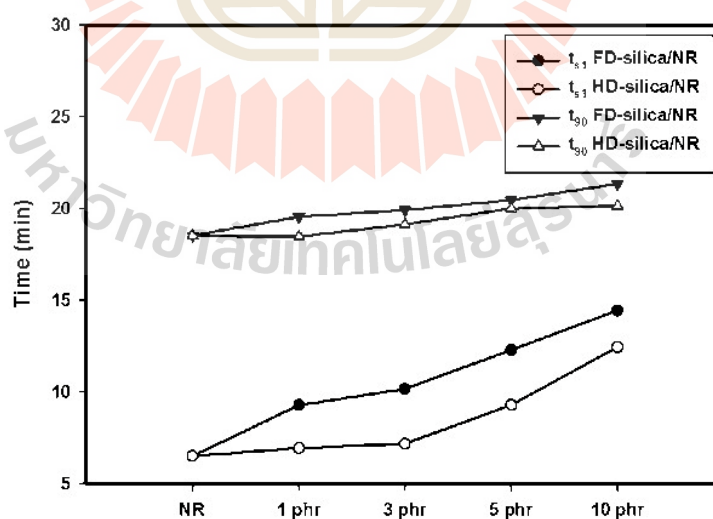


Fig. 5 Scorch time and cure time of NR and NR composites



may be due to higher specific surface area of FD-silica surface leading to highly active surface and high interaction with chemicals in vulcanization process [3].

Maximum torque (MH) and minimum torque (ML) of NR were lower than NR composites as shown in Fig. 6. ML value indicated the initial viscosity of rubber compounds. An increase in ML of NR was related to increased viscosity with the presence of silica nanoparticles. This enhancement was attributed to a physical crosslink network. The mobility of rubber chains was restricted by the filler; therefore, ML was enhanced [21]. ML can be related to the specific surface area of filler [22]. Increasing the ML value indicated that a larger amount of rubbers were immobilized on the filler surface; so reinforcement took place. MH measured the maximum viscosity and stiffness of the fully vulcanized rubber and was an approximate measure of the chemical crosslink density in the sample [23]. Increasing MH was related to degree of crosslink during vulcanization process [24]. When silica nanoparticles content increased, MH and ML of the composites also increased. FD-silica/NR composites had higher MH and ML than HD-silica/NR composites because of high specific surface area of FD-silica leading to high filler–matrix interaction.

Cure rate index (CRI) of NR and NR composites is shown in Fig. 7. CRI is a measure of cure rate of rubber. NR composites had higher CRI compared to NR. This suggested that adding silica nanoparticles accelerated vulcanization process. Moreover, increasing silica nanoparticle content resulted in the composites with enhanced CRI. This was because the incorporation of silica nanoparticles increased a level of hydroxyl groups which can speed up crosslinking reaction and enhance vulcanization rate [25, 26]. FD-silica/NR composites exhibited higher CRI than HD-silica/NR composites. This can be explained by the physical crosslink which was related to ML. ML of FD-silica/NR composites was higher than HD-silica/NR composites. Formation of the physical network changed the accessibility of the surface

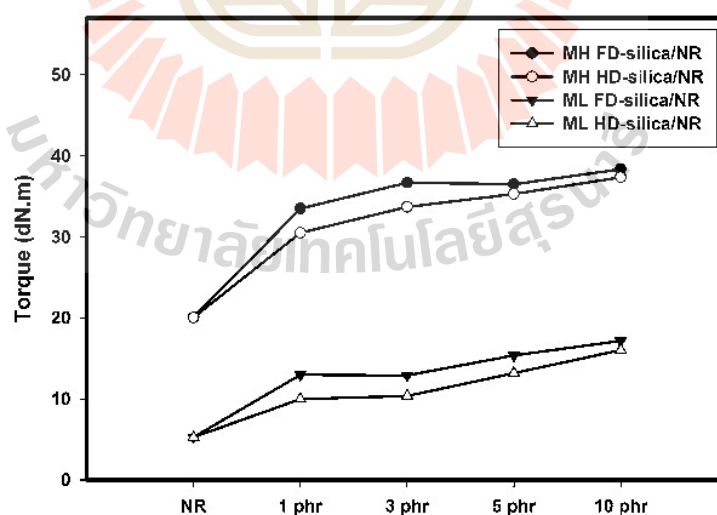


Fig. 6 Maximum torque and minimum torque of NR and NR composites



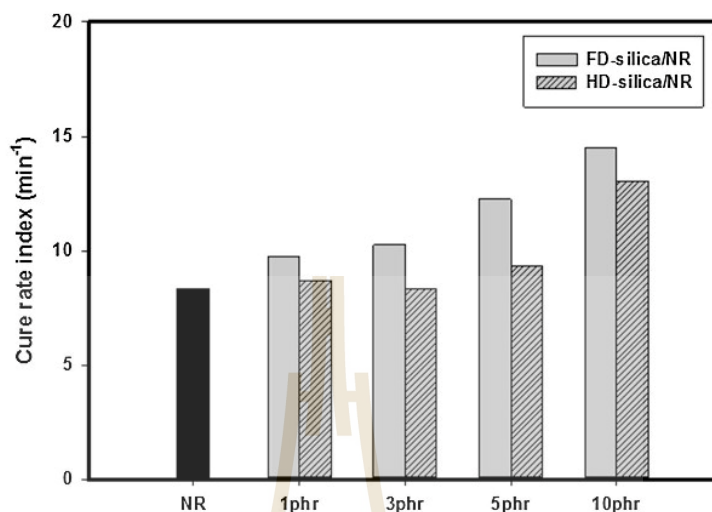


Fig. 7 Cure rate index of NR and NR composites

groups. This resulted in less adsorption of accelerators on the surface of FD-silica/NR composites compared to HD-silica/NR composites. Therefore, the inclusion of FD-silica accelerated the vulcanization and increased the chemical crosslink [21].

### Mechanical properties

Modulus at 100% elongation (M100) and modulus at 300% elongation (M300) and hardness of NR and NR composites are shown in Figs. 8, 9 and 10, respectively. As expected, the addition of silica nanoparticles into NR enhanced M100, M300 and hardness of the composites. In addition, these properties increased with an increase in silica content. This may be because silica nanoparticles reduced the elasticity of NR molecular chain leading to increased stiffness of composites [27]. On the other hand, increasing silica nanoparticle contents resulted in a decrease in elongation at break of the composites due to the reduction in elasticity of NR molecular chains as shown in Fig. 11. FD-silica/NR composites showed higher M100, M300 and hardness compared to HD-silica/NR composites due to higher specific surface area and porosity resulted in high filler–matrix interaction of the composites.

Tensile strength and tear strength of NR and NR composites are shown in Figs. 12 and 13, respectively. The incorporation of silica nanoparticles at contents of 1, 3 and 5 phr resulted in improved tensile strength and tear strength of NR composites. This may be because at low content of silica, silica nanoparticles well dispersed in NR matrix leading to the formation of thin filler network around NR chains. Crosslinks between NR chains along with diffusion across NR led to reinforcement [28, 29]. At 10 phr of silica nanoparticles, tensile strength of the composites was remarkably decreased, while tear strength was slightly changed when compared to the composite filled with 5 phr of silica nanoparticles.

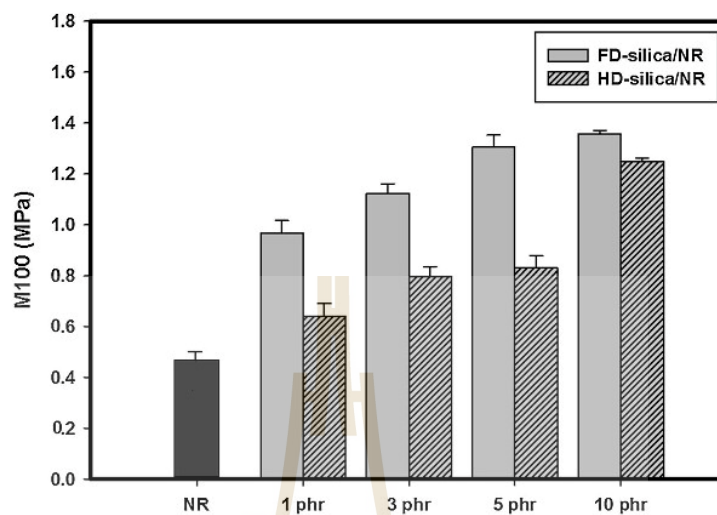


**Fig. 8** Modulus at 100% elongation of NR and NR composites

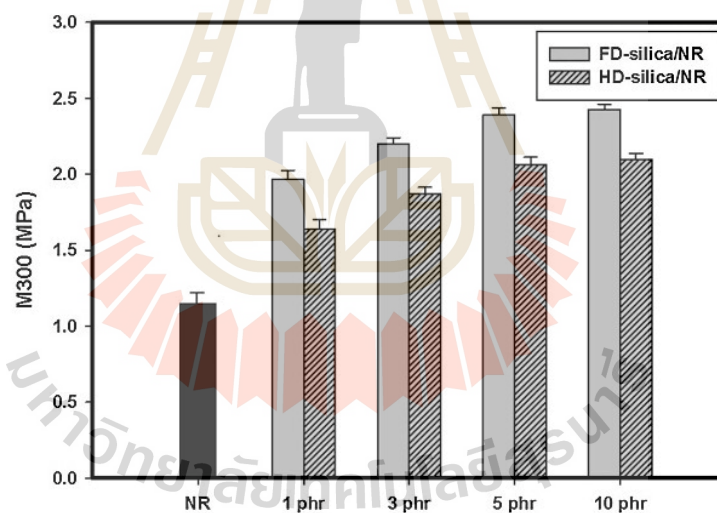


**Fig. 9** Modulus at 300% elongation of NR and NR composites

This was because at higher silica content, the aggregation occurred due to the filler–filler interaction between segregated networks [30]. This resulted in the prevention of molecular diffusion between the natural rubber chains. FD-silica/NR composites showed higher tensile strength and tear strength than HD-silica/NR composites due to higher specific surface area of FD-silica leading to better filler–rubber interaction [31].

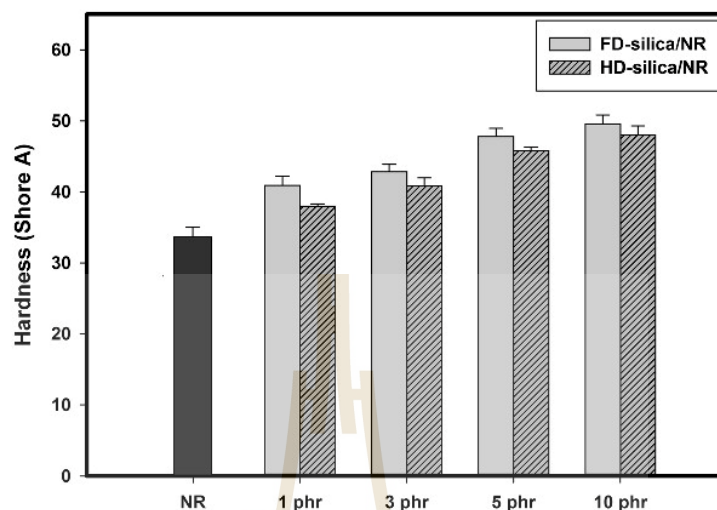


Fig. 10 Hardness of NR and NR composites

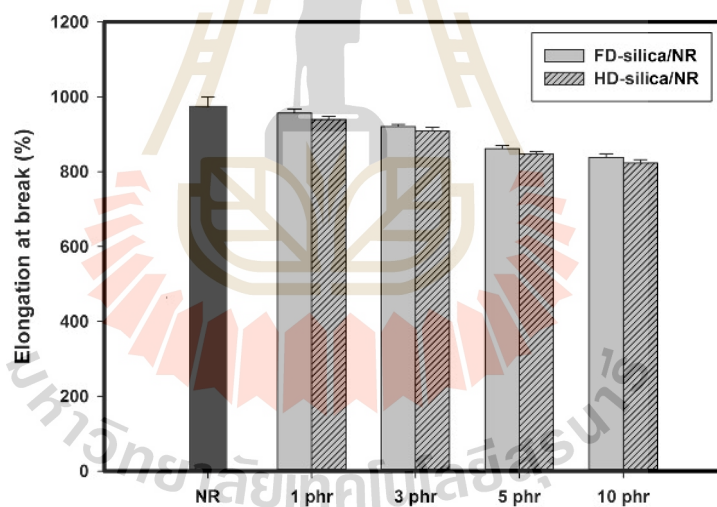


Fig. 11 Elongation at break of NR and NR composites

### Morphology

Tensile fractured surface of NR and NR composites are shown in Fig. 14. The fractured surface of NR without filler showed smooth surface. Filler dispersion significantly affects the performance and rubber–filler interaction of rubber composites. The good dispersion of filler in rubber matrix resulted in the enhancement of

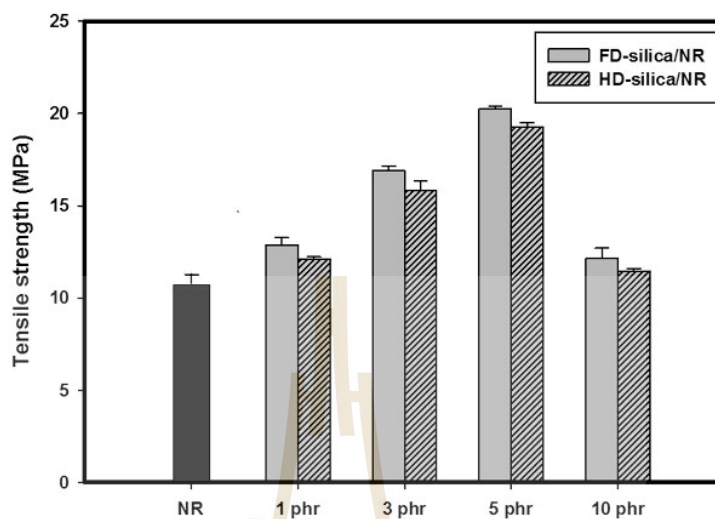


Fig. 12 Tensile strength of NR and NR composites

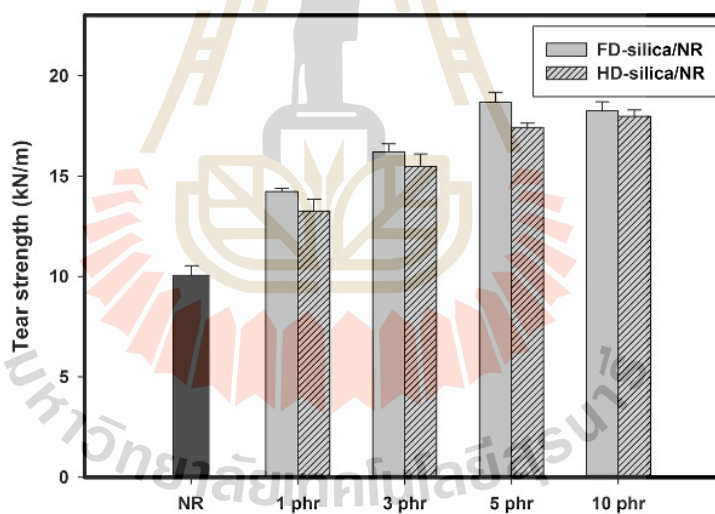
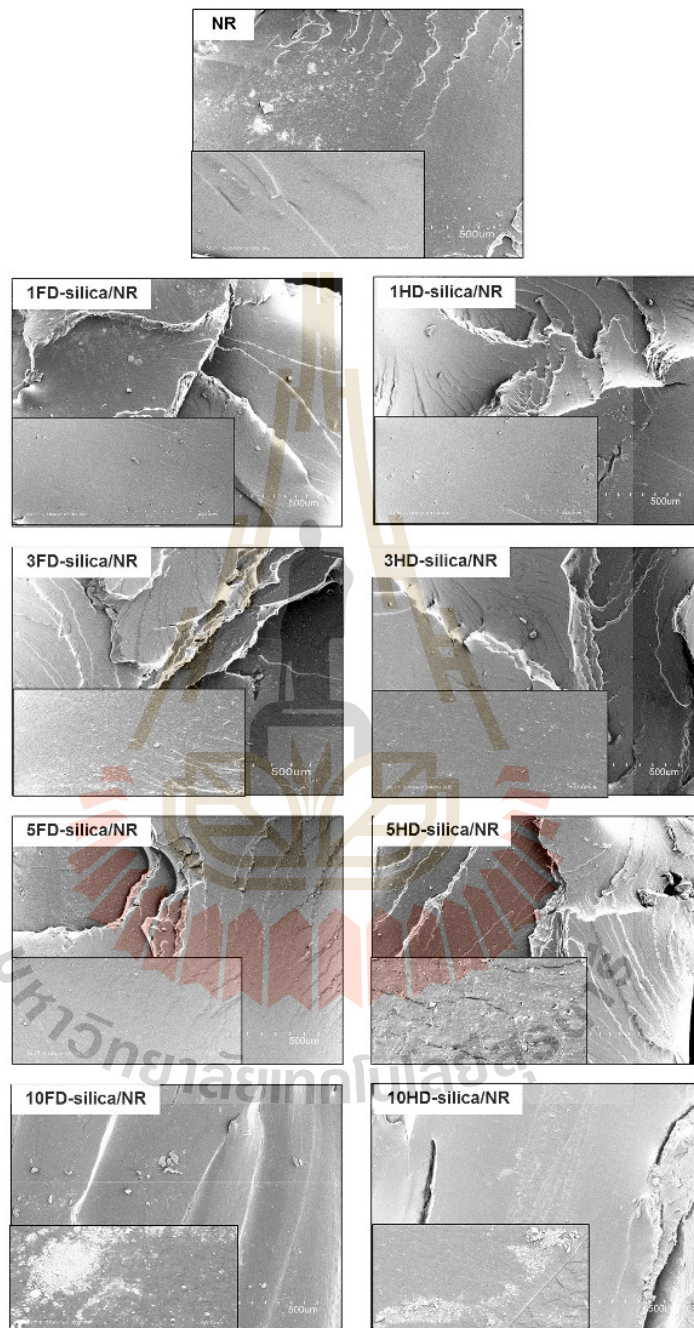


Fig. 13 Tear strength of NR and NR composites

mechanical properties of rubber composites [32]. With the addition of 1, 3 and 5 phr of both silica nanoparticles into NR matrix, roughly and many layer surfaces were observed due to good dispersion of silica nanoparticles in NR chains [4]. This was corresponded with the improvement in tensile strength and tear strength of the composites. Good dispersion of silica in rubber matrix led to high interaction between silica and rubber [31]. Smooth surface with micropores was found in the composites





**Fig. 14** SEM images at 100× and 1000× magnification of NR and NR composites

with the addition of silica nanoparticles at 10 phr due to high filler–filler interaction and non-homogenous dispersion of silica nanoparticles in NR matrix. This caused a negative effect on tensile strength of the composites.

## Conclusions

Silica nanoparticles in the size range of  $90 \pm 10$  nm were successfully prepared from sugarcane bagasse ash in alkaline medium. FTIR spectrum of prepared silica nanoparticles represented the absorption band which confirmed silica characteristics. Silica nanoparticles with 98.8% and 98.5% purity were obtained from freeze dry and heat dry techniques, respectively. Freeze drying technique provided higher specific surface area and porosity compared to conventional heat drying technique due to slow removal of water through sublimation process. NR composites reinforced with silica nanoparticles showed longer scorch time than NR and further increased with an increase in silica nanoparticle content due to the disturbance in vulcanization process by silica surface. Scorch time and cure time of FD-silica/NR composites were longer than HD-silica/NR composites due to higher specific surface area of FD-silica surface leading to highly active surface and high interaction with chemicals in vulcanization process. Adding silica nanoparticles led to increased cure rate index of the composites. The improvement of MH, ML, M100, M300 and hardness of NR composites was found with silica nanoparticle content due to increased stiffness of the composites. Tensile strength of NR composites increased with silica nanoparticle content up to 5 phr and decreased at 10 phr because of silica aggregation. FD-silica/NR composites presented higher modulus, hardness, tensile strength and tear strength than HD-silica/NR composites due to higher specific surface area and porosity of FD-silica.

**Acknowledgements** The authors are grateful to Suranaree University of Technology for financial supports, Khonburi Power Plant Co., Ltd. subordinated to Khonburi Sugar Public Co., Ltd. for supplying sugarcane bagasse ash and PI Industry Co., Ltd. for supplying chemicals used in rubber compounding.

## References

1. Rattanasom N, Saowapark T, Deeprasertkul C (2007) Reinforcement of natural rubber with silica/carbon black hybrid filler. *Polym Test* 26(3):369–377
2. Ahmed K, Nizami SS, Riza NZ (2014) Reinforcement of natural rubber hybrid composites based on marble sludge/silica and marble sludge/rice husk derived silica. *J Adv Res* 5(2):165–173
3. Chuayjuljit S, Eiumnroh S, Potiyaraj P (2001) Using silica from rice husk as a reinforcing filler in natural rubber. *J Sci Res Chula Univ* 26(2):127–138
4. Lay M, Azura AR, Othman N, Tezuka Y, Pen C (2013) Effect of nanosilica fillers on the cure characteristics and mechanical properties of natural rubber composites. *Adv Mater Res* 626:818–822
5. Jafarzadeh M, Rahman IA, Sipaut CS (2009) Synthesis of silica nanoparticles by modified sol-gel process: the effect of mixing modes of the reactants and drying techniques. *J Sol-Gel Sci Technol* 50(3):328–336
6. Rahman IA, Vejayakumaran P, Sipaut CS, Ismail J, Chee CK (2008) Effect of the drying techniques on the morphology of silica nanoparticles synthesized via sol-gel process. *Ceram Int* 34(8):2059–2066
7. Weichold O, Tigges B, Bertmer M, Moller M (2008) A comparative study on the dispersion stability of aminofunctionalised silica nanoparticles made from sodium silicate. *J Colloid Interface Sci* 324:05–109

8. Zulfiqar U, Subhani T, Husain SW (2016) Synthesis of silica nanoparticles from sodium silicate under alkaline conditions. *J Sol-Gel Sci Technol* 77(3):753–758
9. Norsuraya S, Fazlena H, Norhasyimi R (2016) Sugarcane bagasse as a renewable source of silica to synthesize santa barbara amorphous-15 (SBA-15). *Procedia Eng* 14:839–846
10. Premaratne WAPJ, Priyadarshana WMGI, Gunawardena SHP, De Alwis AAP (2013) Synthesis of nanosilica from paddy husk ash and their surface functionalization. *J Sci Univ Kelaniya* 8:33–48
11. Huabcharoen P, Wimolmala E, Markpin T, Sombatsompop N (2017) Purification and characterization of silica from sugarcane bagasse ash as a reinforcing filler in natural rubber composites. *BioResources* 12(1):1228–1245
12. Ghorbani F, Sanati AM, Maleki M (2015) Production of silica nanoparticles from rice husk as agricultural waste by environmental friendly technique. *Environ Stud Persian Gulf* 2(1):56–65
13. Rani KM, Palanisamy PN, Sivakumar P (2014) Synthesis and characterization of amorphous nanosilica from biomass ash. *Int J Adv Technol Eng Sci* 2(10):71–76
14. Alayande SO, Dare EO, Ayinde WB, Bamigbose J, Ayedun PA, Osinkolu GA (2012) Development of ordered and disordered macroporous silica from bagasse ash. *J Pure Appl Chem* 6(1):10–14
15. Alves RH, Reis TVS, Rovani S, Fungaro DA (2017) Green synthesis and characterization of biosilica produced from sugarcane waste ash. *J Chem* 2017:1–9
16. Chen G, Wang W (2007) Role of freeze drying in nanotechnology. *Dry Technol* 25(1):29–35
17. Lu P, Hsieh YL (2012) Highly pure amorphous silica nano-disks from rice straw. *Powder Technol* 225:149–155
18. Pongdong W, Nakason C, Kummerlowe C, Vennemann N (2015) Influence of filler from a renewable resource and silane coupling agent on the properties of epoxidized natural rubber vulcanizates. *J Chem* 2015:1–15
19. Mathew L, Narayanankutty SK (2010) Synthesis, characterisation and performance of nanosilica as filler in natural rubber compounds. *J Rubb Res* 13(1):27–43
20. Prasertsri S, Rattanasom N (2012) Fumed and precipitated silica reinforced natural rubber composites prepared from latex system: mechanical and dynamic properties. *Polym Test* 31(5):593–605
21. Tabaei TA, Bagheri R, Hesami M (2015) Comparison of cure characteristics and mechanical properties of nano and micro silica-filled CSM elastomers. *J Appl Polym Sci*. <https://doi.org/10.1002/app.42668>
22. Li ZH, Zhang J, Chen S (2008) Effects of carbon blacks with various structures on vulcanization and reinforcement of filled ethylene-propylene-diene rubber. *J Exp Polym Lett* 2(1):695–704
23. Marković G, Radovanović B, Marinović-Cincović M, Budinski-Simendić J (2009) The Effect of accelerators on curing characteristics and properties of natural rubber/chlorosulphonated polyethylene rubber blend. *J Mater Manuf Process* 24(10):1224–1228
24. Santos RJD, Agostini DLDS, Cabrera FC, Reis EAPD, Ruiz MR, Budenberg ER, Job AE (2014) Sugarcane bagasse ash: new filler to natural rubber composite. *Polímeros* 24(6):646–653
25. Nakason C, Kaesaman A, Eardrod K (2005) Cure and mechanical properties of natural rubber-g-poly (methyl methacrylate)-cassava starch compounds. *Mater Lett* 59:4020–4025
26. Nor NM, Othman N (2016) Effect of filler loading on curing characteristic and tensile properties of palygorskite natural rubber nanocomposites. *Proc Chem* 19:351–358
27. Sarkawi SS, Aziz Y (2003) Ground rice husk as filler in rubber compounding. *J Teknol* 39(1):135–148
28. Francis LF, Grunlan JC, Sun J, Gerberich WW (2007) Conductive coatings and composites from latex-based dispersions. *Colloids Surf A Physicochem Eng Asp* 311:48–54
29. Arun KJ, Francis PJ, Joseph R (2010) Mechanical properties of NR latex-nano silica composites. *J Optoelectron Adv M* 4:1520–1525
30. Yin C, Zhang Q, Liu J, Liu L, Gu J (2018) Preparation, properties of In-situ silica modified styrene-butadiene rubber and its silica-filled composites. *Polym Compos* 39(1):22–28
31. Yin C, Zhang Q, Gu J, Zheng J, Gong G, Liang T, Zhang H (2013) In situ silica reinforcement of vinyltriethoxysilane-grafted styrene-butadiene rubber by sol-gel process. *J Appl Polym Sci* 128(4):2262–2268
32. Roy K, Debnath SC, Potiyaraj P (2019) A critical review on the utilization of various reinforcement modifiers in filled rubber composites. *J Elastom Plast*. <https://doi.org/10.1177/0095244319835869>

**Publisher's Note** Springer Nature remains neutral with regard to jurisdictional claims in published maps and institutional affiliations.



## Mechanical Properties and Cure Characteristics of Silica Nanoparticles from Sugarcane Bagasse Ash/Natural Rubber Composites

**Anupong Boonmee** and Kasama Jarukumjorn\*

School of Polymer Engineering, Institute of Engineering, Suranaree University of Technology,  
Nakhon Ratchasima 30000, Thailand

Phone +66 4422 4437, Fax +66 4422 4605 \* E-mail: kasama@sut.ac.th

### Abstract

Silica nanoparticles were prepared from sugarcane bagasse ash (SBA) by sol-gel method. Chemical composition, chemical structure and surface properties of SBA and prepared silica nanoparticles were characterized. Silica contents in SBA and prepared silica nanoparticles were 64.8 and 98.8%, respectively. FTIR spectrum of prepared silica nanoparticles showed Si-O-Si peak which confirmed silica characteristics. The prepared silica nanoparticles were used as a reinforcing filler in natural rubber (NR). The effect of silica nanoparticles contents (0, 1, 3, 5 and 10 phr) on cure characteristics, mechanical properties and morphology of NR composites were studied. Scorch time and cure time of the composites were increased with silica nanoparticles content. With increasing silica nanoparticles content, the improvement of maximum torque, minimum torque, modulus, hardness of the composites was found. The composite filled with 5 phr of silica nanoparticles showed the highest tensile strength.

**Keywords:** Silica nanoparticles, Natural rubber, Mechanical properties, Cure characteristics

### 1. Introduction

Natural rubber (NR) is one of the main rubbers and widely used to prepare many rubber products. It combines excellent and wide range of mechanical and dynamical properties for various applications. Properties and performances of rubber compounds depend mainly on the right compounding ingredient combination. Different reinforcing fillers affect significantly on the properties of NR compounds [1,2]

Silica nanoparticles ( $n\text{SiO}_2$ ) have been used widely in various application e.g. medical application, cosmetic application as well as used as a reinforcing filler in natural rubber for improving mechanical and thermal properties of NR composites [2]. The commercial methods used to synthesize silica nanoparticles are flame synthesis and sol-gel. However, the production of silica nanoparticles for commercial applications is still high cost, high energy consumption and hazardous to the worker [3]. Extensive researchers have carried out to extract sodium silicate from sugarcane bagasse ash (SBA) for use as a precursor to

produce silica particles [4,5]. Sugarcane bagasse ash is waste in sugar industry and by-products from Bio-power station. It needs to be disposed properly, otherwise it may cause a major environmental sustainable issue. Using SBA as a source of sodium silicate for produce silica nanoparticles for natural rubber composite applications not only provides a solution for waste disposal but also recovers a valuable materials from agricultural wastes.

The objective of this work was to prepare silica nanoparticles from SBA by sol-gel method. Moreover, the effect of prepared silica nanoparticles contents on cure characteristics, mechanical properties and morphology of NR composites was investigated.

### 2. Experimental

#### 2.1 Materials

SBA was supplied from Khonburi Power Plant Co., Ltd. subordinated to Khonburi Sugar Public Co., Ltd. (Thailand). Chemicals used in silica preparation were hydrochloric acid (HCl), sodium hydroxide (NaOH),

ethanol and ammonia. Natural rubber (NR, STR XL) was obtained from Natural Art and Technology Co., Ltd. Silica ULTRASIL VN2 (Evonik) was supplied from PI Industry Co., Ltd. Other ingredients used to vulcanize natural rubber were stearic acid, zinc oxide, N-cyclohexyl-2-benzothiazole-2-sulphenamide (CBS) and sulfur.

## 2.2 Methods

100 g of SBA was refluxed with 1 M HCl at 100°C for 4 hours to remove dirt and metal oxides impurity. Then the solution was filtered. The remaining solid portion was washed with distil water until pH 7 was obtained then filtered and dried in a vacuum oven at 120°C for 6 hours to remove moisture. The acid leached SBA was then dispersed and vigorous stirring in 50 ml of 3 M NaOH for 4 hours at 80°C. The suspension was then filtered. The solution was sodium silicate supernatant that was used as a precursor to produce silica nanoparticles [4].

10 ml of sodium silicate was added into 20 ml of distil water. Then, the sodium silicate solution was added drop-wise into the ethanol/ammonia mixture in ratio 30:90 ml. The solution was aged for 1 hour to form silica gel. Then, it was centrifuged and washed with distilled water. Finally, the silica gel was dried using freeze dry in deep vacuum overnight [6].

Chemical compositions of samples were analyzed using wavelength dispersive X-ray fluorescence spectrometer (XRF, PAN analysis, Axios). FTIR spectra of the samples were performed in the attenuated total reflection mode (ATR) in the range 400–4000 cm<sup>-1</sup> using Fourier transform infrared spectrometer (FTIR, Bruker, T27/Hyp2000). Surface properties of silica nanoparticles was characterized using BET method (BELSORP-mini II). Particle size of silica nanoparticles was measured using a laser diffraction particle size distribution analyzer (Malvern, Zetasizer-zs).

Formulations of natural rubber composites are shown in Table 1. The compounds were mixed in an internal mixer (Chareontut). The total mixing time was 25 min. Test specimens were prepared using a compression molding machine (Labtech LP20-B) under a pressure of 150 MPa and a temperature of 150°C.

Cure characteristics of NR and NR composites were investigated using a moving die rheometer (MDR, GOTECH/GT-M200F) at 150°C.

Tensile properties of NR and NR composites were tested according to ASTM D412 using a universal testing machine (UTM, INSTRON/5565) with a load cell of 5 kN and a crosshead speed of 500 mm/min.

Hardness of NR and NR composites was determined using a shore A durometer (Bar Eiss, Type BS61 II) according to ASTM D2240.

Tensile fractured surfaces of NR and NR composites were examined using a scanning electron microscope (SEM, Hitachi S3400N) at 5 keV. The samples were coated with gold before examination.

Table 1. Formulation of NR composites

Materials	Content (phr)				
	100	100	100	100	100
Natural rubber	100	100	100	100	100
ZnO	5	5	5	5	5
Stearic acid	2	2	2	2	2
CBS	1.5	1.5	1.5	1.5	1.5
Sulfur	1	1	1	1	1
nSiO <sub>2</sub>	-	1	3	5	10

## 3. Results and discussion

FTIR spectrum of prepared silica was similar to commercial silica nanoparticles as illustrated in Figure 1. Vibration signal at 1091 cm<sup>-1</sup> was attributed to the asymmetric vibration of Si-O-Si. Peak at 800 cm<sup>-1</sup> represented the symmetric stretching vibration of Si-O-Si. Peak at 467 cm<sup>-1</sup> was assigned to the bending vibration of Si-O-Si. Moreover, peak at 950 cm<sup>-1</sup> was hydroxyl group in the sample [7,8].

Chemical compositions of SBA and silica nanoparticles are listed in Table 2. SBA contained 64.8% of SiO<sub>2</sub> and major metal oxide impurities were K<sub>2</sub>O, Fe<sub>2</sub>O<sub>3</sub>, CaO and TiO<sub>2</sub> with 15.2%, 8.9%, 5.2% and 0.9%, respectively. On the other hand, silica purities of 98.8% were obtained after the purification process and metal oxides were reduced. This indicated that the process was useful for removing metallic impurities resulting in improved purity of silica.

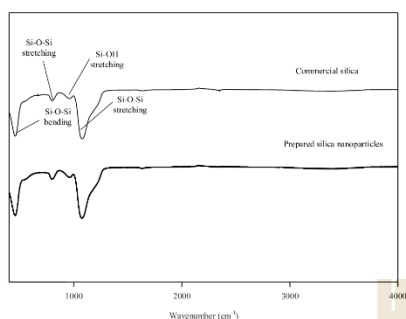


Figure 1. FTIR spectra of commercial silica and prepared silica nanoparticles

Table 2. Chemical composition of SBA and prepared silica nanoparticles

Compound	SBA (%)	nSiO <sub>2</sub> (%)
SiO <sub>2</sub>	64.8	98.8
CaO	5.2	0.4
TiO <sub>2</sub>	0.9	-
K <sub>2</sub> O	15.2	0.1
Fe <sub>2</sub> O <sub>3</sub>	8.9	0.4

Surface properties and particles size of prepared silica nanoparticles are shown in Table 3. The results revealed that prepared silica nanoparticles had smaller particles size ( $91.06 \pm 10.00$  nm) than commercial silica ( $16.12 \pm 6.37$   $\mu$ m). Surface area of prepared silica nanoparticles ( $155.89$  m<sup>2</sup>g<sup>-1</sup>) was higher than commercial silica ( $82.35$  m<sup>2</sup>g<sup>-1</sup>).

Table 3. Surface properties and average particle size of silica nanoparticles prepared from SBA

Properties	nSiO <sub>2</sub>
BET surface area (m <sup>2</sup> g <sup>-1</sup> )	155.89
Pore area (m <sup>2</sup> g <sup>-1</sup> )	125.89
Pore volume (cm <sup>3</sup> g <sup>-1</sup> )	1.35
Mean pore diameter (nm)	35.25
Average particles size (nm)	$91.06 \pm 10.00$

Scorch time ( $t_{s1}$ ) and cure time ( $t_{90}$ ) of NR and NR composites are shown in Figure 2. Scorch time and cure time of the composites increased with increasing silica nanoparticles content due to the disturbance in

vulcanization process of silica nanoparticles. The silanol group at silica surface can interact with accelerator and activator leading to delay scorch time and cure time the composites [9,10]. Maximum torque ( $M_H$ ) and minimum torque ( $M_L$ ) of NR composites were higher than that of NR as displayed in Figure 3 due to increased stiffness of the composites [11, 12,].

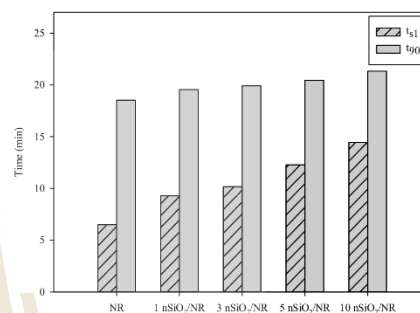


Figure 2. Scorch time and cure time of NR and NR composites

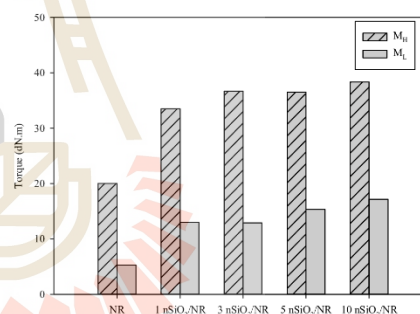


Figure 3.  $M_H$  and  $M_L$  of NR and NR composites

The addition of silica nanoparticles into NR enhanced modulus at 100% elongation ( $M_{100}$ ), modulus at 300% elongation ( $M_{300}$ ) and hardness of the composite as shown in Figure 4 and Figure 5, respectively. Moreover, those properties increased with increasing silica nanoparticles content. This may be because silica nanoparticles reduced the elasticity of NR molecular chain leading to increased stiffness of the composites [7,10,11]. On the other hand, adding silica nanoparticles led to a decrease in elongation at break of the composite due to the

reduction of elasticity of NR molecular chains as shown in Figure 6.

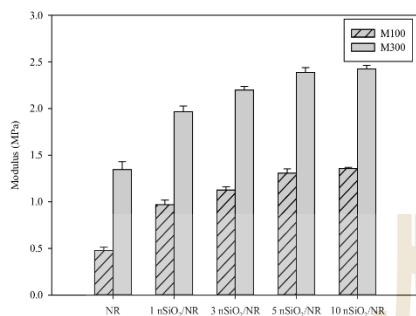


Figure 4. Modulus of NR and NR composites

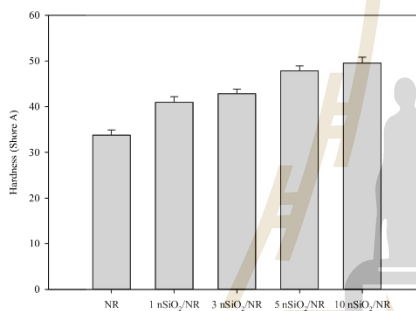


Figure 5. Hardness of NR and NR composites

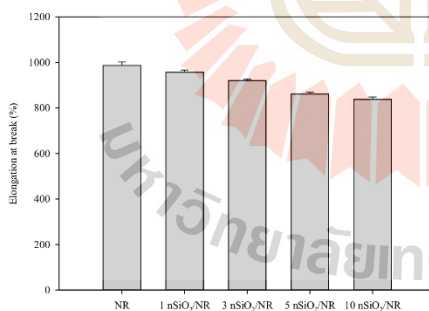


Figure 6. Elongation at break of NR and NR composites

Incorporating silica nanoparticles at 1, 3 and 5 phr resulted in the increment of tensile strength of NR composites as shown in the Figure 7. This may be because silica nanoparticles well dispersed in NR matrix leading to

the formation of thin filler network around NR chains [13,14]. Crosslinks between NR chains along with diffusion across NR resulted in the reinforcement.

At 10 phr of silica nanoparticles, tensile strength of the composite was remarkably decreased. This was because at higher silica content, the agglomeration occurred as shown in Figure 8 due to the filler-filler interaction between segregated networks [15]. The uniform distribution efficacy of filler has affect the stiffness of the composites as well as tensile modulus [16].

The fractured surface of NR showed smooth surface as displayed in Figure 8. With the addition of 1, 3 and 5 phr of silica nanoparticles into NR matrix, roughly and many layer surfaces were observed. This may be due to the strong interfacial adhesion between NR chains and silica nanoparticles [17]. Agglomerate formation was found in NR composite filled with 10 phr of silica nanoparticles due to high filler-filler interaction [17,18]. Moreover, the smooth surface with micro pore was seen in NR composite filled with 10 phr of silica nanoparticles. This was corresponded to a decrease in tensile strength of the composite.

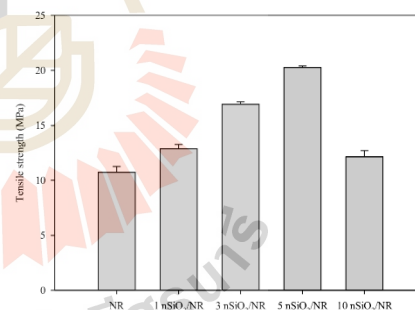


Figure 7. Tensile strength of NR and NR composites

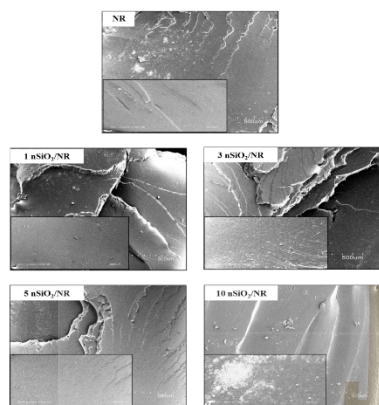


Figure 8. SEM images at 100X and 1000X of tensile fractured surface of NR and NR composites

#### 4. Conclusion

Silica nanoparticles with 98.8% purity were successfully prepared from SBA. FTIR spectrum of prepared silica nanoparticles represented the absorption band which confirmed silica characteristics. Scorch time and cure time of NR composites were longer than those of NR due to the disturbance in vulcanization process by silica surface.  $M_H$ ,  $M_L$ ,  $M_{100}$ ,  $M_{300}$  and hardness of NR composites enhanced but elongation at break decreased with increasing silica nanoparticles content due to increased stiffness of the composites. Tensile strength of the composites improved with silica nanoparticles content up to 5 phr and tended to reduce at 10 phr of silica nanoparticles because of silica nanoparticles agglomeration.

#### Acknowledgements

The authors are grateful to Suranaree University of Technology for financial supports, Khonburi Power Plant Co., Ltd. subordinated to Khonburi Sugar Public Co., Ltd. (Thailand) for supplying sugarcane bagasse ash and PI Industry Co., Ltd for supplying chemicals used in rubber compounding.

#### References

1. Rattanasom, N.; Saowapark, T.; Deeprasertkul, C. *Polym. Test.* **2007**, *26*(3), 369-377.
2. Ahmed, K.; Nizami, S. S.; Riza, N. Z. *J. Adv. Res.* **2014**, *5*(2), 165-173.
3. Faizul, C. P.; Abdullah, C.; Fazlul, B. *Adv. Mat. Res.* **2013**, *626*, 997-1000.
4. Norsuraya, S.; Fazlena, H.; Norhasyimi, R.; *Procedia Eng.* **2016**, *14*, 839-846.
5. Mokhtar, H.; Tajuddin, R. M. *Int. J. Chem. Eng. Appl.* **2016**, *7*(5), 323-326.
6. Jafarzadeh, M.; Rahman, I. A.; Sipaut, C. S. *J. Sol-Gel Sci. Technol.* **2009**, *50*(3), 328-336
7. Huabcharoen, P.; Wimolmala, E.; Markpin, T.; Sombatsompop, N. *Bioresources.* **2017**, *12*(1), 1228-1245.
8. Ghorbani, F.; Sanati, A. M.; Maleki, M. *Environmental Studies of Persian Gulf.* **2015**, *2*(1), 56-65.
9. Pongdong, W.; Nakason, C.; Kummerlowe, C.; Vennemann, N. *J. Chem.* **2015**, *2015*, 1-15
10. Mathew, L.; Narayanankutty, S. K. *J. Rubb. Res.* **2010**, *13*(1), 27-43.
11. Sarkawi, S. S.; Aziz, Y. *J. Teknol.* **2003**, *39*(1), 135-148.
12. Prasertsri, S.; Rattanasom, N. *Polym. Test.* **2012**, *31*(5), 593-605.
13. Francis, L. F.; Grunlan, J. C.; Sun, J.; Gerberich, W. *W. Colloids. Surf. A. Physicochem. Eng. Asp.* **2007**, *311*, 48-54.
14. Arun, K. J.; Francis, P. J.; Joseph, R. *J. Optoelectron. Adv. M.* **2010**, *4*, 1520-1525.
15. Yin, C.; Zhang, Q.; Liu, J.; Liu, L.; Gu, J. *Polym. Compos.* **2018**, *39*(1), 22-28.
16. Ismail, H.; Rozman, H. D.; Jaffri, R. M.; Ishak, Z. M. *Euro. Poly. J.* **1997**, *33*, 1627-1632.
17. Bailly, M.; Kontopoulou, M.; Mabrouk, K. *Polymer.* **2010**, *51*(23), 5506-5515.
18. Lay, M.; Azura, A. R.; Othman, N.; Tezuka, Y.; Pen, C. *Adv. Mat. Res.* **2013**, *626*, 818-822.

## BIOGRAPHY

Anupong Boonmee was born on November 14, 1993 in Surin, Thailand. He finished high school from Thatum Prachasermwit School in 2012. He attended Suranaree University of Technology (SUT) and graduated in 2016 with a Bachelor's degree in Polymer Engineering. He then continued his Master's degree in Materials Engineering at School of Polymer Engineering, Institute of Engineering, Suranaree University of Technology. During his graduate study, he got a research assistant scholarship from Suranaree University of Technology. His research was about silica nanoparticles reinforced natural rubber composites. In the period of his study, he presented two poster presentations entitled: "Preparation and Characterization of Rice Husk Ash for Using as a Filler in Natural Rubber" at The First Materials Research Society of Thailand International Conference (1<sup>st</sup> MRS Thailand International Conference) in Chaing Mai, Thailand and "Mechanical properties and cure characteristics of silica nanoparticles from sugarcane bagasse ash/natural rubber composites" at The International Polymer Conference of Thailand 2019 (PCT-9) in Bangkok, Thailand. His work was published two papers entitled of "Preparation and characterization of silica from sugarcane bagasse ash as filler in natural rubber" in Suranaree Journal of Science and Technology (Suranaree J. Sci. Technol.) and "Preparation and characterization of silica nanoparticles from sugarcane bagasse ash for using as a filler in natural rubber composites" in Polymer Bulletin (Polym Bull).